Journal of Materials Chemistry A

Accepted Manuscript

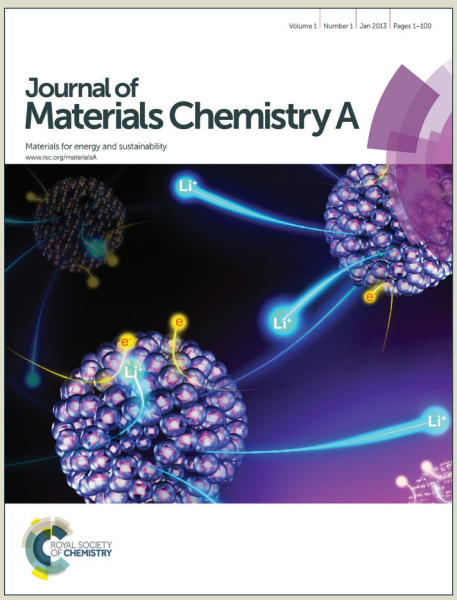

ROYAL SOCIETY OF CHEMISTRY

www.rsc.org/materialsA

Journal Name

RSCPublishing

ARTICLE

Recent Advances in the Potential Applications of Bioinspired Superhydrophobic Materials

Cite this: DOI: 10.1039/xoxxoooooox

Thierry Darmanin and Frederic Guittard[a]

Received ooth January 2012,
Accepted ooth January 2012

DOI: 10.1039/xoxxoooooox

www.rsc.org/

This review allows to give an overview of recent advances in the potential applications of superhydrophobic materials. Such properties are characterized by extremely high water contact angle and various adhesion properties. The conception of superhydrophobic materials has been possible by studying and mimicking natural surfaces. Now, extremely various applications have emerged such as anti-icing, anti-corrosion and anti-bacteria coatings, microfluidic devices, textiles, oil/water separation, water desalination/purification, optical devices, sensors, batteries and catalysts. At least two parameters were found to be very important for many applications: the presence of air on superhydrophobic materials with self-cleaning properties (Cassie-Baxter state) and the robustness of the superhydrophobic properties (stability of the Cassie-Baxter state). This review will allow to researchers to envisage new ideas and to industrialists to advance in the commercialization of these materials.

1. Introduction

Superhydrophobicity is characterized by the repellency of water on a surface with an apparent contact angles of water (θ_w) above 150° and various adhesive properties characterized by dynamic contact angle measurements. The potential applications of superhydrophobic materials are extremely wide and include anti-icing coatings, anti-corrosion coatings, anti-corrosion coatings, anti-bacteria coatings, textiles, oil/water separation, water purification and desalinization, microfluidic devices, optical devices, batteries, sensors, drug delivery or heterogeneous catalysis. Recent advances in the potential applications of superhydrophobic materials will be carefully described in this review.

Biomimetic and bioinspired approaches have been necessary to well understand and reproduce non-adhesion phenomena.[1-3] Indeed, the nature have produced since millennia several plants, insects and animals with superhydrophobic surface properties. The possession of superhydrophobic properties is a major trump for these species to survive in very aggressive environments. The most famous example is the lotus leaf associated with self-cleaning properties and robustness due to the presence of micro- and nanostructures of hydrophobic waxes (Fig. 1a and Fig 1b).[1-5] Very recently, it has been reported that soil-dwelling wingless arthropods such as pringtails (*Orthonychiurus stachianus* and *Tetrodontophora bilanensis*) are able to resist to the wetting of low surface tension liquids (Fig. 1f), such as oils, due to the presence of surface structures with positive re-entrant structures (serif T structures).[6-8] We can also cite the antireflective[9] and anti-fogging[10] properties of moth and mosquito eyes to have a large and clear view of the surroundings, the structural color of butterfly wings to warn the predators (Fig. 1d),[11-12] and the bactericidal properties of cicada wings.[13] Other species are also able to collect water in very dry and hot media (Fig. 1c),[14-15] collect air underwater (Fig. 1b),[16] while others are able to slip on water (Fig. 1e)[17-18] or to walk on vertical surfaces (Fig. 1g). These various ability are especially due to differences of surface adhesion.[19]

The superhydrophobicity is governed by two main parameters as described by the Wenzel[20] and Cassie-Baxter[21] equations: the intrinsic hydrophobicity of the materials present at the extreme surface and a roughness parameter, which combines surface roughness and topography, as described by Marmur.[22-23] Various strategies could be used to reproduce these properties such as lithographic processes, templating, electrospinning, electrodeposition, sol-gel processes and layer-by-layer deposition.[24-27]

Because the scientific community have worked very intensively since about 10 years, it is now appropriated to give a very exhaustive overview of the importance of the superhydrophobicity for various potential applications. After the description of the wetting theories as well as self-cleaning properties and robustness, which are extremely important for applying superhydrophobic materials, we will summarize each application such as a "mini-review".

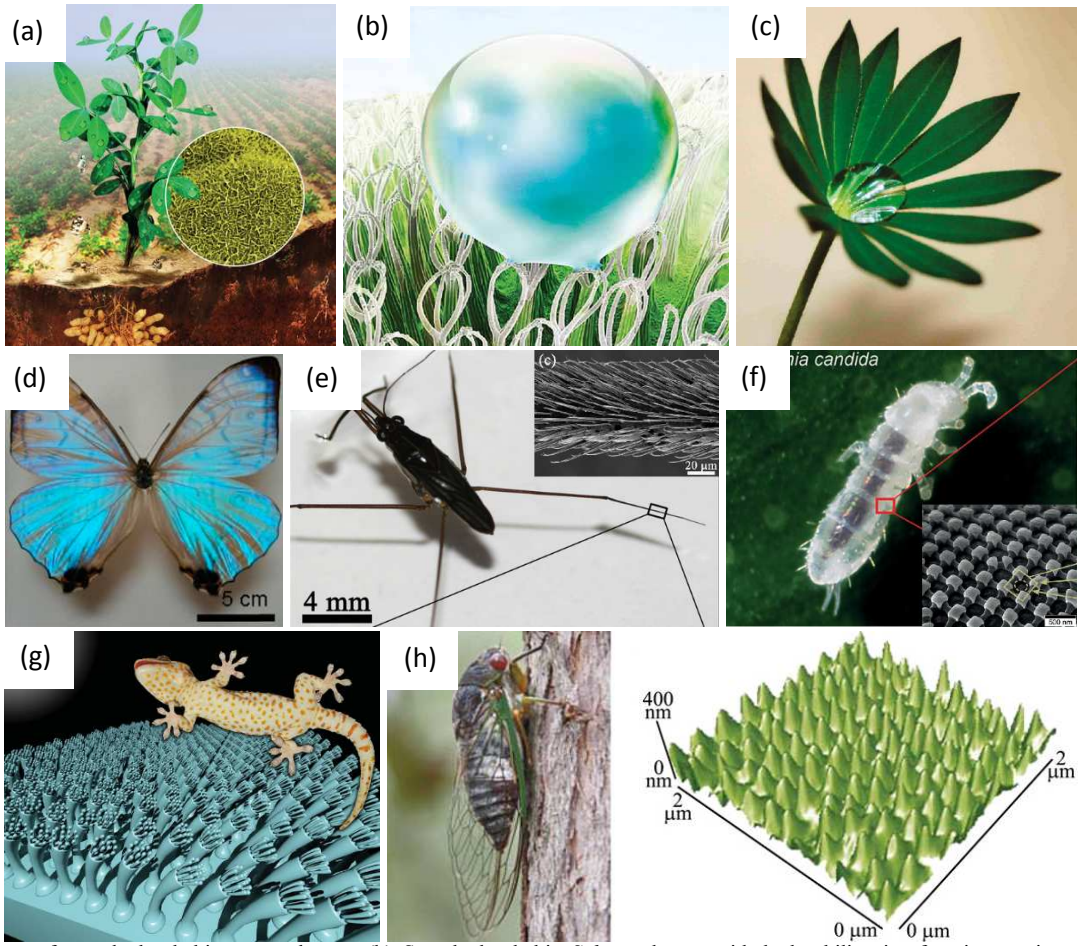

Fig. 1. (a) Picture of superhydrophobic peanut leaves; (b) Superhydrophobic *Salvinia* leaves with hydrophilic pins for air retention; (c) Picture of a superhydrophobic lupin with superhydrophilic channels to guide water droplets; (d) Picture of a blue *Morpho Aega* with directional adhesion; (e) Picture of a water strider capable of walking on water; (f) Picture of superoleophobic *Folsomia candida*; (g) Picture of a gecko capable of walking on vertical surfaces;[19] (h) Picture of cicada with superhydrophobic and self-cleaning wings.
Panel a reprinted with permission from ref. 4, copyright 2014, Wiley-VCH; Panel b reprinted with permission from ref. 16, copyright 2010, Wiley-VCH; Panel c reprinted with permission from ref. 16, copyright 2009, American Chemical Society; Panel d reprinted with permission from ref. 12, copyright 2013, American Chemical Society; Panel e reprinted with permission from ref. 17, copyright 2010, Elsevier B.V.; Panel f reprinted with permission from ref. 6, copyright 2014, Wiley-VCH; Panel h reprinted with permission from ref. 5, copyright 2013, PNAS.

2. Wetting theories, self-cleaning properties and robustness

When a droplet is deposited on a substrate, it wets more or less the substrate. The apparent contact angle θ_w is taken at the triple point solid-liquid-vapor. For a smooth, homogeneous, rigid, insoluble and non-reactive solid surface,[28] θ_w depends on the solid-vapor tension γ_{SV} (surface free energy), the solid-liquid surface tension γ_{SL} and the liquid-vapor surface tension γ_{LV}, as given by the Yound-Dupre equation (Fig. 2a): $\cos\theta^Y = (\gamma_{SV} - \gamma_{SL})/\gamma_{LV}$.[29] Hence, for a "smooth", θ^Y increases when γ_{SV} decreases or γ_{LV} increases. However, for a smooth surface, θ_w do not exceed 125-130°C, which is the maximum value obtained for some fluorinated materials.

Indeed, it is necessary to increase the surface roughness by creating surface structures, as described by the Wenzel[20] and Cassie-Baxter[21] equations. A liquid droplet in the Wenzel state[20] fully wets the surface by entering in all surface anfractuosities (Fig. 2b). The solid-liquid interface is increased by a roughness parameter r corresponding to the specific/projected area. The Wenzel equation is: $\cos\theta = r\cos\theta^Y$. As a consequence, both superhydrophobic and superhydrophilic properties can be predicted. The surface roughness increases the hydrophobicity of intrinsically hydrophobic materials ($\theta^Y > 90°$) and decreases the hydrophobicity of intrinsically

hydrophilic materials ($\theta^Y < 90°$). In the Cassie-Baxter state,[21] the liquid droplet is suspended on top of rugosities and on air trapped inside surface anfractuosities (Fig. 2c). The Cassie-Baxter equation is: $\cos\theta = \varphi_s (\cos\theta^Y + 1) - 1$, where φ_s is the solid fraction in contact with the droplet and $(1 - \varphi_s)$ is the air fraction.

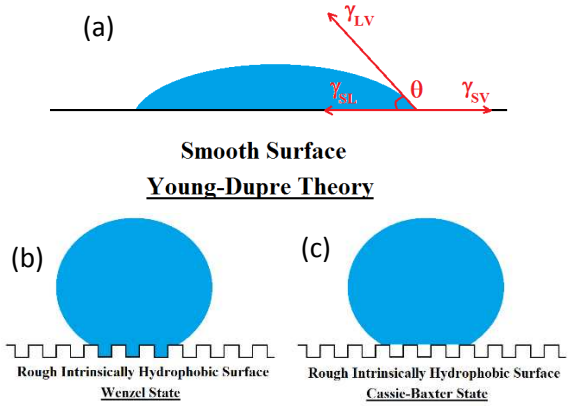

Fig. 2 Schematic representation of a water droplet on a (a) smooth surface, following the Young-Dupre equation, and on a rough surface, following (b) the Wenzel equation and (c) the Cassie-Baxter equation

To determine the superhydrophobic properties of materials, it is necessary to determine not only the water apparent contact angle θ_w but also the dynamic contact angles: the advanced contact angle $\theta_{adv,w}$, the receding contact angle $\theta_{rec,w}$, and as a consequence the hysteresis $H_w = \theta_{adv,w} - \theta_{rec,w}$. H gives an indication on the necessary force to remove a droplet on a substrate. Usually, for superhydrophobic surfaces, the most employed method to determine H is the tilted-drop method. This method consists in the deposition of a water droplet on a substrate. After inclination until a maximum angle, called sliding angle or tilting angle (α), the water droplet rolls off the substrate. H has to be determined just before the droplet rolls off the substrate. Indeed, the gravity inducing a deformation of the droplet allowing to determine $\theta_{adv,w}$ and $\theta_{rec,w}$. When a liquid droplet follows the Wenzel equation, H and α are very high because of the increase in the solid-liquid interface. By contrast, when a liquid droplet follows the Wenzel equation, H and α are very low (usually < 10°) due to the increase in the liquid-vapor interface. The low H and α are also responsible of the self-cleaning properties observed on natural species such as the lotus leaves.[1-5] Indeed, if dusts or particles are present on a superhydrophobic surface, there are more attracted by water droplets than by the surface (Fig. 3).[30-31] As a consequence, during rainfall, a simple surface inclination allows to remove dusts and particles on superhydrophobic surfaces.

Moreover, the Wenzel and Cassie-Baxter states are two extreme states but many other states between these two states can also exist (with a composite interface).[32-34] Indeed, the Cassie-Baxter state is a metastable state and the applying of an extern pressure can induce a Cassie-Baxter–to–Wenzel transition (Fig. 5). A surface supporting a very high pressure is called "robust". The term "robust" is different from the term "mechanical durable", which is also important for many applications.[35]

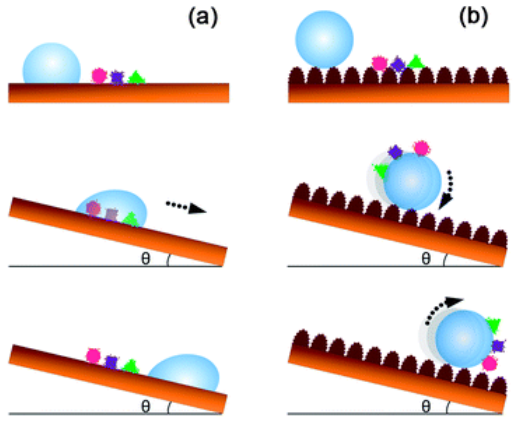

Fig. 3 Schematic representation of (a) a smooth surface without self-cleaning properties and (b) a superhydrophobic surfaces with self-cleaning properties (Cassie-Baxter state).[30]

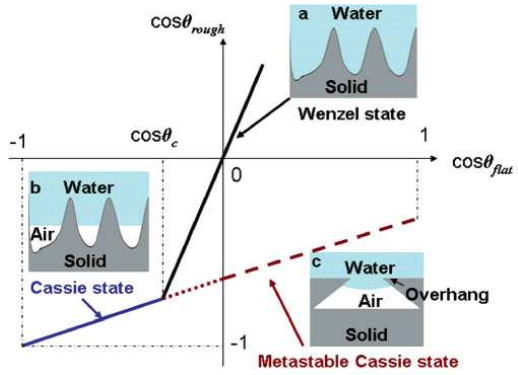

Fig. 4 Relationship of $\cos\theta$ with $\cos\theta^Y$: the black, blue, correspond to the Wenzel state, the Cassie-Baxter state while the red dotted and red dashed lines to the metastable Cassie-Baxter state when $\theta^Y > 90°$ and the metastable Cassie-Baxter state when $\theta^Y < 90°$.
Reprinted with permission from ref. 32, copyright 2007, American Chemical Society.

The robustness is highly depending on the surface topography. For example, the presence on both micro- and nanostructures was found to be an important parameter to obtain robust superhydrophobic properties.[36] It was even demonstrated the possibility to stabilize the Cassie-Baxter state using intrinsically hydrophilic materials ($\theta^Y_w < 90°$) as well as superoleophobic properties with using intrinsically oleophilic materials ($\theta^Y_{oils} < 90°$).[37] The main parameter was found to be the presence of re-entrant surface structures, as observed in springtails (Fig. 1f) and in leafhopper (Fig. 5), such as overhangs, T-like structures or mushroom-like structures. Indeed, their presence often affects the interface meniscus and induces a negative capillary effect helping to support the liquid.[35,39]

3. Potential applications of superhydrophobic surfaces

3.1 Anti-icing coatings

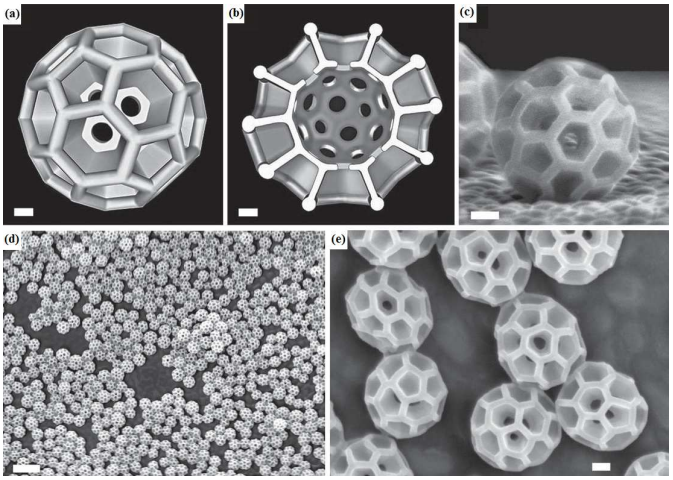

Fig. 5 Superoleophobic bronchosomes observed at the surface of leafhoppers (*Insecta*, *Hemiptera*, *Cicadellidae*). Scale bars: 50 nm (a,b), 100 nm (c,e) and 1 μm (d).
Reprinted with permission from ref. 38, copyright 2013, The Royal Society.

The development of anti-icing coatings can increase the energy efficiency as well as the safety of materials and systems such as aircrafts or turbines.[40] The surface topography/roughness necessary to obtain superhydrophobic surfaces can lead also in certain conditions to anti-icing properties. However, if water and ice are composed of the same molecules, their adhesion on a substrate is clearly different. First of all, it was demonstrated that superhydrophobic properties can delay the formation of freeze.[41-47] Indeed, the presence of air trapped on superhydrophobic surfaces favoring the Cassie-Baxter can induce the formation of a thermal barrier between the solid and the liquid. This characteristic was demonstrated by depositing water on cold solids.[41] Hence, if the substrate is tilted, water droplets can be removed without freezing. The group of Song showed, using superhydrophobic surfaces made of ZnO nanorods, that condensed micro-droplets below the freezing points were always spherical indicating that the surfaces were superhydrophobic to these droplets.[42] Moreover, they observed a dependence of the delay of the freeze formation with the dimension of the ZnO nanorods. Other groups worked on the ice nucleation on superhydrophobic surfaces using supercooled water droplets.[43-46] They observed a delay for superhydrophobic surfaces but also a nucleation mechanism highly depending on the temperature. As a consequence, it is extremely difficult to obtain anti-icing properties for all temperature ranges. Gao et al. also studied anti-icing properties of superhydrophobic surfaces made of nanoparticle/polymer composites using supercooled water droplets.[47] They observed that their anti-icing capacity was highly depending on the size of the particles. Second, the adhesion of ice can be higher or lower on superhydrophobic surfaces than on smooth surfaces. It was demonstrated that there is a relationship between the water wettability and the ice adhesion with the quantity [1 + cos θ_{rec}].[48-49] More precisely a surface should exhibit a $\theta_{rec} > 118.2°$ to induce a significant decrease of the ice adhesion. As a consequence, superhydrophobic textured surfaces favoring the Cassie-Baxter state are preferable to reduce the ice adhesion and more precisely a water droplet should freeze in the Cassie-Baxter state.[48-53] Such surfaces should also resist to freezing rain and condensation of moisture within the surface structures. Indeed, it was shown that the anti-icing efficiency is lower in a humid atmosphere because the water condensation can enter inside the surface roughness leading to higher values of ice adhesion strength.[52] The surfaces should be also mechanically resistant to the icing and deicing phenomena.[54]
Moreover, the mechanism of water and ice adhesion are clearly different,[55-58] as showed by the group of Nosonovsky. When a piece of ice is present on a surface, it can be removed by dewetting or can fracture (Fig. 6).[55] When a superhydrophobic in the Cassie-Baxter state is used, the freezing of water changes the air pockets into air voids, which can act as stress concentrators (microcracks). It was showed that the forces necessary to remove a piece of ice are depending on the receding contact angle and the initial size of the interfacial cracks. Hence, a superhydrophobic surface can lead to high ice adhesion if there are not sufficiently large voids at the interface. The hardness of the materials is also important for the process. For example, flexible and rigid materials were tested against icing and deicing cycles.[59a] The results showed that the rigid materials were more efficient against icing and deicing cycles. Indeed, the icing and deicing can deteriorate the surface structures and also the chemical compounds present on the surface. However, Zheng et al. also reported than flexible materials containing PDVF microspheres and coated by ZnO nanocones have excellent anti-icing and deicing properties.[59b]

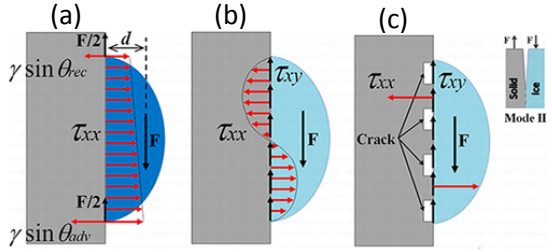

Fig. 6 Normal and shear forces during shear the loading of (a) a water droplet and (b) an ice frozen droplet on a flat and (c) textured (Cassie-Baxter state) surface.
Reprinted with permission from ref. 57, copyright 2012, American Chemical Society.

Hence, many strategies were used to reduce the ice adhesion using superhydrophobic surfaces. The group of Aizenberg also reported the elaboration of a predictive model for the formation of ice on superhydrophobic surfaces with the possibility to vary the surface morphology and the surface chemistry.[60]
In the last section, we will report examples of ice-phobic materials reported in the literature.
Robust anti-icing coatings were reported on stainless steel. To obtain such properties, the substrates were etched, modified with silica nanoparticles and treated with a fluorinated silane.[61] Anti-icing coating were reported in freezing rain at -6°C and

humidity 97% with robustness even after 100 icing/deicing cycles. Superhydrophobic aluminum alloy substrates obtained by chemical etching or anodization (θ_w = 159.1° and H = 4° for the etched substrates) were tested from room temperature (16°).[62] In comparison to smooth aluminum, the authors observed a delay in the ice formation at -2.2° of 270 s while the icing temperature could be decreased from -2.2° to -6.1°. Moreover, the tilting of the surface could highly reduce the utilization temperature of these materials. The resistance to ice of superhydrophobic anodized aluminum substrates were also confirmed by other works.[63]

Copper foils were treated by immersion in KOH and $K_2S_2O_8$ to form superhydrophobic (θ_w = 156.2°) flower-like structures after surface modification with a fluorinated silane.[64] The authors showed that the water droplet was smaller and more dispersive on these surfaces, in comparison with smooth copper foils, reducing both the icing and deicing time. Glass substrates were also modified in the literature to form anti-icing properties.[65-66] The strategies involved the use of silica nanoparticles and calcium carbonate/polymer composites.

Another strategy to form robust ice-repellent coatings was to infuse a water-immiscible liquid inside the structures of a porous superhydrophobic materials.[67] The group of Aizenberg worked on aluminum substrates coated by a porous layer of polypyrrole and reported that when this materials is infused in a perfluorinated lubricant (perfluoroalkylether), the resulting materials can reduce the ice adhesion with 1-2 orders of magnitude in comparison to conventional materials (Fig. 7).[67a]

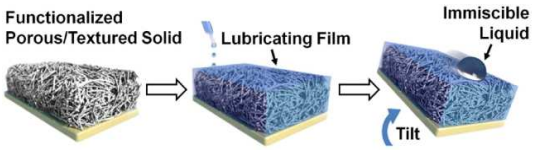

Fig. 7 Schematic representation of a slippery, liquid-infused porous surface (SLIPS) for anti-icing coatings.
Reprinted with permission from ref. 67b, copyright 2012, American Chemical Society.

3.2 Anti-corrosion coatings

The corrosion of metals is one of the more major concern in the worlds and represents about 3% of the world GDP. Today, most of the coatings used contain chromium (VI) ions for anti-corrosion properties and due to its toxicity all the strategies to replace it have to be tested. It was shown in the literature that superhydrophobic materials can also act as anti-corrosion barrier without adding chemicals.[68-69] Superhydrophobic surfaces with different adhesions but with the same surface chemistry were reported in literature and especially superhydrophobic surfaces with self-cleaning properties (Cassie-Baxter state) and with high adhesion (Wenzel state).[68] The authors observed that the surfaces with the self-cleaning properties have the more promising anti-corrosion properties with a very high impedance value of 10^{10} Ω cm^2 (at 10^{-2} Hz). They proposed that the air layer between the surface and water, when the superhydrophobic surface possess self-cleaning properties, may inhibit ion transport from the electrolyte to the metal substrate (Fig. 8). As a consequence a robust superhydrophobic surface keeping their properties in seawater has to be used for anti-corrosion properties.

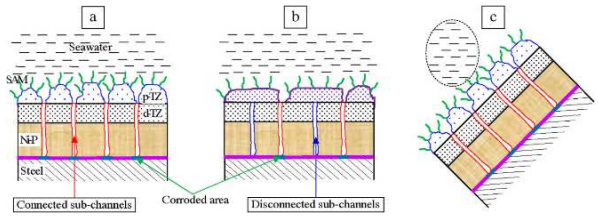

Fig. 8 Mechanism of corrosion of (a) superhydrophobic and (b) hydrophobic metals; (c) experiments on inclined superhydrophobic films with self-cleaning properties.
Reprinted with permission from ref. 69, copyright 2014, Elsevier B.V.

Superhydrophobic metals were used in the literature to reach anti-corrosive materials. A metal (M) can be oxidized to form M^{n+} ions. In acidic media, the substrate can be etched while in neutral or basic media, the M^{n+} ions can react to form metal oxide, hydroxide, or complex nanostructures. The group of Wang etched Mg, Al, and Ti alloys in HNO_3, HCl, HF as well as oxidized Mg and Al alloys in hot water and Ti alloys in H_2O_2 or H_2O_2/HF.[70] The surfaces were superhydrophobic after modification with a perfluorinated silane. The authors showed that the surfaces treated in hot water or H_2O_2 are much more efficient against corrosion than the surfaces etched in acidic media. This is probably due to the presence of the oxide layer which adds a barrier effect and also strengthens the interfacial bindings between the surfaces and the perfluorinated silane. Similar results were also reported by other research groups.[71-74] To induce a more controlled oxide layer, aluminum and titanium surfaces with excellent ant-corrosion properties were also obtained by anodization.[75-76] Zhang et al. elaborated $Cu[CH_3(CH_2)_{12})COO]_2$ flower-like structures by electrochemical oxidation of Cu plates in the presence of tetradecanoic acid (Fig. 9).[77] The films presented excellent anti-corrosion properties and it was observed a decrease of more than four orders of magnitude of the anodic and cathodic polarization current densities. The films were stable after more than 20 days immersion in 3.5 wt.% NaCl even if a decrease of θ_w to around 140° was observed. The authors could also play on the surface morphology replacing tetradecanoic acid by laurylamine or 3-undecyl-4-amino-5-mercapto-1,2,4-triazole as well as the copper substrate by a zinc one.[78-80] Carambola-like CuO structures were also reported by immersing Cu plates in hot water containing copper acetate and hexamethylenetetramine.[81] It was also possible to deposit metal nanostructures on a substrate composed of another metal by galvanostatic deposition. When the potential difference between the metal and the metal ion is sufficiently important, the growth is spontaneous at room temperature.

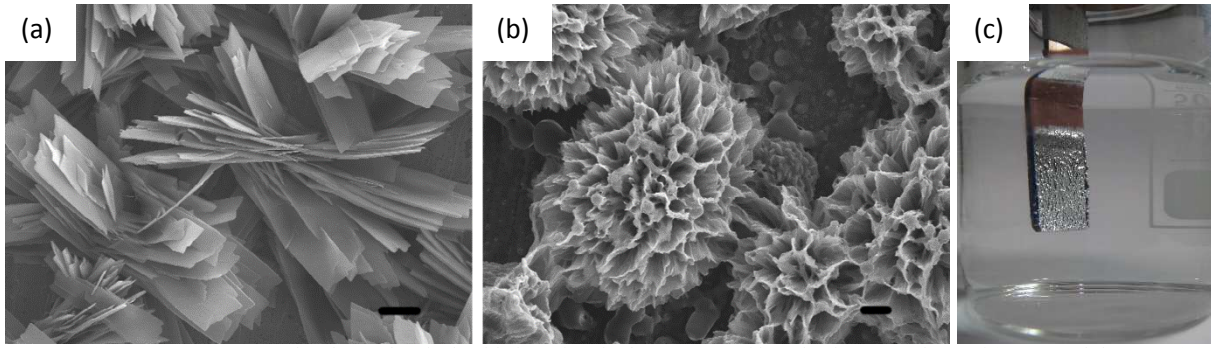

Fig. 9 $Cu[CH_3(CH_2)_{11}N]_2C$ nanostructures by electrochemical oxidation of Cu in the presence of laurylamine at a voltage of (a) 5 V and (b) 50 V. (c) Picture of a superhydrophobic film immersed into 3.5% NaCl solution. Scale bars: 100 µm (a) and 20 µm (b).
Reprinted with permission from ref. 78, copyright 2014, Elsevier B.V.

For example, $Fe[CH_3(CH_2)_{12})COO]_3$ were reported at the surface of Mg alloy substrates as well as Pt nanostructures at the surface of Zn substrates.[82] Otherwise, the deposition can be performed by electrodeposition.

To increase the surface roughness and to improve the anti-corrosion properties, SiO_2 and TiO_2 nanoparticles were used in the literature.[84-88] For example, the group of Rao reported the elaboration of large SiO_2 particles at the surface of Cu substrates with superhydrophobic properties (θ_w = 158°) and low sliding angles (α = 7°).[84] The coating was able to resist to an immersion for 100 h in 50% HCl solution even if a decrease of θ_w from 158° to 146° was observed after 120 h. To increase the surface properties, a fluorinated silane could also be grafted to the nanoparticles.[86-88] Fibrous szaibelyite structures and leaf-like boehmite structures were also applied on Mg alloy and Al substrates, respectively.[89-90] After surface modification, the substrates displayed anti-corrosion properties with a decrease in the corrosion current density of three orders of magnitudes in comparison to smooth substrates.

Polymer materials were also found to be suitable for anti-corrosion properties. Rough polysiloxane materials deposited on Mg alloys by plasma-enhanced chemical vapor deposition highly improved their corrosion resistance.[91] However, the films were stable in acidic and neutral media but not in alkaline media. To improve the adhesion between a polymer layer and a metal substrate, the polymer should be grafted on the surface. An electrospun diblock copolymer was used to improve the corrosion of Al and also the adhesion to Al.[92] The first block (poly(heptadecafluorodecylacrylate-*co*-acrylic acid)) was used to increase the surface hydrophobicity and to graft onto Al thanks to carboxylic acids while the second block (polyacrylonitrile) was used to insure the stability during annealing. The best adhesion and corrosion resistances were obtained for 20 µm thickness. The group of Yuan also reported the graft polymerization of a fluorinated polymer after introduction of vinyl groups on copper substrates.[93]

Superhydrophobic polymer surfaces with regular patterns were also obtained by lithographic process. Yeh et al. used of soft lithographic process using natural *Xanthosoma sagittifolium* leaves as molds and used polyaniline, electroactive polyimide, or an electroactive epoxy for the replication (Fig. 10).[94-96] Here, the electroactivity of the polymer enhanced the protection of the polymer against the corrosion. The same group also used an UV-curable epoxy-acrylate to induce a very fast curing and without any solvent.[97] Here, the corrosion potential and the corrosion current were found to shift from -730 mV and 5.44 µA cm^{-2} for the smooth surfaces to -394 mV and 2.30 µA cm^{-2} for the structured superhydrophobic ones. Colloidal lithography was also used in the literature. To induce microstructures, the group of Advincula formed ordered PS nanoparticles on steel substrates before electrodeposition of a polythiophene-derived polymer.[98] They observed an increase of the anti-corrosive efficiency of 96.2% and 81.3% for the superhydrophobic films and the corresponding smooth surface, in comparison with the steel substrate. Wang et al. also used the deposition of PS nanoparticles by colloidal lithography but as removable template.[99] After deposition of SiO_2 nanoparticles, the PS template was removed by heating at 550°C. The as-prepared materials possessed good anti-corrosive properties.

Hence, several kinds of materials (metal, inorganic, polymer…) were used in the literature to enhance the anti-corrosion properties of metals by formation of superhydrophobic films. Composites films were also reported in the literature for this application.[100-101]

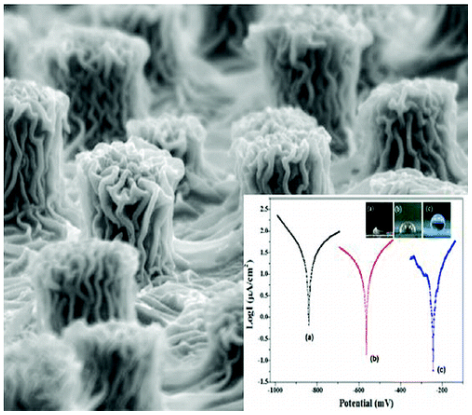

Fig. 10 Superhydrophobic surfaces with anticorrosive properties obtained by soft lithography and using natural *Xanthosoma sagittifolium* leaves as molds. The inset represents Tafel plots for different materials measured in 3.5 wt % NaCl aqueous solution.

Reprinted with permission from ref. 94, copyright 2011, American Chemical Society.

3.3 Anti-bacteria surfaces

The biocontamination of materials and devices is a major problem in various industrial sectors including in medicine and environment fields. In these fields the growth of biofilms can be problematic as observed by nosocomial infections in hospitals. The formation of biofilm is a natural and spontaneous process taking place in four steps: transport, adhesion, strengthening and colonization. Two strategies are often employed: to kill them or to reduce their adhesion.

3.3.1 Bactericidal surfaces

The first strategy to reduce the presence of bacteria on surfaces is to kill them. It was shown that the superhydrophobic and nanopatterned wings of cicada *Psaltoda claripennis* possess this ability.[13,102] The wings are able to consistently kill Gram-negative bacteria (*Branhamella catarrhalis*, *Escherichia coli*, *Pseudomonas aeruginosa*, *Pseudomonas fluorescens*) but do not kill Gram-positive bacteria (*Bacillus subtilis*, *Planococcus maritimus*, *Staphylococcus aureus*), independently of the bacteria shape (Fig. 11).

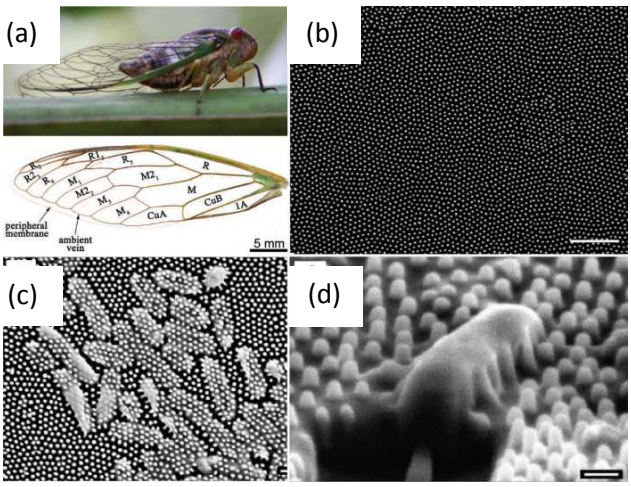

Fig. 11 (a) Picture of cicada *Psaltoda claripennis* with nanopatterned superhydrophobic wings; (b), (c) and (d) SEM images of the wings with dead bacteria.
Reprinted with permission from ref. 13, copyright 2012, Wiley-VCH.

Otherwise, biocides can be used such as Ag^+, or highly reactive species such as hydroxyl radical, hydrogen peroxide and superoxide produced by the photocatalysis of TiO_2. Ag nanoparticles immobilized in polyelectrolytes were used to prevent bacterial adhesion.[103-105] The authors reported that the presence of superhydrophobic properties can reduce the release of Ag^+ ions due to the presence of air between the substrate and seawater, which reduces the contact between the substrate and seawater (Fig. 12). Hence, superhydrophobic properties enhanced the stability of the Ag-based coating and prolonged the duration of release of antibacterial Ag^+ ions. To control the release of Ag^+ ions, superhydrophobic mesoporous silica microcapsule-supported Ag nanoparticles were also elaborated.[106] In this strategy, the release of Ag^+ was controlled by mesopore channels.

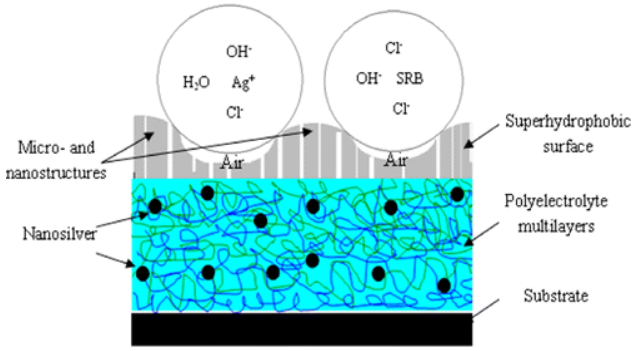

Fig. 12 Mechanism of Ag^+ ions released on a polyelectrolyte superhydrophobic film.
Reprinted with permission from ref. 103, copyright 2012, American Chemical Society.

Other research groups elaborated superhydrophobic surfaces using Ag nanoparticles for antibacterial properties. For example, fibrous Ag-perfluorodecanethiolate complexes were elaborated by reaction between $AgNO_3$ and perfluoroodecanethiol.[107] After UV irradiation to form Ag nanoparticles, the film showed antibacterial properties. To use the antibacterial photocatalytic effect of TiO_2 but under-visible light, N-doped TiO_2 nanoparticles were used as well as Cu/WO_3 ones.[108-109] Composites obtained with these materials and PTFE showed a bacterial activity against *Escherichia coli*. Cotton textiles with antibacterial properties were also reported by incorporation of Ag nanoparticles, Cu nanoparticles or ammonium moieties.[110-115]

3.3.2 Anti-bioadhesion surfaces

Hence, if the use of bactericidal materials allows to kill bacteria with high efficiency, the increase in bacterial resistance allowed to envisage another way without killing the bacteria. This strategy is based on the reduction of the bacteria adhesion on surfaces.

3.3.2.1 Protein and Cell Adhesion

The control of the cell and protein adhesion has a potential application in bio-sensors and the implanting of biomaterials. This control is also important to control and reduce the adhesion of pathogenic bacteria, germs and cancel cells.
It is admitted in the literature that the adhesion of proteins and cells is depending on the surface chemistry. The question is how the presence of a surface topography in superhydrophobic surfaces can affect the interactions between the surface and proteins or cells.[116-117]

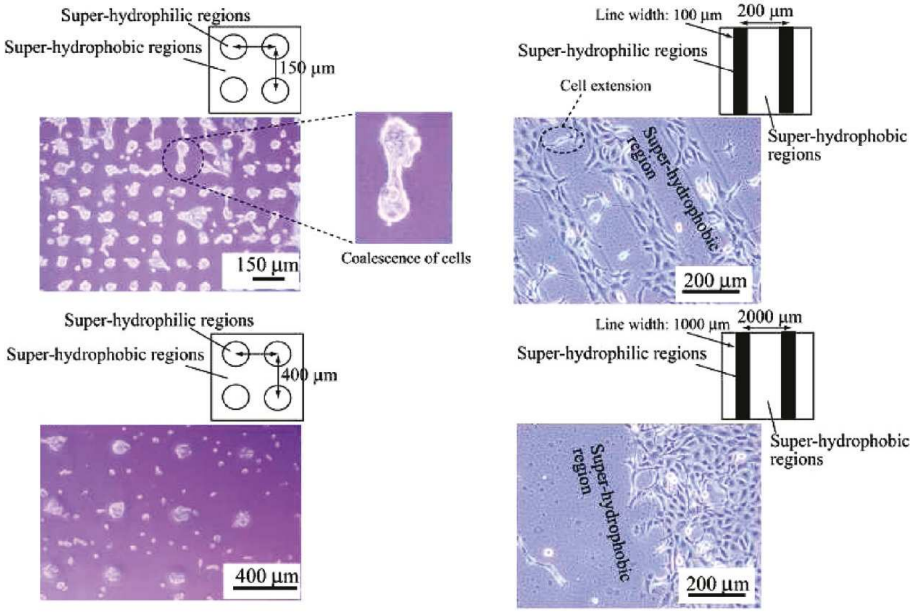

Fig. 13 Cell adhesion on micropatterned superhydrophobic/superhydrophilic surfaces. Reprinted with permission from ref. 119, copyright 2010, American Chemical Society.

The group of Salmeron-Sanchez studied the influence of the superhydrophobicity on the fibronectin adsorption and MC3T3-E1 cell adhesion.[118] They used superhydrophobic PS substrates and compared their results to smooth PS ones. They observed that the superhydrophobic surfaces reduce the density of adsorbed fibronectin and alter their conformation, leading to cell adhesion without formation of mature focal adhesion plaque and scarce phosphorylation of FAKs. However, cells were able to proliferate on superhydrophobic surfaces and maintain a stable population up to 21 days even if their density was lower than on smooth surfaces. On the one hand, Ishizaki et al studied the impact of the surface chemistry and physics by investigated the cell adhesion on superhydrophobic, superhydrophilic (with the similar roughness) and micropatterned superhydrophobic/superhydrophilic surfaces (Fig. 13).[119] On micropatterned surfaces, the cells attached to the superhydrophilic regions in a highly selective manner. When the distances between superhydrophilic regions were lower than 400 μm, the cells partially extended to the neighboring cells. Moreover, the cells adhered and proliferated much easier on superhydrophilic surfaces than on superhydrophobic ones. The authors also observed that the amount of adsorbed proteins was greater on smooth hydrophilic surfaces than on smooth hydrophobic ones.

On the other hand, the group of Moon studied the impact of the topography on the adhesion of mouse liver cancer cells on nanostructured superhydrophobic and superhydrophilic surfaces.[120] They observed that the growth of the cancer cells is suppressed on superhydrophilic surfaces with high aspect ratio nanostructures (hair shaped) due to the limited sites for focal adhesion. The adhesion and the growth was further restricted on superhydrophobic surfaces with high aspect ratio nanostructures. More precisely, they observed that their cell activity was extremely low and that their spherical shape was maintained.

Other groups were interested in the evaluation of the role of air trapped on superhydrophobic surfaces on the protein and cell adhesion. Indeed, it is thought that the air trapped can act as a resistance to protein and cells.[121-122] The group of Lin investigated the influence of air trapped within the interstices of TiO_2 nanotubes by the elaboration of micropatterned superhydrophobic/superhydrophilic surfaces.[122] The effect of air was investigated by displacing the air by sonication. The authors observed that the proteins bind much more on superhydrophobic surfaces when the air is displaced. However, they also showed that the air trapped in superhydrophobic surfaces does not block short or long-term cell attachment.

Finally, the adhesion of proteins and cells was also investigated on switchable superhydrophobic surfaces. To study this effect, superhydrophobic GaN nanowires were deposited by CVD while their wettability could be switched to superhydrophilic by UV irradiation with an increase in the protein adsorption and cell adhesion (Fig. 14).[123] Chen et al. also fabricated nanostructured Teflon AF with superhydrophobic properties and resistance to protein adsorption.[124] After electrowetting, the surfaces changed into superhydrophilic with a promotion of the protein adhesion. The group of Advincula was also interested in such materials.[125] They developed superhydrophobic surfaces combining colloidal lithography with an electrodeposited polythiophene derivatives. In its undoped state, the film was superhydrophobic and inhibited the adhesion of fibrinogen protein and *Escherichia coli*. By changing the voltage, the doped polythiophene film was hydrophilic and increased the adhesion of protein and *Escherichia coli*.

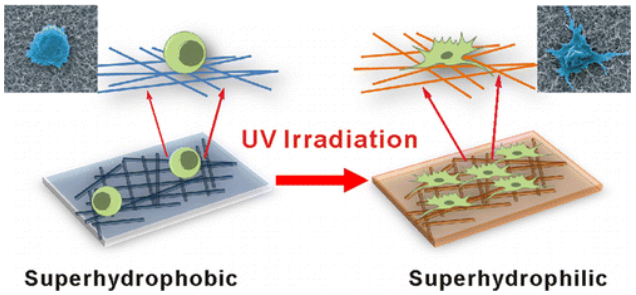

Fig. 14 Effect of irradiation on protein adsorption and cell adhesion of GaN nanowires.
Reprinted with permission from ref. 123, copyright 2013, American Chemical Society.

3.3.2.2. Bacteria Adhesion

In this last sub-section, we will discuss on the surface able to limit the adhesion bacteria also called anti-bioadhesive surfaces. If protein and cell adhesions can give information and strategies to reduce the bacteria adhesion, it should be noticed that bacteria are extremely complex microorganisms having various surface chemistry, hydrophobicity, cell membrane, surface charges, shape, and hardness and can also have pili and flagella to modify their adhesion.[126-130] Hence, the elaboration of surfaces repelling all kinds of bacteria is to date not possible.
The group of Dowling studies the adsorption of proteins of siloxane and fluorinated materials ranging from superhydrophilicity to superhydrophobicity.[131] A reduction of the protein adsorption was observed on superhydrophilic surfaces in comparison to hydrophobic one, but the highest reduction was measured on superhydrophobic surfaces. The authors also observed a reduction of *Staphylococcus aureus* on their surfaces. Superhydrophobic xerogels made of fluorinated silica nanoparticles were reported in the literature.[132] Such surfaces were able to reduce the bacterial adhesion (tests realized with a parallel plate flow cell) of *Staphylococcus aureus* and *Pseudomonas aeruginosa* by 2.08 ± 0.25 log and 1.76 ± 0.12 log in comparison with a "smooth" similar surface. Superhydrophobic surfaces containing nanoparticles of an elastomer silicone (Sylgard 184) obtained by aerosol assisted CVD were also studied. The surfaces were able to reduce the bacterial adhesion of *Escherichia Coli* and methicillin-resistant *Staphylococcus aureus*.[133]
Khine et al. reported the antibacterial properties of superhydrophobic plastics (PS, PC and PE) with wrinkles as surface structures.[134] They reported that these surfaces were able to prevent the growth of *Escherichia Coli*. Moreover, they authors suggested that the self-cleaning of superhydrophobic surfaces with low hysteresis and sliding angles is the key factor to control the anti-bioadhesion properties.
On another hand, the group of Ivanova observed that the bacteria adhesion is highly depending on the nature of the bacteria.[135] They created superhydrophobic (θ_w = 166°) titanium surfaces by femtolaser ablation with low hysteresis (H = 10°) and with a possibility of water droplets to bounce on these surfaces. The authors revealed that *Staphylococcus aureus* was able to colonize these superhydrophobic surfaces with an increase in the number of attached cells in comparison with smooth substrates. However, *Pseudomonas aeruginosa* was not able to colonize these superhydrophobic surfaces. They suggests that one of the main factor may be the shape of the bacteria. Indeed, the spherical shape of *Staphylococcus aureus* may need less contact with the surface to be attached than *Pseudomonas aeruginosa*, which have a rod-like shape.
The surface topography is another parameter studied in the literature. The group of Lin revealed that natural plants of the genus *Nelumbo nucifera* and *Colocasia esculenta* possess both self-cleaning and biofouling properties under submerged conditions.[136] They showed that this resistance is due to the presence of dense nanostructures, which reduce the adhesion force of the plant. Other works on superhydrophobic PP and PS obtained by plasma treatments also showed the importance to have surface structures at the bacteria dimension in order to avoid their trapping.[137,138]

3.4 Textiles

The development of fabrics which repel water but also all kind of organic contaminants is highly in demand. However, for this application, the coating should be mechanical resistant to stresses, such as scratching, abrasion or tensile, as well as support many cycles of laundry. Hence, it is absolutely necessary that the superhydrophobic textiles are robust. The robustness of such materials can be controlled with several parameters.[139-141] For example, the Cassie-Baxter state can be highly stabilized by playing with the spacing ratio (D*), defined as the ratio of the distance between the fibers and the region covered by the fibers, the pressure difference across the liquid–vapor interface or the surface chemistry (Fig. 15). Theoretically, nanometric fibers can lead to extremely stable superhydrophobic properties and can even resist to the impact of rainfall. The formation of nanostructures around the textile fibers often also allows to increase its robustness.

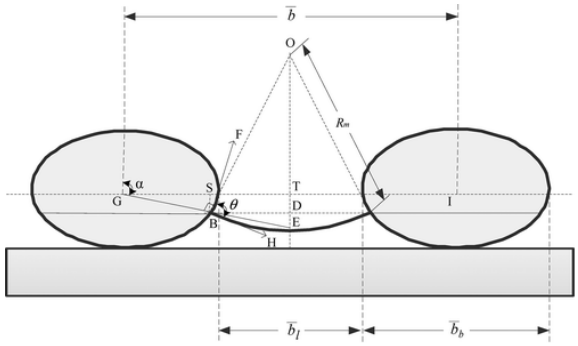

Fig. 15 Schematic representation of the sagging of the liquid–air composite interface on fiber surface in an electrospun nonwoven mat.
Reprinted with permission from ref. 139, copyright 2012, American Chemical Society.

To obtain durable and robust superhydrophobic textiles, it is extremely important to have a resistant interface between the

textile and the coating. To form robust superhydrophobic polyester fabrics, the group of Im reported the possibility to stack polymer film composed of poly(1,3,5,7-tetravinyl-1,3,5,7-tetramethylcyclotetrasiloxane) and poly(1*H*,1*H*,2*H*,2*H*-perfluorodecylacrylate) by initiated chemical vapor deposition (iCVD), a solventless process allowing to form nanostructures.[142] Here, the two polymer layers most likely formed a covalent bonding at their interface. These fabrics were chemically and mechanically stable and also stable after 75 cycles of laundry test. Lin et al. reported the obtaining of robust and durable superhydrophobic fabrics by dip-coating with a solution of perfluorinated SiO_2 nanoparticles and a PDMS elastomer (Sylgard186) to form a composite layer.[143a]

The best strategy to highly enhance the binding of the interface is to graft the coating on the surface of the textile. In the case of cotton textile, hydroxyl groups are already present on the surface. One of most employed strategies is to use silanes to graft hydrophobic materials. Highly durable and robust cotton textiles were reported by grafting diblock copolymers of poly(glycidyl methacrylate) and poly(2,2,2-trifluoroethyl methacrylate).[143b] While the fluorinated segment was necessary to reach superhydrophobic properties, the epoxy groups allowed the grafting of the polymer on the cotton textile. Moreover, the polymer grafting allowed the formation of nanostructures on the textile surface, which is an important parameter to obtain robust textiles. Here, these textiles withstood mechanical abrasion, laundering with strong conditions, UV-light irradiation, ultrasonication in THF and trifluorotoluene and immersions in organic solvents, acid and basic solutions. Nanostructures could also be performed using nanoparticles. SiO_2 nanoparticles were grafted onto cotton fabrics by functionalizing them with azido groups (Fig. 16).[144a] Then, covalent cross-linking was performed under UV-light irradiation.

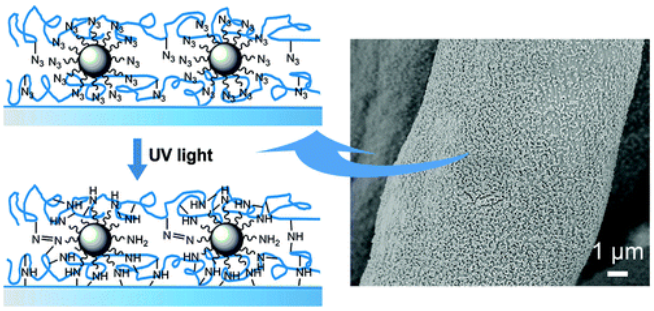

Fig. 16 Grafting of SiO_2 nanoparticles onto cotton fabrics by functionalizing them with azido groups.
Reprinted with permission from ref. 144a, copyright 2012, American Chemical Society.

A fluorinated polyacrylate polymer was also grafted onto the cotton fabric under γ-rays irradiations.[144b] The fabrics were stable against acid and basic solutions and durable for more than 250 launderings. Wool and polyester fabrics were modified with hydrophobic SiO_2 nanoparticles (containing alkyl groups) with the help of triethylamine and ultrasonication to form highly durable and robust textiles.[145a,145b] Robust, self-healing and superoleophobic polyester fabrics were also obtained using SiO_2 nanoparticles functionalized with fluorinated chains following by the reaction with poly(vinylidene fluoride-*co*-hexafluoropropylene) and a fluorinated silane.[149] The as-prepared fabrics were extremely chemically and mechanically resistant and withstand more than 600 cycles of laundry.

Other properties are often required for applications in textile industry. First of all, for anti-soil textiles, it is necessary to induce the repellency of other liquids such as oils. However, due to the much lower surface tension of oils (< 35 mN m^{-1} following the oil used), it is much more difficult to impede their spreading on surfaces.[37,146-149] Indeed, if it was demonstrated that, for example, the formation of micro and nanostructures can allow the obtaining of robust superhydrophobic surfaces, other surface structures are necessary for robust superoleophobicity. Because all materials are intrinsically oleophilic, the surface structures should induce a change from oleophilic to superoleophobic. Surface structures with re-entrant curvatures such as overhang structures, mushroom-like structures or T-like structures were found to be ideal to induce such effect.[37] Indeed, an extremely high pinning effect of the liquid interface on these structures can induce the stabilization of the Cassie-Baxter state even using low surface tension liquids. Fortunately, fibrous structures such as fabric textures can induce such effect but the presence of nanostructures on the fabrics and the surface modification with fluorinated materials is one of the best way to produce stable superoleophobic properties. The stability of the superoleophobic properties is also extremely depending on the geometric parameters on the fabrics such as the fiber diameter the distance between the fibers or the fibers weaving. As shown by the group of McKinley, the maximum pressure that the fabrics can support is highly depending on the surface tension of the liquid and these geometric parameters.[150] They obtained superoleophobic fabrics even against octane and methanol by coating polyester fabrics with fluorodecyl polyhedral oligomeric silsesquioxane (F-POSS) forming nanostructured coating. Similar results were also reported by the group of Lin.[151] They reported the possibility to reach superoleophobic fabrics with UV, acid, mechanical and laundry resistance, in the presence of F-POSS and a fluorinated silane.

Superoleophobic cotton textiles were reported by the group of Ming via a multi-step of grafting process.[152] First, they induced the formation of relatively large SiO_2 nanoparticles (≈ 800 nm) directly grafting on the cotton textile with the Stöber method. Then, the SiO_2 layer was modified to introduce amino groups, which were then protonated into ammonium. In the last step, negatively charged SiO_2 nanoparticles were introduced by layer-by-layer assembly and the surface was modified with a perfluorinated silane resulting in superoleophobic properties. The group of Seeger developed a technique allowing the growing of silicone nanofilaments on the surface of polyester fabrics.[153] A subsequent plasma fluorination led to robust superoleophobic surfaces with resistance to impacts of alkane

drops. Another strategy to obtain superoleophobic properties was to infuse the nanostructures with a lubricant (a perfluoropolyether, for example).[154,155] Here, Aizenberg et al. reported the possibility to reach robust superoleophobic properties to polar and non-polar liquids.

Mesoporous SiO_2 nanoparticles were also used in the literature. The group of Freire showed the possibility to use mesoporous SiO_2 nanoparticles modified with a perfluorinated silane (Fig. 17).[156] Their synthesis by co-condensation in the presence of the textile, hexadecyltrimethylammonium (CTAC) and triethanolamine led to their formation on the surface of the textile. Various morphologies were obtained with different surface area, pore volume with the possibility to obtain superoleophobic surfaces. Finally, Lovingood et al. also reported the possibility to repel chemicals in vapor phase such as chemical weapons (sarin, for example) using SiO_2 nanoparticles and perfluorinated silanes. Such properties are highly important for military applications.[157]

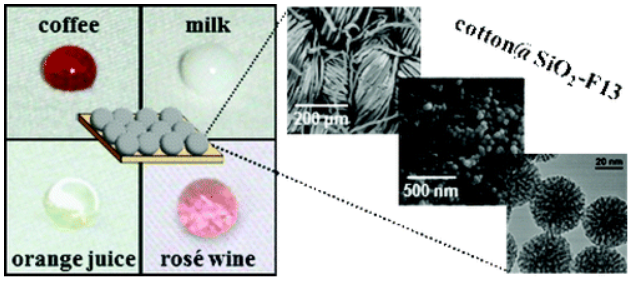

Fig. 17 Superoleophobic textiles modified by mesoporous SiO_2 nanoparticles and a perfluorinated silane.
Reprinted with permission from ref. 156, copyright 2011, American Chemical Society.

The use of metal oxide white pigments such as TiO_2, ZnO, CeO_2 can be introduced for UV blocking. However, the absorption of UV by these materials often also changes their wettability due to the formation of hydroxyl groups on their surface. As a consequence, these pigments should be inserted in nanocomposites or core-shell structures to avoid this effect. ZnO nanorods were used in the literature to coat textiles and obtain superhydrophobic properties.[158,159] Then, a SiO_2 shell was formed around ZnO nanorods. The textiles displayed UV-shielding property and also UV-durability of the superhydrophobic properties. CeO_2 nanoparticles were also used for UV proportion.[160] The surfaces were functionalized with a fluorinated silane to reach also superhydrophobic properties. Benzophenone-type UV organic absorbers were also reported in the literature. The group of Lin intercalated 4-methoxybenzophenone-5-sulfonic acid inside the structure of a layered double hydroxide and structured the surface of cotton textile with nanoplatelets.[161] The textiles exhibited both superhydrophobicity and high increase of UV protection.

Another properties reported in the literature is the improvement of the flame retardancy properties. Commercially, especially two kinds of treatments are known to enhance the flame retardancy of cotton: the use of tetrakis(hydroxymethyl)-phosphonium chloride and the use of *N*-methylol functional phosphorous esters. Another way to impart such properties without using toxic chemicals if to form a nanocoating. Mohamed et al. reported the grafting of coating to introduce epoxy groups, which were then used to graft amino-modified ZnO nanoparticles.[162] The as-prepared cotton displayed both superhydrophobicity and flame retardancy. The group of Wang also reported the modification of cotton textiles with epoxy groups and the grafting of amino-functionalized SiO_2 nanoparticles to reach superhydrophobicity and flame retardancy.[163]

3.5 Oil/water separation

The water decontamination of organic compounds such as petroleum and other oils has become a serious threat to biological and human safety. As present, the methods used to separate oils from water often present low separation efficiency and involve complex separation instruments. Here, using meshes, membranes, textiles, foams or sorbents, the possibility to render all these materials superhydrophobic has opened a very interesting way to separate oils from water with high efficiency. Three different properties are used in the literature: both superhydrophobic and superoleophilic properties, both superhydrophilic and underwater superoleophobic properties, or both superhydrophilic and superoleophobic properties.

3.5.1 Superhydrophobic/superoleophilic materials

To obtain superhydrophobic and superoleophilic membranes, the best strategies is to use meshes as substrates and to form nanostructures around the meshes wires. Indeed, to obtain superhydrophobic and superoleophilic membranes it is necessary that the meshes stabilize the Cassie-Baxter with water but not with oils. Here, hydrocarbon derivatives were very often used to reach superhydrophobic and superoleophilic properties.

The group of Jiang showed that the form of the meniscus of the liquid between the mesh wires is very important to predict the superhydrophobic and superoleophilic properties (Fig. 18).[164,165] Indeed, the liquid will not penetrate the mesh if its hydrostatic pressure $\Delta P = 2\gamma_{LV}/R = -l\gamma_{LV}\cos(\theta_A)/A$ with γ_{LV} the liquid surface tension, R the radius of the meniscus, A the cross-sectional area of the pore and θ_A the advancing contact angle of the liquid. When $\theta > 90°$, the liquid will not penetrate due to a negative capillary effect ($\Delta P > 0$) and reversely. Hence, the permeation is highly depending on the liquid surface tension but also the mesh opening.

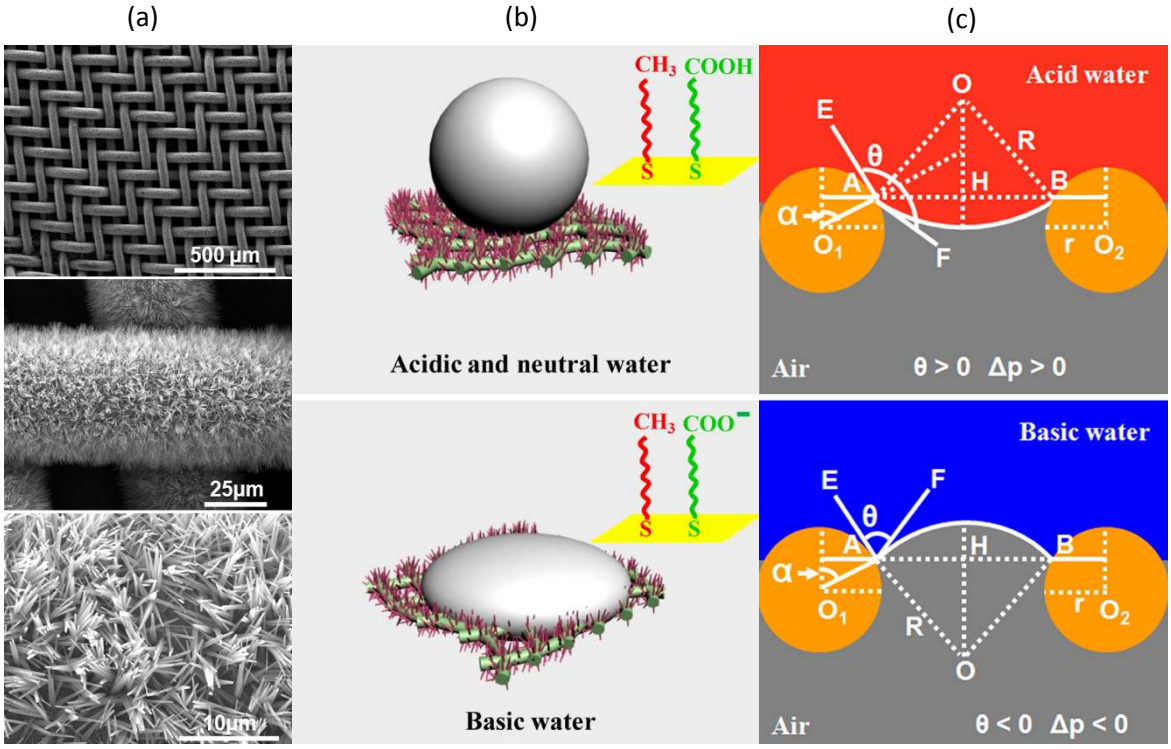

Fig. 19 (a) SEM images of $Cu(OH)_2$ nanoneedles on meshes. (b) Schematic representation of a water droplet and (c) liquid wetting model after modification with a 11-mercaptoundecanoic acid and 1-dodecanethiol mixture in acidic/neutral and basic media.
Reprinted with permission from ref. 169, copyright 2012, American Chemical Society.

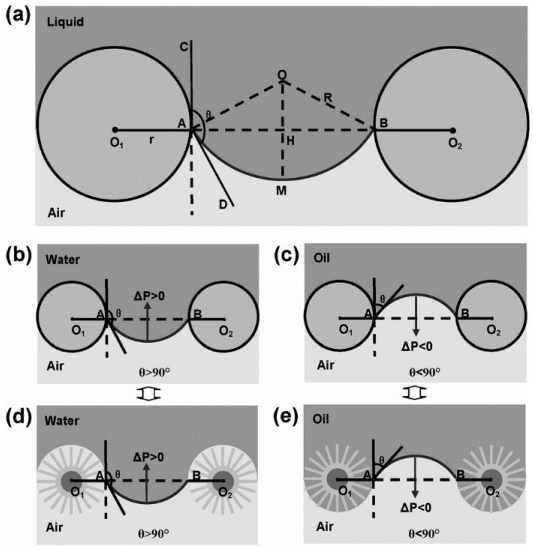

Fig. 18 Liquid wetting model of nanostructured meshes as a function of the hydrostatic pressure (ΔP).[164]

3.5.1.1 Meshes

Meshes could be etched to induce the formation of structures around the meshes. Copper meshes (opening: 44-490 µm) were etched in nitric acid to increase the roughness of the wires.[166] After modification with 1-hexadecanethiol, the meshes were superhydrophobic and superoleophilic whatever the mesh opening. Copper meshes were also etched in alkaline media (NaOH + $K_2S_2O_8$ or anodization) to form $Cu(OH)_2$ nanoneedles around the mesh wires and modified with 1-dodecanethiol to form superhydrophobic and superoleophilic properties.[167,168] The authors reported a higher separation efficiency for the mesh with a short opening (< 600 µm).[167] By surface modification with 11-mercaptoundecanoic acid and 1-dodecanethiol mixture, it was possible to obtain pH-responsive materials (Fig. 19).[169] Indeed, in acid or neutral media, the mesh was superhydrophobic due to the presence of carboxylic acid groups and dodecane chains but in alkaline media, the change of the carboxylic groups into more polar carboxylate ones induced a switch from superhydrophobic to superhydrophilic. Cu_2O cauliflower-like structures were also electrodeposited on stainless steel (opening: 75 µm) meshes at constant potential (3 V) in aqueous solution containing $CuSO_4$, lactic acid and NaOH.[170,171] Superhydrophobic surfaces were obtained from 20 min of deposition. These substrates could separate different kinds of oils from water with separation efficiency above 90%. Cu nanoparticles were also electrodeposited in $CuSO_4$, containing H_2SO_4 and at constant current (0.1 A). Superhydrophobic and superoleophilic meshes were obtained from a deposition time of 240 s after surface modification with 1-octadecylthiol. These meshes could separate chloroform/water mixture with high efficiency.

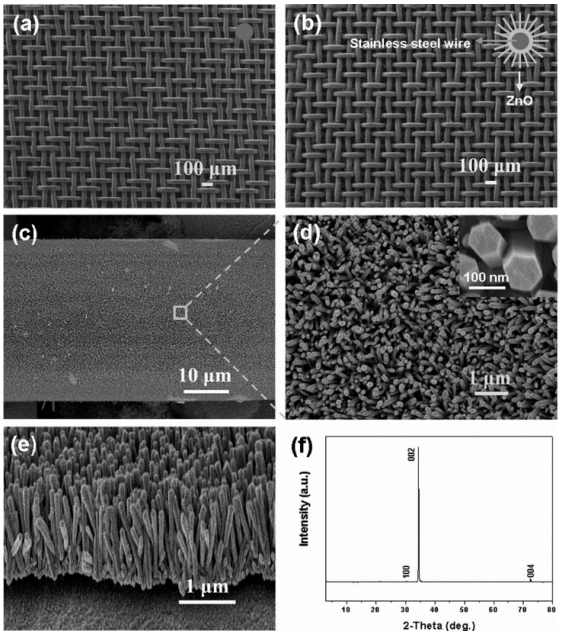

Fig. 20 Aligned ZnO nanorod array-coated stainless steel mesh film obtained by dip-coating of ZnO sol and immersion in $Zn(NO_3)_2.6H_2O$.[164]

Other metal oxide and inorganic nanostructures were also used in the literature. Vertically aligned ZnO nanorods were coated on stainless steel meshes by CVD or in a two-step process including dip-coating of ZnO sol and immersion in $Zn(NO_3)_2.6H_2O$ and methenamine (Fig. 20).[164] The best superhydrophobic surfaces were obtained for an opening of 50-75 µm following the experimental conditions reported of the literature. Another interest to use ZnO is the possibility to have UV-switchable materials (Fig. 21).[172-176] It was showed that meshes with aligned ZnO nanorods could be water-permeable after UV light irradiation due to the formation of hydroxyl groups and become impermeable to water after dark storage. Other strategies were used in the literature to control the growth of other nanostructures. ZnO flower-like structures were formed by spraying ZnO seeds using a zinc acetate solution and growth in Zn acetate solution at pH 10.[177] Using this strategy, oil-water separation meshes were obtaining after coating by PTFE and for an opening of 25-250 µm. ZnO nanoflakes were also formed by depositing an aluminum layer on stainless steel (opening: 75 µm) and immersion in $Zn(NO_3)_2.6H_2O$ and hexamethylenetetramine.[178] After modification with stearic acid, oil-water separation meshes were obtaining with an efficiency of 95%.

TiO_2 nanoparticles were also coated on copper mesh by immersion in $TiCl_3$/NaCl and heating.[179] Surface modification with octadecylphosphonic acid led to oil-water separation meshes with UV-light switchable wettability from superhydrophobicity to superhydrophilicity. Moreover, the photocatalytic effect of TiO_2 could lead to promising effects on water purification. SiO_2 particles were also deposited using the sol-gel process to form superhydrophobic and superoleophilic meshes.[180,181] These properties were depending on the size of the particles, concentration of the chemicals and surface modification. Finally, vertically aligned carbon nanotubes as well as nanocrystalline diamond were also produced on meshes by thermal CVD to separate oil/water mixture.[182,184] In the case of the nanocrystalline diamond, the mesh wettability was also switchable from superhydrophobic to superhydrophilic by hydrogen and oxygen plasma.[184]

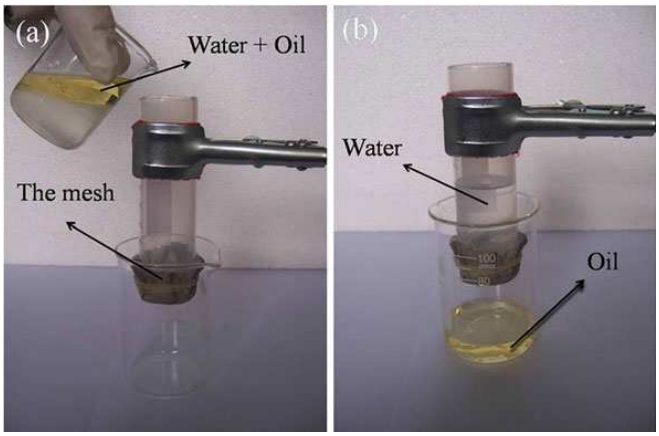

Fig. 21 Experimental process of separation oil and water.[172]

Polymers and polymer composites could also be used to form nanostructures on meshes using different strategies. Copper meshes were coated (opening: 152-297 µm) with rough silicone elastomer (Sylgard 184).[185] The highest separation efficiency (> 99%) with toluene, petroleum ether and hexane were obtained with an opening of 297 µm. PS nanofibers were also electrospun on stainless steel meshes to deposit horizontal nanofibers of about 317 nm average diameter.[186] These meshes easily separated diesel oil from water with excellent efficiency. Conducting polymers were also reported in the literature to modify meshes. For example, polypyrrole micropapilla and polyaniline nanofibers were deposited by electropolymerization and chemical polymerization.[187]

3.5.1.2 Textiles

Textiles were also employed for oil/water separation. The principle is exactly the same than with meshes. Cotton textiles were used by several groups. The group of Guo showed the possibility to induce the growth of metal or metal oxide nanostructures of Fe, Co, Ni, Cu and Ag on textiles.[188] Further modification with perfluroodecanethiol led to superhydrophobic and superoleophilic properties with the possibility to separate oil and water. Wang et al. pre-treated cotton textiles to form hydroxyl groups at the surface of the fibers and the textiles were then coated with SiO_2 nanoparticles and finally modified with octadecyltrichlorosilane.[189] The as-prepared cotton could absorb various oils and organic solvents up to fifty times of its own weight while repelling water completely.

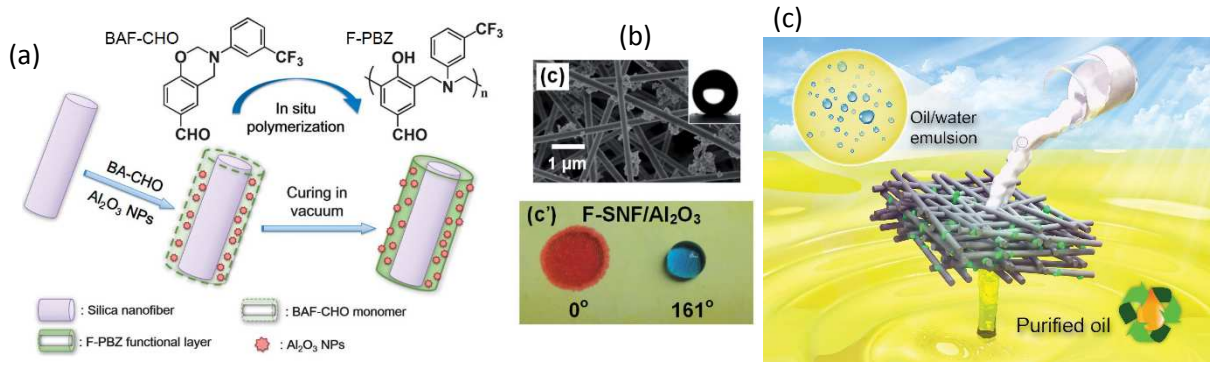

Fig. 22 (a) (b) Silica nanofibrous membranes obtained by modification with Al_2O_3 nanoparticles and a fluorinated monomer derived from benzoxazine and *in situ* polymerization at 200°C; (c) Schematic representation of oil/water separation experiment.[197]

To produce superhydrophobic and superoleophilic cotton in one step, SiO_2/polystyrene as well as ZnO/polystyrene nanocomposites were also used.[190] TiO_2-SiO_2/PDMS were also deposited in the literature.[191] These materials combined an extreme thermal stability (up to 400°C), chemical resistance, photocatalytic properties of TiO_2 with the possibility to clean water, wettability switching from superhydrophobicity to superhydrophilicity by calcination, and oil/water separation. Cotton textiles were also coating with polyaniline and a perfluorinated silane by vapor phase polymerization in the presence of $FeCl_3$ as oxidizing agent.[192] Using this process, nanogranules were deposited on the surface of the textile. These materials displayed oil/water separation with an efficiency of 97.8%. Plastic textiles were used modified in the literature. PET textiles were hydrolyzed on their surface with NaOH to produce hydroxyl and carboxylic groups to graft SiO_2 nanoparticles.[193] The rough PET textiles were able to separate oil/water mixtures.

3.5.1.3 Foams

Some examples of foams were also reported in the literature to reach oil/water separation applications. Ni foams were modified with candle soot nanocoating following by a silicone elastomer (Sylgard 184) to enhance the binding degree of the candle soot.[194] The as-prepared materials were efficient for oil/water separation. Ultralight Fe_2O_3/C, Co/C and Ni/C foams were also prepared by grafting polyurethane foams with poly(acrylic acid) through cerium (IV)-ammonium nitrate (CAN)-catalyzed polymerization, ion exchange with Fe^{3+}, Ni^{2+} or Co^{2+} following by calcination.[195] After coating with PDMS, the foams could be used for oil/water separation with the ability to absorb oil of 100 times of its own weight.

3.5.1.4 Synthetic membranes

Finally, several research groups also fabricated membranes for oil/water separation. PVDF membranes composed of spherical particles were prepared by a phase-inversion process.[196] The membranes could separate with an efficiency higher than 99.95% water-in-oils emulsions such as surfactant-free and surfactant-stabilized emulsions (droplet sizes from micrometer to nanometer range) with high flux. Otherwise, the electrospinning technique was also used to elaborate porous membranes made of nanofibers.[197-199] Silica nanofibrous membranes were fabricated first by calcination of electrospun tetraethylorthosilicate/poly(vinyl alcohol) composite nanofibers (Fig. 22).[197] Further modification with Al_2O_3 nanoparticles and a fluorinated monomer derived from benzoxazine and *in situ* polymerization at 200°C led to the membrane. The membrane could separate water-in-oil microemulsions with high efficiency and with an extremely high flux. Similar results were also reported with electrospun poly(*m*-phenyleneisophtalamide) and SiO_2 nanoparticles.[198]

3.5.1.5 Sorbents

Sorbents can also be used to clean-up water from oils. Common absorbents include activated carbon, zeolites, natural fibers but suffer from low separation selectivity and low absorption capacity.[200] Hence, the strategy was to elaborate superhydrophobic and superoleophilic sorbents such as sponges or aerogels. Wang et al. elaborated oil-absorbent by incorporation of SiO_2 nanoparticles onto natural kapok fibers and surface modification with an alkylsilane.[201] For example, the as-prepared materials displayed an improvement of the oil sorption capacity of 46.6% and 20.2% for diesel oil and soybean oil. Leung et al also used natural cotton fibers to form hollow carbon fibers after carbonization.[202] The enhancement of the oil sorption capacity was of 27-126%. Carbon aerogels as well as sponges were also used in the literature. Yu et al. developed carbon nanofiber aerogels from a template-directed hydrothermal carbonization using glucose as precursor.[203] The carbon aerogels displayed high sorption capacity, high selectivity but especially can maintain their properties over a wide temperature range (≈ -200°C–400°C).

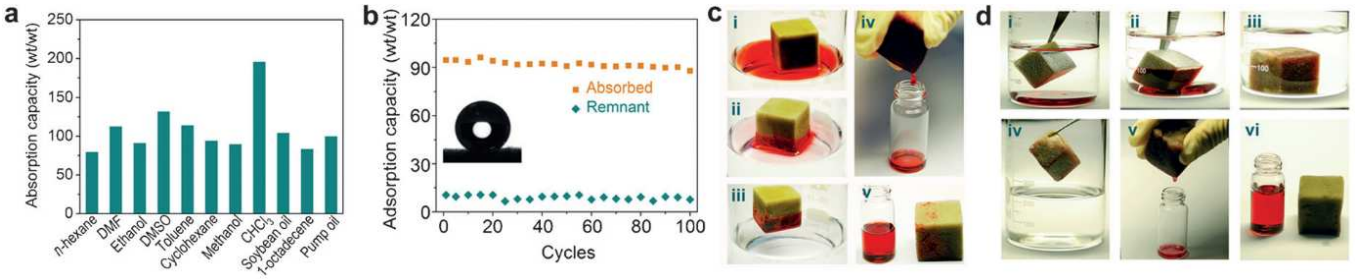

Fig. 23 Superhydrophobic sponge with absorbency and flame retardancy obtained by modifying melamine-formaldehyde sponges with polydopamine layer and a perfluorinated thiol.
Reprinted with permission from ref. 210, copyright 2014, Wiley-VCH.

The group of Qiu reported the properties of multiwall carbon nanotube-graphene hybrid aerogels by functionalization of graphene aerogel with ferrocene and its decomposition into iron particles and cyclopentadienyl, which acted as catalyst and carbon source for the growth of carbon nanotubes.[204] The as-prepared materials displayed rapid oil sorption, large sorption capacity, good recyclability and high compressibility. It was also interesting to develop sponges for their high elasticity and desorption easiness.[205-210] Pan et al. developed robust and easily reusable (> 300 cycles) polyurethane sponges with high oil absorption capacity by surface modification with methyltrichlorosilane. The group of Lu also reported the obtaining of superhydrophobic sponge with excellent absorbency and flame retardancy by modifying a melamine-formaldehyde sponge with polydopamine layer and a perfluorinated thiol (Fig. 23).[210] The flame retardancy properties of these material are due to the high nitrogen content, which releases N_2 after burning and decreases the surrounding O_2.

3.5.2 Superhydrophilic/underwater superoleophobic materials

Because oils droplets are often stabilized in and aqueous media, another strategy to obtain oil/water separation membrane is to use superhydrophilic and underwater superoleophobic properties. Underwater superoleophobicity is the resistance of a surface to the wetting of oils when the surface is immerged in water: solid/liquid(water)/liquid(oil) interface.[211]
Here, hydrophilic derivatives are very often used to reach superhydrophilic and underwater superoleophobic properties. Cu meshes were modified by electrodeposited Cu nanoparticles as well as by formation $Cu(OH)_2$ nanoneedles.[212] After surface modification with 11-mercaptoundecanoic, the meshes displayed pH-switchable underwater superoleophobicity: underwater superoleophilic in acidic and neutral media and underwater superoleophobic in alkaline media. Aligned ZnO nanorods were also found to be suitable for underwater superoleophobicity and oil/water separation (opening: 75 μm).[213] The surface wettability of these materials could be switched by UV-light irradiation. To form materials with controllable porosity, zeolite silicate-1 crystals were used to cover meshes.[214-215] These superhydrophilic and underwater superoleophobic materials showed excellent efficiency for oil/water separation. Moreover, it was possible to tune the flux and intrusion pressure by changing the growth time.
Hydrophilic polymers such as polyacrylic acid, polyacrylamide and polyacrylamide-co-poly(acrylic acid) hydrogels were reported in the literature to reach superhydrophilic and underwater superoleophobic materials.[216,222] Polydopamine was also used to immobilize nanoparticles, as observed in marine mussels, with a tuning of the adhesion by changing the pH or adding 1-dodecanethiol (Fig. 24).[219,220] One of the advantages to use polymer is also the possibility to functionalize by various groups. Hence, sensitive groups could be introduced to obtain "smart" materials with switchable wettability. Thermo and pH dual-responsive meshes were elaborated by coating with poly(dimethylaminoethyl methacrylate) hydrogels.[221] While the amino groups allowed to switch the wettability by varying the pH, the change in the tacticity of the polymer was possible by changing the temperature (T). Here, water could pass through the mesh when T < 55°C and pH < 13.

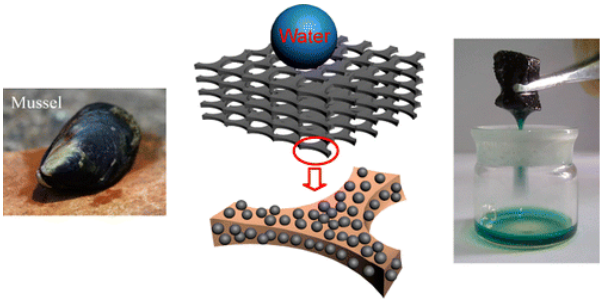

Fig. 24 Immobilization of Fe_3O_4 nanoparticles onto polyurethane foams and application for oil–water separation.
Reprinted with permission from ref. 219, copyright 2014, American Chemical Society.

Other research groups also used nanoparticles to reach superhydrophilic and underwater superoleophobic meshes.[222] pH-switchable textiles and polyurethane sponges were also reported by deposing SiO_2 nanoparticles, silanization to introduce bromide groups and grafting poly(2-vinylpyridine)-*b*-PDMS. In acidic media, the pyridine moiety was protonated and the material was superhydrophilic and underwater superoleophobic while for pH ≥ 6.5 the pyridine moiety was deprotonated and the material was superhydrophobic and

underwater superoleophilic. Moreover, the flexibility of the PDMS block facilitated the reversible switching of the oil wettability.

3.5.3 Superhydrophilic and superoleophobic materials

Because the surface tension of oils is lower than that of water, almost all the superoleophobic surfaces reported in the literature are also superhydrophobic.[37,223-227] As a consequence the elaboration of materials with higher oleophobicity than hydrophobicity, when the media is the air, is extremely rare. In all these examples, it was found the importance to use a material with both a hydrophilic moiety and an oleophobic one to induce this property.[228-231] Zhou et al. reported, to our knowledge, the unique example of superhydrophilic and superoleophobic coatings (Fig. 25).[232] They produced superhydrophilic and superoleophobic meshes by coating with poly(diallyldimethylamonium perfluorooctanoate). The resulting rough meshes were able to separation oil/water mixtures (tests done with hexadecane, vegetable oil, gasoline and diesel).

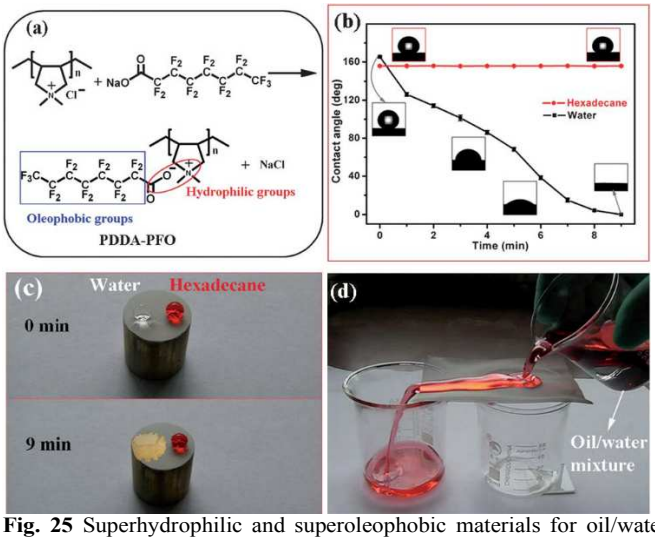

Fig. 25 Superhydrophilic and superoleophobic materials for oil/water separation by coating of poly(diallyldimethylamonium perfluorooctanoate).[232]

3.6 Membrane distillation and water desalination

The desalination of seawater is a worldwide concern especially in countries where drinkable water is little available. Different strategies are used in the industry for water desalination, such as reverse osmosis, multi-stage flash distillation or the use of membrane distillation. In the last case, a hot feed steam containing non-volatile species has to pass across a hydrophobic membrane. On the other side of the membrane, a cooling stream creates a vapor difference. Then, The feed liquid evaporates and passes through the pores of the membrane. This method is often limited by low mass-flux across the membrane and fouling issues, which are both depending the microstructures and materials of the membranes including the ratio of the pore diameter, porosity and vapor pressure difference. If microporous membranes are made superhydrophobic, the allowable pore sizes can be larger, which can increase the mass flux. Hence, it is necessary to have both superhydrophobic properties but with vapor permeability. This dual functionality was reported in several publications. Glass membranes with ordered arrays of nanospiked microchannels were fabricated by glass fiber drawing, template dissolving and chemical etching (Fig. 26).[233] These membranes had higher antifouling capacity and high flux than existing polymer membranes especially at high salt concentration.

Superhydrophobic and superoleophobic polyurethane membranes with gas permeability were reported. Nanofibrous membranes were elaborated by electrospinning of polyurethane containing fluorinated segments (Fig. 27).[234] The membranes showed high water resistance (39.3 kPa), good air permeability (8.46 L m^{-2} s^{-1}) and water vapor transmittance (0.384 kg m^{-2} h^{-1}). SiO_2 nanoparticles could also be incorporated inside the membranes to enhance the roughness of the fibers.[235] Stretchable polyurethane with gas permeability were also performed by electrospinning of an elastomer polyurethane following by the surface modification with polyaniline nanofibers and PTFE.[236] Superhydrophobic PS nanofibrous membranes with micro- and nanoscale hierarchical structures were also obtained by electrospinning.[237] The membranes allowed to maintain a high and stable permeable water vapor flux.

Superhydrophobic aligned multiwalled carbon nanotubes (MWNTs) were reported by thermal CVD followed by the deposition of a PDMS layer.[238] Here, the interstitial space of nanotubes allowed high gas permeability with even a selectivity as high as 2.10^5 for H_2/H_2O. The use of carbon nanotubes for water desalination was also reported in other works.[239]

PDVF membranes were highly used in the literature for water desalination for their high chemical stability.[240-246] PVDF membranes were modified by CF_4 plasma.[241] The authors observed an increase in the water flux of about 30%. Li et al. also studied the effect of the modification of PVDF membranes by spraying a solution containing SiO_2 nanoparticles and PDMS.[242] These membranes showed NaCl rejection of above 99.99% with an excellent anti-fouling property. PVDF membranes were also modified with TiO_2 nanoparticles and a fluorinated silane.[243,244] The authors showed that the use of a templating agent such as polyethylene glycol results in porous, multi-level microstructures with improved salt rejection and desalination performance. PVDF membranes were also modified with poly(vinyl acetate) or PDMS functionalized carbon nanotubes for water desalination.[245,246]

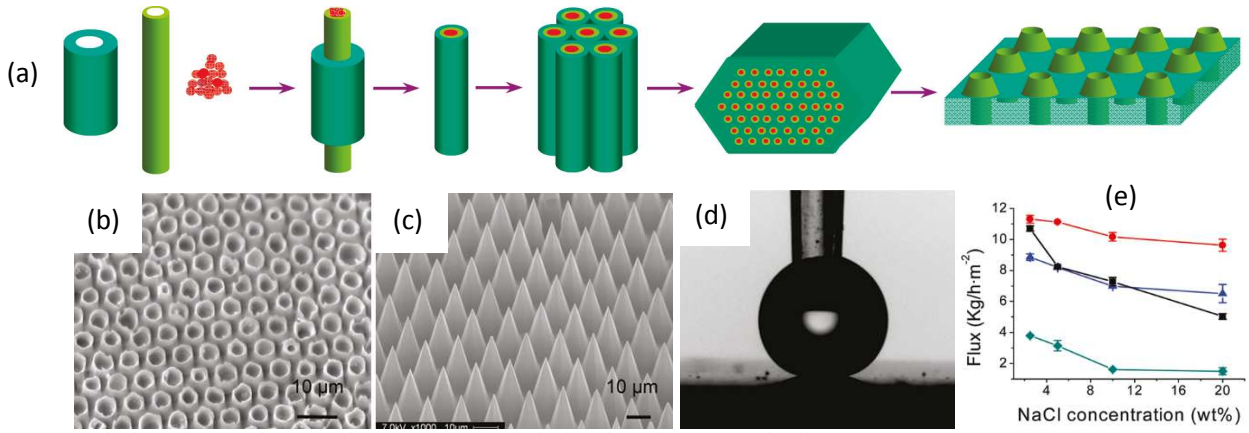

Fig. 26 Superhydrophobic membranes with arrays of nanospiked microchannels for water desalination. Reprinted with permission from ref. 233, copyright 2009, American Chemical Society.

.

3.7 Water purification

When superhydrophobic materials are made from semiconductors or TiO_2 they can also have intrinsic photocatalytic properties due to the formation of superoxides under light-irradiation. Such properties can reduce the bacterial adhesion, induce anti-misting properties, increase the self-cleaning properties or purify soiled water.[247-253] Superhydrophobic materials composed of Ag_2Se complex nanostructures were reported.[249] The authors observed an excellent degradation of rhodamine B (RhB) dye (89.8% after 15 hr) under UV-light irradiation. The group of Cao also reported the photocatalytic activity of $In(OH)_3$ nanocubes synthesized with an amino-assisted hydrothermal process (Fig. 28).[250] The surfaces displayed superhydrophobic properties with extremely low α and photocatalytic effect on the degradation of RhB (93.25% after 16 hr). Superhydrophobic surfaces with photocatalytic properties were also obtained with Ag-NPs@ZnO-nanorods.[251] After exposure to visible or UV-light, the surfaces changed from superhydrophobic to superhydrophilic due to the formation of hydroxyl groups. To overcome the problem of the change on the wettability after light exposure, the photocatalytic materials could be incorporated as nanoparticles in a polymer matrix.[252-254] The group of Parkin elaborated superhydrophobic surfaces incorporating TiO_2 nanoparticles into PDMS via an aerosol-assisted CVD.[252] The polymer remained superhydrophobic even after UV-exposure. The materials displayed photocatalytic effect with a discoloration of resazurin dye after 90 min under UV-light irradiation. Yamashita et al. also reported the photocatalytic properties of a composite made of TiO_2 nanoparticles and PTFE by radio frequency-magnetron sputtering deposition.[253] The surfaces was superhydrophobic and composed of nanofibers. The photocatalytic effect was confirmed with the discoloration of methylene blue under UV-light irradiation. The surfaces also displayed photocatalytic self-cleaning properties (test realized with oleic acid).

3.8 Microfluidic devices

Controlling the transport and manipulation of liquid is very important for microfluidics devices. Many researches were reported on the enhancement of transport properties, which are very important for the manipulation of liquids in microfluidic devices.

Many works were dedicated to the reduction of the drag of a flux on a surface, a pipeline or a channel, which impacts on the necessary energy and the flux rate. This drag is due to the shear stress induced by the flux on the surface. In the nature, the shark skin was found to have low drag properties while rice leaves (*Oryza sativa*) and butterfly wings (*Blue Morpho didius*) combine both low drag properties (anisotropic flow) and self-cleaning properties (Fig. 29).[255-257] The surface of the rice leaves is composed of micropapillae superimposed by epicuticular waxy nanobumps and that of butterfly wings of hierarchical scales with microgrooves. Replicas of these natural surfaces were realized in order to evaluate the effect of superhydrophilicity/phobicity and superoleophilicity/phobicity on the drag reduction with various fluids (water, oil, air) in laminar and turbulent flows. In the case of oil flux, superoleophilic and superoleophobic surfaces could reduce the drag. The air drag could be reduced by increasing the smoothness of the surface structures. The highest drag reduction was observed in turbulent water flow with the rice leaf and shark skin replicas. Hence, these natural surfaces could provide new ideas to reduce the drag and the surface topography seems to be essential to control these properties.

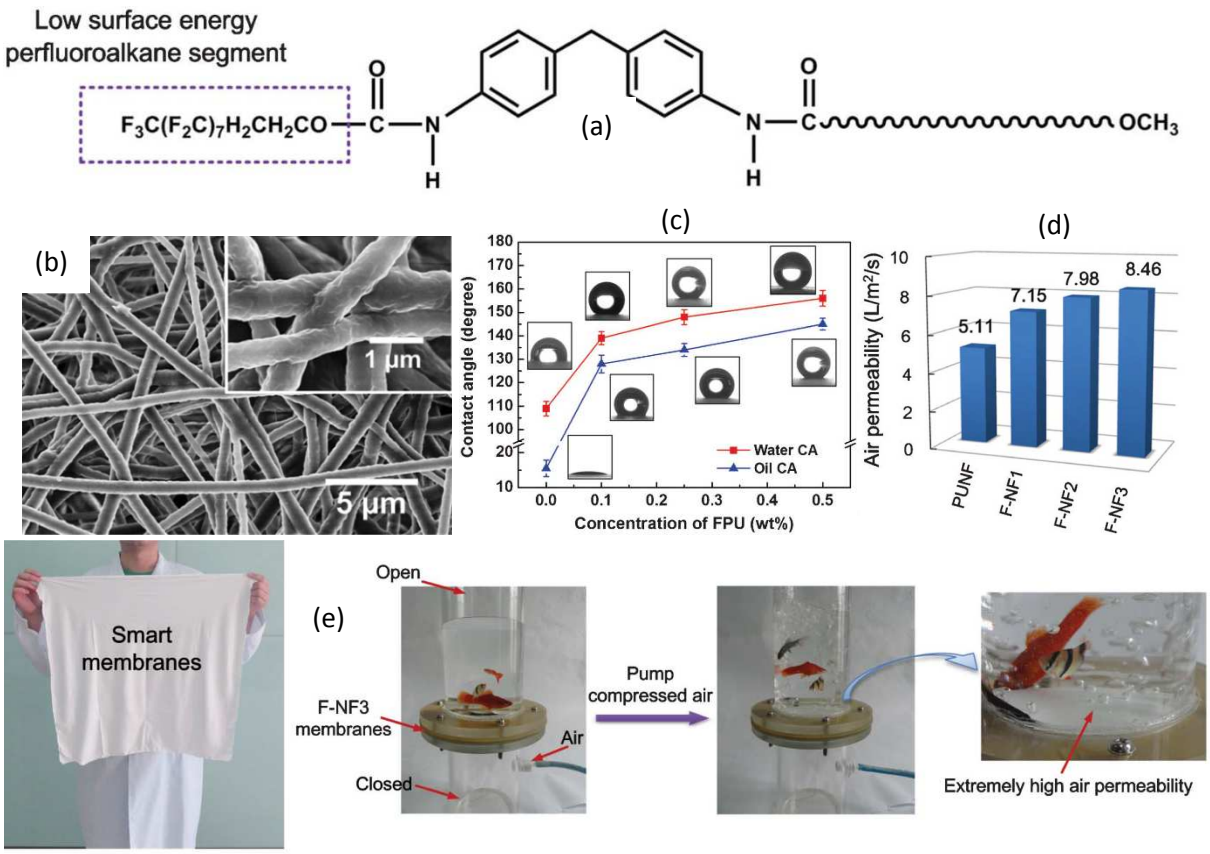

Fig. 27 (a) Fluorinated polyurethane segments to produce (b) (b) superoleophobic nanofibrous membranes with (d) (e) high air permeability.[234]

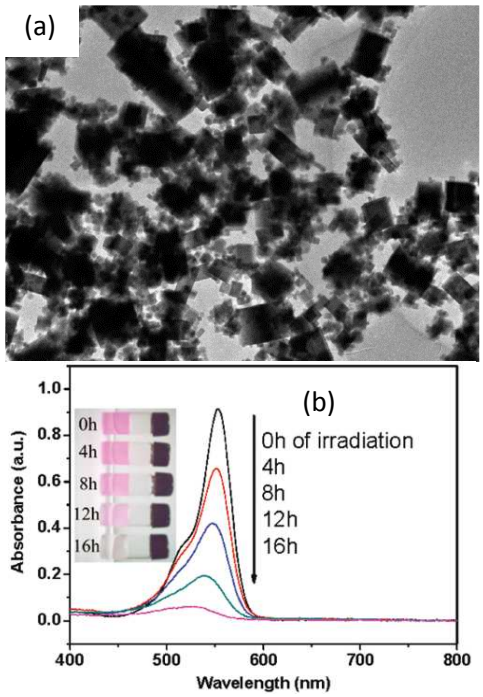

Fig. 28 (a) TEM images of $In(OH)_3$ nanocubes with photocatalytic effect on the (b) degradation of rhodamine B (RhB) dye.
Reprinted with permission from ref. 250, copyright 2010, American Chemical Society.

First of all, it was found that the air trapped inside superhydrophobic surfaces with self-cleaning (Cassie-Baxter state) is responsible for the reduction of the drag.[258-262] Indeed, works on the immersion of superhydrophobic materials in water demonstrated that the main parameter to reduce the drag is if the superhydrophobic materials are able to keep an air layer, also called plastron, when immersed into water.[259] This ability is obviously depending on the surface topography. Lu et al. also experimented in determining the speed of superhydrophobic and superhydrophilic hollow glass balls on water.[260] They found that, the movement of superhydrophobic ball is faster than that of superhydrophilic one because the presence of air in superhydrophobic surfaces provides extra supporting force.

In the case of a water flux, the change of the surface hydrophobicity from hydrophilic to hydrophobic can induce the slipping of the liquid flowing, which can be highly amplified by the air trapped on rough superhydrophobic surfaces. The group of Rothstein fabricated micropatterned superhydrophobic surfaces consisting in regular parallel grooves in the flow direction and studied the effect of the topography.[268] They observed the possibility to reduce the drag of about 50% with structures 60 μm wide and spaced 60 μm apart, if the number of Reynolds (Re) is important (Re > 2500).

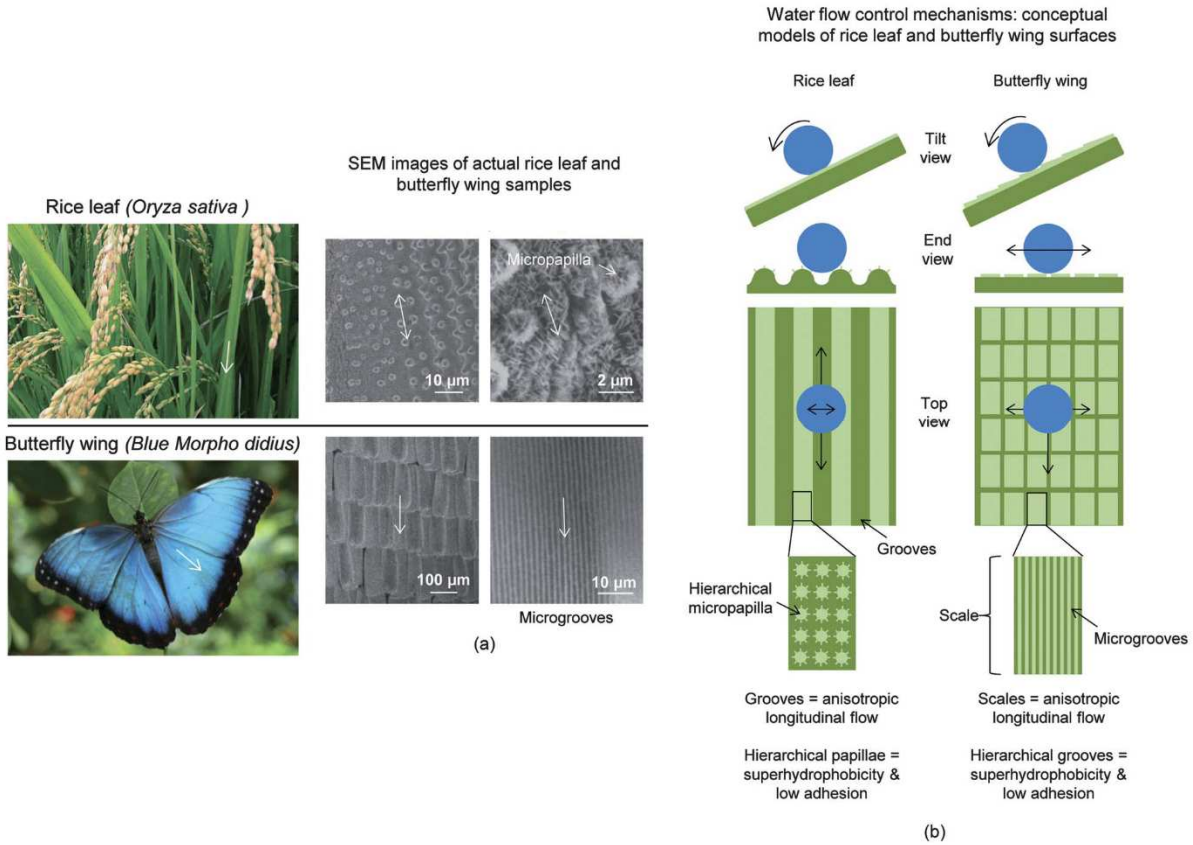

Fig. 29 Rice leaves (*Oryza sativa*) and butterfly wings (*Blue Morpho didius*) with low drag (anisotropic flow) and self-cleaning properties due to the presence of grooves and scales, respectively.[255]

The reduction is due to the presence of a shear-free air-water interface.[268-272] Moreover, the presence of these parallel structures induced the formation of an anisotropic flux.[273-275]

Teo et al. also studied the influence of the pattern (longitudinal grooves, transverse grooves, square holes and square posts) as a function of Re and on the drag reduction.[276] They showed that when Re is low, square posts are the most effective structures while longitudinal grooves are the best at high Re. The group of Gad-el-Hak also demonstrated that high drag reduction can also be obtained on superhydrophobic surfaces with randomly distributed roughness, if the air fraction is high and that the air-water interface is stable (the stability is depending on the average spacing between the roughness).[277] The group of Yoon elaborated superhydrophobic surface with micro and nanostructures by anodization of aluminum plate following by the treatment with a fluorinated silane.[278] They revealed a considerable drag reduction for Re < 200000, with an increase of the drag reduction as the Re decreases.

Ming et al. studied the fluid drag reduction of superhydrophobic surfaces composed of carbon nanotube forests obtained by CVD.[279] They determined the effect of the superhydrophobic properties by measurements of apparent viscosity to calculate the slip length. They observed that this slip length can reach 10 µm. Hence, by coating a microchannel of 90 µm with these carbon nanotubes, it was possible to reduce the drag by about 10%. To obtain mechanically durable structures with low drag, carbon nanotube/epoxy composites were also sprayed on micro-patterned surfaces.[280]

Superhydrophobic PMMA micro-channels were also fabricated by O_2 plasma etching and using a photosensitive PDMS as a resist.[281] The authors measured the electroosmotic flow induced by voltage between the anode and the cathode. In comparison with hydrophilic and non-treated PMMA channels, the superhydrophobic treatment induced an increase in the electroosmotic velocity.

In droplet-based, also called digital, microfluidic devices, reactant solutions are confined in discrete droplets, which can be moved, mixed and analyzed on the surface of a chip. In most of the techniques, the moving of droplets is possible through closed channels or using actuation method such as electrowetting on dielectric (EWOD), dielectrophoresis using electrode arrays, among others.[282-299] Based on these considerations, microfluidics systems were elaborated using superhydrophobic micro-channels. First of all, when a micro-droplet enters into a superhydrophobic microchannel, a high capillarity force can be induced on the droplet due to Laplace pressure difference. Tolonen et al. studied EWOD technique with superhydrophobic surfaces obtained by crystallization of alkylketene dimer (AKD).[300] In this system based on electrowetting, two electrodes are necessary to move of

droplets: a working electrode covered by dielectric materials and the superhydrophobic coating, and a counter-electrode also coated by the superhydrophobic coating. The applying of a voltage induces a decrease in the contact angle of the droplet in contact to the working electrode but not in that in contact to the counter-electrode. As a consequence, a difference pressure is induced on the droplet, which leads to its moving. Here, the authors succeeded in the stepwise moving of water droplets by switching the electrode voltage. The advantages to use superhydrophobic coatings in EWOD are various such lower applied voltage, higher average speed, greater motion and deformation of the droplet or more important contact angle variation.[293-299] Indeed, the electrowetting of superhydrophobic surfaces can induce a Cassie-Baxter-to-Wenzel transition.

As example of application, Di Fabrizo et al. reported the possibility to study the biomineralization of $CaCO_3$ by *in situ* SAXS/WAXS by coalescence of a droplet containing $CaCl_2$ with another droplet containing Na_2CO_3 in a EWOD device.[301] The group of Boukherroub also succeeded in the realization of reversible electrowetting on superhydrophobic surfaces by deposition of silicon nanowires and coating with a fluorinated polymer.[302-306] They could use these superhydrophobic materials in EWOD for matrix-free mass-spectrometry analyses (DIOS analysis). By applying voltage with very narrow frequencies, it was also possible to induce the jumping of the droplet in EWOD.[307-308] Carbon nanofiber superhydrophobic surfaces were also reported in the literature to obtain reversible electrowetting.[309]

Manipulation of water droplets could be realized in the literature by introducing paramagnetic carbonyl-iron microparticles inside the droplets.[310] Here, the moving of droplets was possible by applying a magnetic field. Kaler et al. also used liquid dielectrophoresis liquid actuation to move droplets.[311] This method uses passivized metallic electrodes in order to induce a spatially non-uniform electric field. The group of Sikorski proposed a digital microfluidic chip based with inlets, outlets, sample storage and mixing areas using wire guidance to move the droplets.[312] This technique is based on the realization of arrays of superhydrophobic dimples. Here, the modification with superhydrophobic CuO nanowire only in the dimples was performed with a mask and by electrodeposition and subsequent modification with a perfluorinated thiol. In this technique, the guidance is based on direct contact between the droplet and the rod: if the adhesion between the droplet and the rod is larger than that between the droplet and the surface, the droplet follows the rod, and reversely.

EWOD is a technique also used in biotechnology to displace biological liquids. The advantages are for example the reduction of consumption of expensive reagents and the high surface-to-volume ratio.[313-317] However, due to the desorption of proteins and other analytes, the droplet motion is often reduced. Freire et al. showed the possibility to move biological liquids using superoleophobic materials made by coating of candle soot and subsequent surface modification.[316] The authors were able to move bovin serum albumin droplets even at concentration 2000 times higher. To control the protein adsorption on microfluidic channels, Gogolides et al. used a lithographic process on PMMA following by anisotropic O_2 plasma etching and fluorinated plasma deposition to obtain superhydrophobic channels.[317] Using the biotin-streptavidin system, they showed that the superhydrophobic properties can enhance the sensitivity of the protein detection by two orders of magnitude in comparison to flat microchannels.

Another method to confine the flow is to use superhydrophobic/superhydrophilic contrasts. Shirtcliffe et al. showed that some superhydrophobic plants have the ability to collect water from their environment without the possibility to move (Fig. 30).[14] Similar behavior was also reported on the surface of beetles in the Namib Desert.[15] This ability is due to a combination of topography and more precisely both superhydrophobic and highly "sticky" states designed in order to induce effective water collection. Here, the water droplets are collected by the sticky regions and then the size becomes critical than can roll off them. However, on some plants such as *Echeveria* and *Euphorbia*, the leaves acted like channels steering the water to the stem by gravity where they are trapped. They also showed the possibility to artificially collect water by creating superhydrophilic artificial grooves surrounded by superhydrophobic walls to channel the water. It was also reported that the cactus *Opuntia microdasys* is able to collect water thanks to structured spines having wettability gradient[318] whereas the endemic Namib Desert grass *Stipagrostis sabulicola* uses microgrooves parallel to the axis of the plant to guide water.[319] By contrast, *Cotula fallax* uses a 3D arrangement formed by its leaves and the fine hairs covering them to collect a high amount of water.[320a] We can also cite the spider *Uloborus walckenaerius*, which uses silk constituted of periodic spindle-knots made of nanofibrils to collect water.[320b]

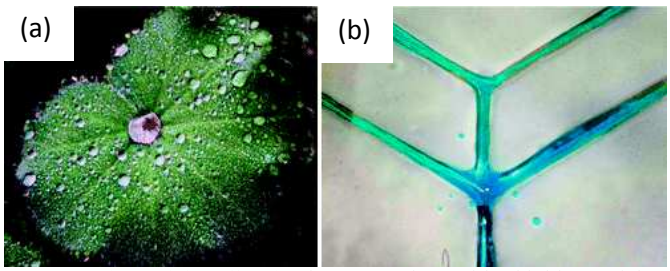

Fig. 30 (a) *Alchemilla* (Lady's Mantle) with highly "sticky" superhydrophobic leaves (Wenzel state) to collect water and superhydrophilic channels to guide the water to the stem; (b) artificial superhydrophilic channels surrounded by superhydrophobic walls. Reprinted with permission from ref. 16, copyright 2009, American Chemical Society.

Hence, other authors worked to the biomimetism and the reproduction of this ability to collect water. Cohen at al. elaborated hydrophilic patterns of superhydrophobic surface using water/2-propanol solution of poly(fluorescein isothiocyanate allylamine hydrochloride) polyelectrolyte.[321] Gogolides showed the interest to produce superhydrophilic microchannels in microfluidic devices while superhydrophobic patches could be used as passive valves.[322a] Boukherroub et al. used also superhydrophobic/superhydrophilic contrasts to

induce the move of small biomolecules in a EWOD system coupled to a surface-assisted laser desorption-ionization (SALDI) for mass spectrometry.[322b] They showed that analyses of low molecular weight compounds can be achieved with a very high sensitivity.

Finally, another important interest to use these properties was the possibility to create open microfluidic devices and more precisely on paper substrates.[323-324] Indeed, paper could made superhydrophobic for example by immersion in poly(hydroxybutyrate) solution. Then, it was possible to render regions superhydrophilic just by writing or printing.

3.9 Floating Properties

The principle of the possibility to walk on water is based on that of water striders (Fig. 1e).[18] These insects are this ability thanks to densely packed nano-hairs on their legs, which allows the trapping of a high amount of air between the legs and water surface. To construct microrobots capable of walking on water surface, nanostructured legs were fabricated (Fig. 31).[325] These legs are able to support the weight of the microrobot. Here, the legs consisted in copper wires covered with $Cu(OH)_2$ nanoribbons and treated with *n*-dodecanoic acid to induce superhydrophobic properties. Microrobots capable of jumping on water surface were also created with superhydrophobic nickel foam legs.[326] Pan et al. used copper meshes and induced the galvanic deposition of Ag nanodendrites by a simple immersion process in $AgNO_3$.[327] After surface modification with *n*-dodecanoic acid, loading capacities (> 11 g for a boat of 8 cm^3, for the best results) as a function of the pore size of the copper meshes were reported. Aerogels were also used in the literature to support an important weight.[328]
The use of smart materials can also lead to the motion of a microrobot. To induce the on-off motion of a superhydrophobic boats by changing the pH based on the Marangoni effect, the group of Shi used three functional materials: a material to reduce the drag, a gold substrate with platinum nanostructures to give a hydrogen peroxide-responsive surface and a nickel mesh coated with a mixture of 1-dodecanethiol and 11-mercaptoundecanoic acid to induce a pH-responsivity.[329-330] The microrobot could move on water by changing the pH from 1 to 13.

3.10 Printing Technologies

The use of superhydrophobic properties was also used in printing technologies. Indeed, in these technologies it is important to have high contrast of wettability between the image areas and non-image areas.[331] Nishimoto et al. were interested in the improvement of offset printing.[332-333] In a classical process, a wettability-patterned surface is formed by coating an anodized Al plate with a photosensitive polymer, light illumination through a mask and development treatment. During the printing, the hydrophilic areas are filled with water. Then, the ink injected adheres only in the areas without water and the pattern is transferred to the paper. While conventional printing plates cannot be reused, the authors reported this possibility using TiO_2-based superhydrophobic-superhydrophilic patterns and also to have a very high contrast of wettability. Indeed, the remaining patterned hydrophobic organic molecules could be photocatalytically decomposed by TiO_2 under light irradiation.

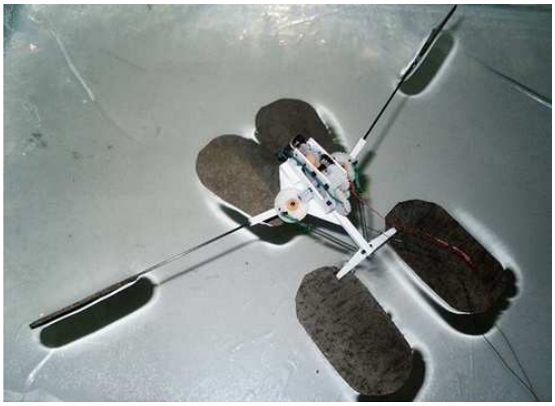

Fig. 31 Picture of a microrobot with superhydrophobic legs capable to move on water like a water strider.
Reprinted with permission from ref. 325, copyright 2012, American Chemical Society.

Law et al. worked on the improvement of the impression to paper from a fuser surface (Fig. 32).[334-336] In this process, a toner is usually fused at a temperature ranging from 130 to 180°C under pressure (300-700 kPa) in 10-20 ms. In this technology, the molten toner has to adhere onto the paper rather than to the fuser surface. Otherwise, the quality of the images decreases after each use. Usually, the fuser surface is in Teflon but this material is oleophilic with a contact angle of hexadecane of ≈ 48°. As a consequence, the molten toner, which is close to a wax, can be attracted but the fuser surface. Here, the authors proposed to developed robust superoleophobic fuser surface to reduce this possibility. They developed textured pillars using the Bosch etching process and modified them with a perfluorinated silane. Superoleophobic properties, with contact angle of ink or toner up to 168°, were reported.

3.11 Optical Devices

3.11.1 Transparency

To obtain superhydrophobic properties, it is necessary to structure the surface of a material. The surface structures can decrease the transparency of the material due to the scattering of the light in the surface roughness. However, the transparency is absolutely fundamental for various applications such as windows, glasses, lenses or optical instruments. The light scattering on superhydrophobic surfaces can be predicted by the Rayleigh scattering and Mie scattering if we suppose that the roughness acts such as spherical, non-absorbing particles (dielectric) to redirect the incident light.[337]

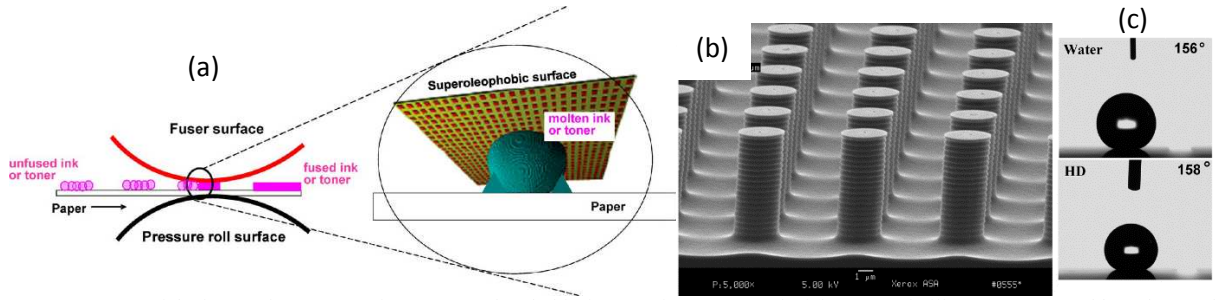

Fig. 32 (a) Improvement of the impression to paper from a superoleophobic fuser surface composed of (b) textured pillars; (c) water and hexadecane droplets on the surface.
Reprinted with permission from ref. 334, copyright 2012, American Chemical Society.

For roughness dimension below that of the light wavelength, in intensity of scattered light I is given by the equation:

$$\frac{I}{I_0} = \frac{1+\cos^2\theta}{2S^2}\left(\frac{2\pi}{\lambda}\right)^4\left(\frac{n^2-1}{n^2+1}\right)^2\left(\frac{d}{2}\right)^6$$

where λ is wavelength light, n is the refraction index of the particle, d is particle diameter and S is the distance between the particle and the detector. Hence, using visible light the Rayleigh scattering is negligible for roughness size lower than 100 nm. Moreover, for antireflection, the refractive index of the material should be low.

Hence, most of the techniques used to produce transparent superhydrophobic particles are based on the use of nanoparticles (SiO_2, TiO_2, ZnO, C, polymers,…), for example with the sol-gel process, electrospinning, vapor deposition or by colloidal lithography, and also based on plasma treatments.[337-339]

A very interesting potential application was given by the group of Xiao (Fig. 33).[340] They showed that nanoporous polymer chalk such as polydivinylbenzene can be used to obtain transparent superhydrophobic paintings. This materials could be used to coat, paper, PDMS and even the skin.

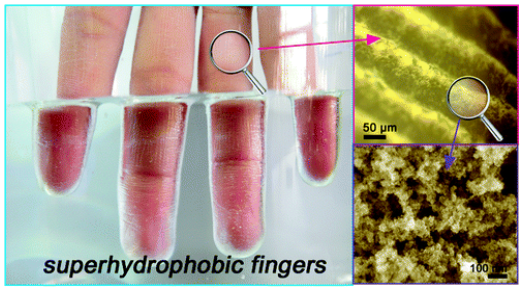

Fig. 33 Fingers coated with a transparent superhydrophobic paint.
Reprinted with permission from ref. 340, copyright 2011, American Chemical Society.

3.11.2 Anti-reflection coatings

An anti-reflection property is useful to increase the light transmittance ration and to reduce the glare, and are widely used in various optical devices such as cameras or cell phones. Usually, an anti-reflection property can be introduced as a multiple layer thin film with various refractive indices and thicknesses, or by structuring the surface of a material. In order to produce superhydrophobic properties and anti-reflection properties it is necessary to have ordered surface structures with controlled dimension. In nature, the moths and flies are known to have eyes with anti-reflective properties.[9,341-344] The moth eyes are composed of hexagonal arrays of nonclose-packed nano-nipples (Fig. 34) to reduce the reflectivity. The sub-wavelength size of the nipples induces of grade transition of refractive index. As a consequence, the reflection is minimized over a broad range of wavelengths and incidence angles.

Fig. 34 SEM image of a fly's eye with antireflection properties.[344a]

Different research groups tried to reproduce these properties.[345-350] The group of Jiang produced anti-reflection coatings composed of nano-pillars with self-cleaning properties.[345] They reported the reactive ion etching process using silica nanoparticles to induce the formation of nano-pillars with various aspect ratios on silicon and glass. They observed that a high aspect ratio (≈ 10) is necessary to reach also self-cleaning properties. For example, in the case of Si wafer, the nano-pillars allowed to reduce the reflectivity from > 30% for smooth silicon wafers to < 2.5% for the structured ones. In a similar way, Yang et al. produced silica arrays of different shape using colloidal crystal of PS as mask and reactive ion etching.[346] The surfaces were finally modified with a perfluorinated silane to reach superhydrophobic properties. The best surfaces displayed anti-reflective properties < 2.5% over the range 800–2500 nm.

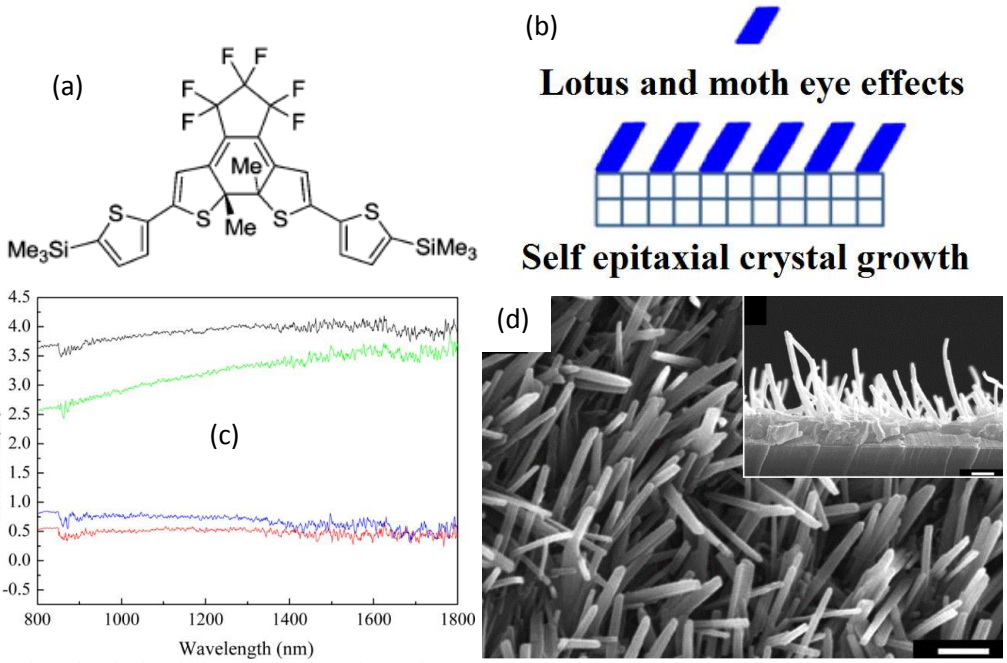

Fig. 35 (a) Molecule used for (b) (d) photoinduced self-epitaxial crystal growth with (c) anti-reflection properties.
Reprinted with permission from ref. 349, copyright 2013, American Chemical Society.

Moreover, the transmittance was > 99% in the range 1600–2130 nm.

In a similar approach, Huang et al. reported the formation of Si nanopillar arrays with properties depending on the height of the pillars.[347] Reflectance < 10% were observed with the longer pillars. The substrates also displayed superhydrophobicity, photoluminescence and surface-enhanced Raman scattering by metal deposition onto the pillars.

Superhydrophobic substrates with self-cleaning and anti-reflective properties composed needle-shaped microcrystals (∅ = 0.2-0.3 μm, length = 2.2-2.5 μm) were reported by Uchida et al. by photoinduced self-epitaxy of a fluorinated diarylethene derivative (Fig. 35).[349] The reflectance of the substrates was < 0.5%. The group of Sung also reported the elaboration of antireflective and superhydrophobic properties on large-area flexible substrates (PET) by UV-nanoimprint lithography roll-to-roll process, plasma etching and surface modification with a perfluorinated silane.[350] The best results were obtained with nanostructures of 82 nm height, 300 nm pitch and 283 nm diameter.

3.11.3 Anti-fogging coatings

The formation of fog appears by condensation of vapor into water droplets.[351-355] The condensation nuclei diameter is larger than 190 nm, which is approximately half of the shortest wavelength of the visible light. As a consequence, the visibility of transparent materials can be reduced by light scattering and reflection. Indeed, the formation of water droplets on superhydrophobic surfaces is a very complex phenomena and superhydrophobic properties can sometimes increase and sometimes decrease the water condensation. Jiang et al. reported that the eyes of mosquitoes and flies are able to repel micrometer-size water droplets (Fig. 36).[10] They showed that this ability is due to specific ordered structures in both at the microscale and the nanoscale: hexagonally close-packed ommatidia (∅ ≈ 26 μm) at the microscale and hexagonally non-close-packed nipples (∅ ≈ 101 μm and interparticle spacing ≈ 48nm) at the nanoscale. Moreover, they could reproduce the structures by a complex process including photolithography, heating, transfer by soft lithography and incorporation of SiO_2 nanoparticles.

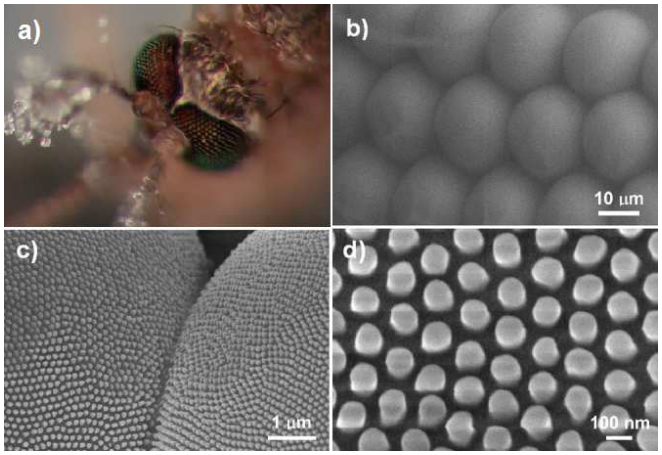

Fig. 36 Corneal nipple arrays with anti-fogging properties of the mosquito, at different magnification.
Reprinted with permission from ref. 10a, copyright 2007, Wiley-VCH.

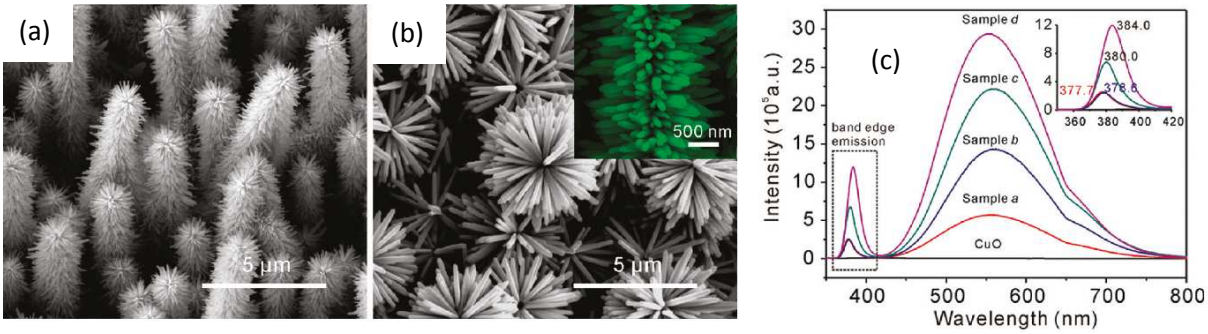

Fig. 38 Growth of ZnO nanorods on CuO nanowires in $Zn(NO_3)_2$ aqueous solution at a concentration of (a) 0.05 M and (b) 0.1 M; (c) photoluminescence spectra at different concentration of $Zn(NO_3)_2$.
Reprinted with permission from ref. 364, copyright 2011, American Chemical Society.

Other research groups also reported the anti-fogging properties of superhydrophobic materials.[356-358] The group of McKinley reported robust superhydrophobic surfaces with ordered arrays of nanoplots of conical shape by a complex lithographic process using reactive ion etching and followed by a modification with a perfluorinated silane.[356] The as-prepared materials displayed optical transmission (> 98% over a broad range of wavelength and incident angles) and anti-fogging properties. Krupenkin et al. fabricated transparent Ta_2O_5 containing nanoplots using anodized Al as mold to transfer the pattern.[357] After plasma deposition of a fluorinated polymer the thin film was transparent and with self-cleaning and anti-fogging properties.

3.11.4 Photoluminescence

The elaboration of one-dimensional nanostructures of semiconductor such as nanorods, nanoneedles, nanowires, nanotubes or nanobelts can yield to unique properties including photoluminescence. Hence, the deposition of these nanostructures on surfaces can yield to both photoluminescence and superhydrophobicity. In the literature, ZnO is probably one of the most studied semiconductors for photoluminescence properties due to the possibility to form extremely various nanostructures with controllable dimension such as nanorods.[359-364] Indeed, the exceptional properties of ZnO are in part due to its wide band gap (≈ 3.37 eV) with a large excitation binding energy of 60 meV at room temperature and its hexagonal wurzite-type crystalline structure.
The photoluminescence is an important technique to characterize the purity and crystalline quality of semiconductors. For example, Patil et al. elaborated superhydrophobic ZnO nanoplatelets by spray pyrolysis.[359] They observed a strong UV emission at ≈ 398 nm with three shoulder at 373 nm, 382 nm and 410 nm, with weak blue emission at 471 nm and green emission at 520 nm. The UV emission at 398 nm, corresponding to the near band edge emission of ZnO and responsible for the excitonic recombination, can be taken as indicator of good crystallinity. In the opposite, the green emission peak is due to crystal defects such as vacancies or interstitial sites. A study of crystalline defects was also performed by Ozer et al. comparing ZnO nanorods and ZnO nanoneedles obtained by hydrothermal process with different seed-to-growth solution concentration ratios (Fig. 37).[360] Indeed, they concluded that the ZnO nanoneedles had a higher degree of crystallinity. The position of the peaks can also give information about the dimension of the crystalline structures. For example, Huang et al. studied the growth of ZnO nanorods on CuO nanowires (Fig. 38).[364] They observed that the UV emission peaks shift from 377.7 nm to 384.0 nm due to the increase in the diameter and length of the ZnO nanorods. Moreover, the substrates also displayed self-cleaning properties. Superhydrophobic and photoluminescent ZnS nanostructures were also reported in the literature using thiourea as a sulfur source.[365] The authors observed difference in the photoluminescence spectra for ZnS nanowires and ZnS nanorods arrays with a strong yellow UV emission centered at 574.9 nm and 587.7 nm respectively.

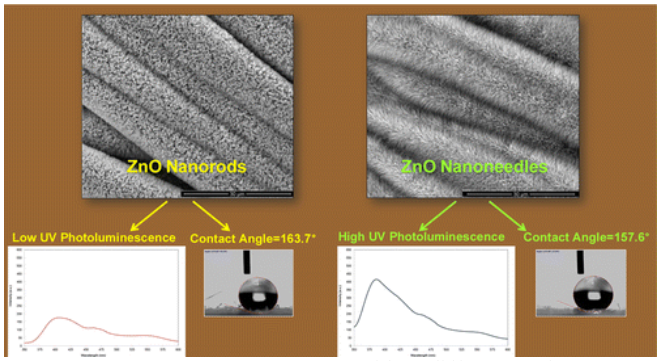

Fig. 37 ZnO nanostructures with different shapes and photoluminescence properties.
Reprinted with permission from ref. 360, copyright 2013, American Chemical Society.

Other nanomaterials with superhydrophobicity and photoluminescence were also explored in the literature. Jaouad et al. reported the properties of vertically aligned Ge nanoneedles.[366] In comparison with bulk Ge, the Ge nanoneedles showed and broad emission peak centered at 650 nm. The other materials include Si flower-like structures,[367] BN nanosheets,[368] PbSe nanodendrites,[369] Bi_2S_3 urchin-like

structures,[370] $In(OH)_3$ nanocubes,[371] $In_xGa_{(1-x)}N$ nanotips[372] and different C nanostructures.[373-374]

Another strategy to obtain superhydrophobic materials with photoluminescence was to introduce quantum dots (QDs) such as CdS, CdSe or CdTe. Zhai et al. induced the growth of CdS QDs directly on TiO_2 nanotube arrays using chemical bath deposition method. Superhydrophobic properties were obtained after modification with a perfluorinated silane.[375] In order to obtain superhydrophobic properties in one step and to induce a good compatibility with organic monomer and polymer matrix, other research groups preferred to synthesize CdS QDs in solution following by an exchange with a hydrophobic ligand.[376-380] The group of Chen modified CdS QDs with dodecanethiol.[376] The authors could introduce these QDs in a PMMA matrix. The same author also reported the incorporation of CdTe QDs after modification with dodecaneamine.[377] Then, they elaborated superhydrophobic fibrous structures by electrospinning. Photoluminescent analyses confirmed that the QDs were well dispersed in the matrix: as expected, just a shift was observed as a function of the size of the CdTe QDs. To enhance the resistance of nanocrystals against photooxidation, various dithiocarbamates were tested (Fig. 39). Various crystalline structures were obtained as a function of the dithiocarbamate while superhydrophobic properties were obtained using dithiocarbamates with long alkyl chains.[379]

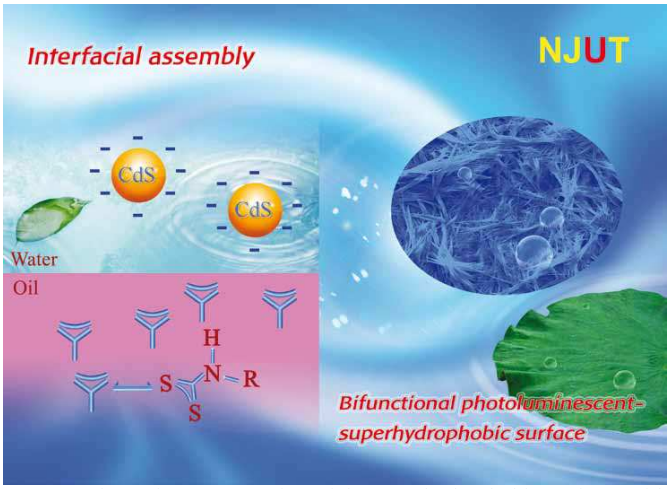

Fig. 39 Schematic representation of the superhydrophobic surfaces with photoluminescence using CdS quantum dots and dithiocarbamates.[379]

Finally, the last strategy discussed in this review was the use of Eu complexes for their high photoluminescent properties.[401-402] Hou et al. reported the photoluminescent properties methylsilicone polymer just by dissolving the polymer in ethanol and mixing with Eu(benzoic acid)$_3$(1,10-phenanthroline).[401] YBO_3/Eu^{3+} with various crystalline structures and hydrophobicity were hydrothermally synthesized by adjusting the ratio of surfaces PEG-6000 to octadecylamine. For example, the rose-like structures displayed photoluminescence with three strong emission peaks at 591, 610 and 615 nm. The group of Jin reported the formation of structured silica of various crystalline structures in the presence of poly(ethylenimine) and additives.[402] Then, the surfaces could be modified with perfluorinated chains to reach superhydrophobic properties and containing Eu^{3+} complexes for photoluminescence.

3.11.5 Photonic crystals

The butterflies of the genus *Morpho*, which display brilliant blue color, intrigued the scientific community.[403-406] The brilliant colors of their wings are useful against predators while their self-cleaning properties are an advantage when they fly. It was shown that their color was not due to the presence of pigments or dye but to the presence of ordered structures on their wings diffracting light and inducing interference effects. Hence, the replacement of pigments and dyes by introduction of structured materials is very interesting to increase the lifetime of colored materials. An example of complex skeleton of butterfly is given in Figure 40b. Moreover, the butterflies of the genus *Morpho* also display superhydrophobic properties.[11,407] For example, the blue butterfly *Morpho Aega* possess anisotropic superhydrophobic properties due to the presence of directional arrangement of micro-scales. The group of Goodwyn studied superhydrophobic white translucent butterfly's wings of the genus *Parantica sita* (Nymphalidae) and transparent butterfly's wings of the genus *Parnassius glacialis* (Papilionidae) (Fig. 40).[408] They observed that the white zones of *Parantica sita*'s wings are due to the presence of highly porous and ordered scales (ridge-lamella connected by cross ribs) as observed in *Morpho* species. Similar effects were also found to be responsible of the iridescence of insects and animals such as damselfish,[409] the neon tetra *Purucheirodon innesi*,[410] *Pentapodus paradiseus* whiptail,[411] *Loligo pealeii* squid,[412] *Beroë cucumis* comb-jellyfish,[413] *Pachyrhynchus argus*,[414] *Hoplia coerulea*[415] and *Charidotella egregia*[416] beetles, *Ancyluris meliboeus* Fabricius[417] and *Papilio palinurus* butterflies.[418] It was demonstrated that these color changes are due to changes in refractive index, periodic nanostructures and incident light angle.

The group of Gu, tried to reproduce the properties of *Morpho* species using colloidal crystals, also called colloidal lithography, using poly(methyl methacrylate-co-divinylbenzene-co-methacrylic acid) spherical particles.[419] Indeed, this method based on the deposition of highly ordered particles (inorganic or polymer) allowed the tuning of the surface wettability and the material color with the surface topography.[419-422] These properties were confirmed by the group of Zhu using PS spheres.[423] Moreover, the introduction of dyes as dopant could improve the brightness of the materials by the suppression of light scattering. The use of colloidal crystals is extremely interesting to tune the optical properties, for example with the diameter of the particles, their refractive index, the incidence angle of the light, but also by swelling or by stretching as well as using sensitive polymers and by post-functionalization.[424-425]

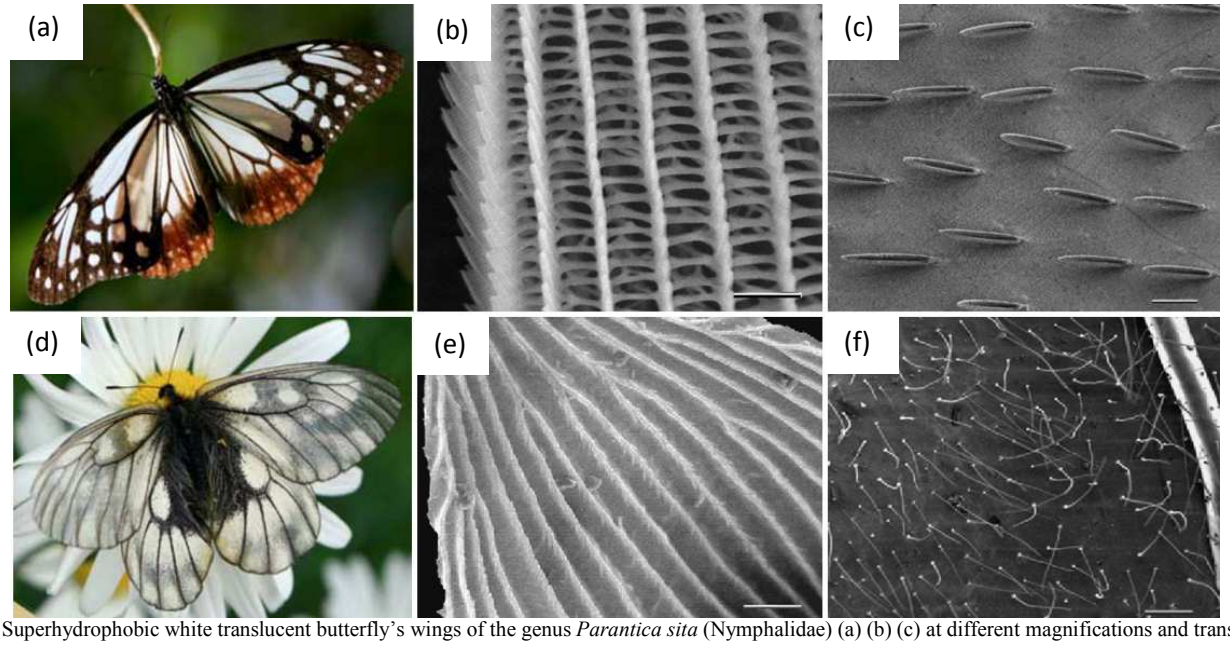

Fig. 40 Superhydrophobic white translucent butterfly's wings of the genus *Parantica sita* (Nymphalidae) (a) (b) (c) at different magnifications and transparent butterfly's wings of the genus *Parnassius glacialis* (Papilionidae) (d) (e) (f) at different magnifications.
Reprinted with permission from ref. 408, copyright 2009, Springer.

Indeed, in nature the iridescence of opal (a hydrated amorphous form of silica) is due to the presence of closely packed silica spheres (150 to 300 nm in diameter).[426-427] Moreover, other strategies can be used to deposit these materials such as spray coating, ink-jet printing or deposition on low-adhesive superhydrophobic substrates,[428-436] which allows to increase the interest of these properties for various applications.

To tune the surface hydrophobicity of colloidal crystal without changing in the photonic bandgap, the group of Jiang used PS-*block*-PMMA-*block*-poly(acrylic acid) particles.[437] The surface wettability could be changed from superhydrophilic to superhydrophobic by controlling the assembly temperature. The authors explained this possibility by changing the chemical groups present at the extreme surfaces of the spheres as a function of the assembly temperature.

In order to obtain both structural color and self-cleaning properties, inverse opal films were fabricated using suspension of PS spheres (∅ = several 100 nm) and SiO_2 nanoparticles (∅ ≈ 6 nm) (Fig. 41).[438] Then, the materials were calcined at 450°C to remove the PS sphere and to solidify the SiO_2 nanoparticles, and modified with a perfluorinated silane to reach superhydrophobic properties. Moreover, different colors were obtained depending on the center-to-center distance between two neighboring holes (275 nm for blue, 310 nm for green and 400 nm for red). Moreover, the assembly of colloidal particles is possible only if the surface is hydrophilic.[439] Hence, surfaces with hydrophobic/hydrophilic contrasts were also elaborated combining colloidal lithography and photolithography. To enhance the mechanical and thermal properties of the materials, Song et al. also reported the properties of superhydrophobic inverse opal films using polyimide and with close-cell structures.[440] These structures were produced with poly(styrene-methyl methacrylate-acrylic acid) core-shell: a rigid PS core and an elastomer poly(methyl methacrylate-acrylic acid) shell. Here, the elastomeric properties of the shell are responsible of the formation of core-shell structures. The materials kept their superhydrophobic properties and photonic band gap after heating at 400°C for 2 h. To obtain tough materials, these core-shell polymers were also used for the formation of SiC inverse opals.[441] The authors showed the possibility to obtain photonic crystals covering the entire UV-vis-NIR range. To elaborate materials with switchable wettability and conductivity, inverse opal of polypyrrole were fabricated from poly(styrene-methyl methacrylate-acrylic acid) core-shell.[442] While the surface wettability could be reversely changed from highly hydrophobic to hydrophilic by dedoping/doping processes with a change in conductivity but also in color, due to change in polypyrrole refractive index and volume.

Finally, other strategies were employed to obtain photonic crystals with similar or different ordered structures. Yang et al. achieved to obtain structures close to that obtain with inverse opals using holographic lithography.[443] In order to increase the superhydrophobic properties (θ_w = 161.4°), they could controlled the formation of nano-roughness on the microstructures using epoxy-functionalized POSS. The nano-roughness was generated due to microphase separation during the rinsing step of holographic lithography. Here, nano-roughness did not significantly affect the bang gap of the photonic crystal. Moreover, these materials had very high ability of dye adsorption (6 times higher) in comparison with smooth surfaces.

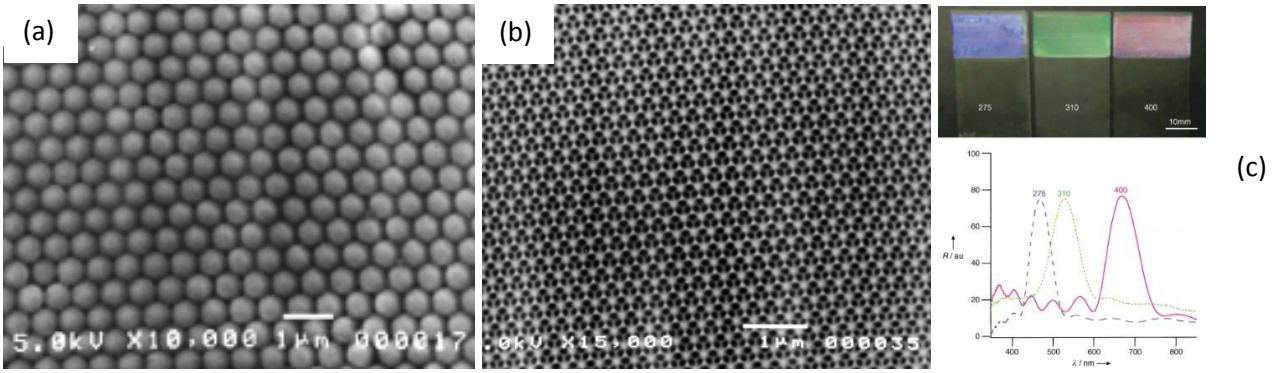

Fig. 41 (a) Opal structures obtained by colloidal lithography with PS spheres and SiO_2 nanoparticles, and (b) inverse opal structures obtained after calcination to remove the PS spheres; (c) color and transmission spectra of the inverse opal structures with different center-to-center distances. Reprinted with permission from ref. 438, copyright 2003, Wiley-VCH.

The group of Sun used a multibeam holographic lithography, sensitization with $SnCl_2$ and Ag electroplating to produce photonic crystal with regular nano-nipples arrays.[444] The as-prepared material displayed superhydrophobic properties and iridescence.

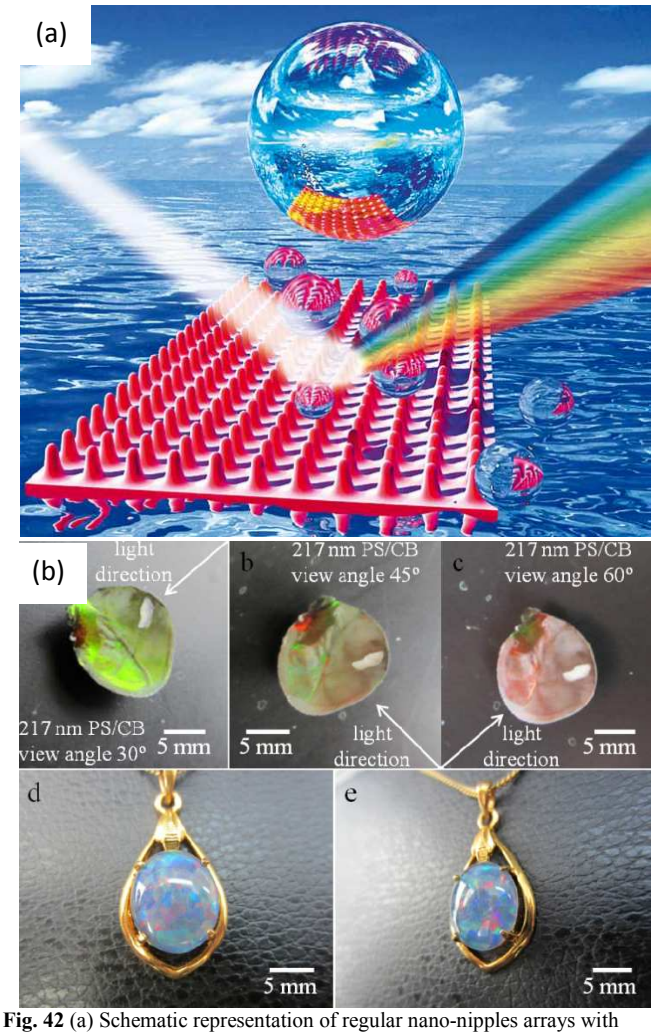

Fig. 42 (a) Schematic representation of regular nano-nipples arrays with superhydrophobic and iridescence properties;[444] (b) man-made polymer opals with different colors and iridescence properties.[426]

3.11.6 Solar Cells

The low conversion efficiency is a major problem for solar cells. The energy efficiency can be enhanced by reducing the light reflection, increasing the transparency and/or increasing the light absorption. As shown in the previous sections a surface can be made superhydrophobic while being transparent and anti-reflective, by controlling the surface topography. Another important interest to use superhydrophobic coatings is the possibility to reduce the dust on the solar cells, which is to date an important problem (the dust reducing the energy performance).

It was possible to induce transparent and anti-reflective properties by producing nanostructures close to the moth eyes.[9,341-344] Wong et al. elaborated superhydrophobic and self-cleaning solar cells containing Si micropyramids modified with ZnO nanowires (Fig. 43).[445] Here, the micropyramids were obtained by etching Si wafer in KOH water/isopropyl alcohol solution. ZnO nanowires were produced by magnetron sputtering to form a ZnO seed layer before immersion in zinc nitrate and hexamethylenetetramine solution.

The solar cells displayed an increase in the anti-reflection by 3.2% over the 300-1200 nm range and a high conversion efficiency of 16%. The performance of solar cells based on ZnO nanostructures was also reported in others works. To improve the UV-resistance of the materials, Beaujuge et al. also proposed to add an ultra-thin layer of SiO_2 around the ZnO nanostructures, while Nuraje et al. electrospun PS and PVC fibers incorporating TiO_2 nanoparticles and graphene nanoflakes.[446-447] Other research groups also reported the possibility to reduce the dust accumulation on flexible and transparent PDMS or PET substrates by creating microshells and nanofibers, respectively.[448-449] They developed their substrates by replication from a patterned mold.

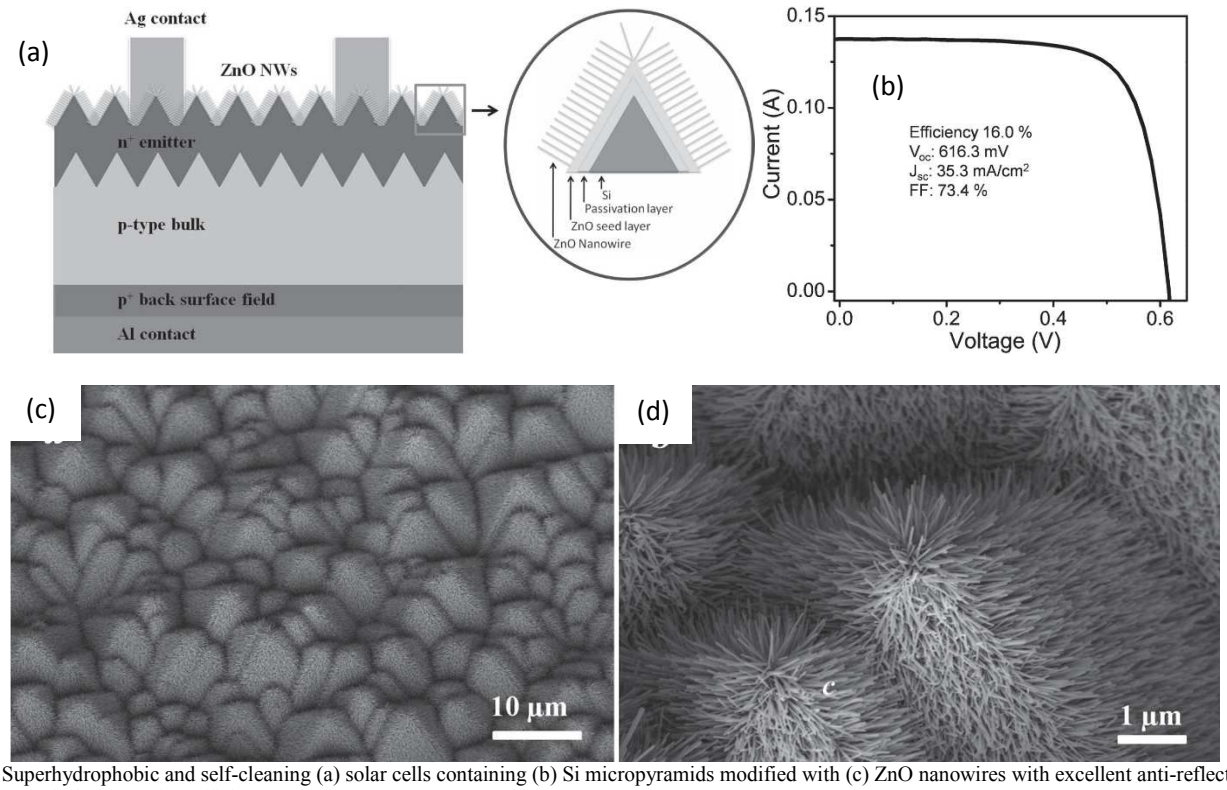

Fig. 43 Superhydrophobic and self-cleaning (a) solar cells containing (b) Si micropyramids modified with (c) ZnO nanowires with excellent anti-reflection properties and (d) conversion efficiency.
Reprinted with permission from ref. 445, copyright 2012, Wiley-VCH.

This process as well as the UV-nanoimprint process were also used on PET substrates by Lee at al. to replicate the moth eyes structures and as a consequence increase the anti-reflective properties.[450] The authors also reported an increase in accumulated electric energy of the solar cell of until 3.9%. Finally, the use of superhydrophobic properties in dye-sensitized solar cell was also reported.[451] Kim et al. incorporated an anti-reflective layer with moth eye-like structures in this device.[452] The layer could increase the transmittance up to 82% at 540 nm. The dye-sensitized solar cells displayed an enhancement of the efficiency to 7.3% at 100 mW cm^{-2}.

To combine self-cleaning properties with anti-reflectivity and high absorption properties, nanodomes of an active absorber (hydrogenated amorphous silicon) were created by pattern transfer from a mold.[453] The as-prepared materials could absorbed 94% of the light in the range 400-800 nm, higher than the corresponding smooth substrate (65%). They also reported a high power efficiency of 5.9% (25% more than the corresponding smooth substrate). Patsalas et al. used nanocomposites of metal nanoparticles (Ni, Fe, Mo, Sn) included in diamond-like carbon matrices to form various nanostructures depending on the experimental conditions.[454] The interlinked star-shaped Ni structures displayed superhydrophobic properties, extreme optical absorbance over the visible range, low optical reflection (< 10^{-4}) and high thermal conductivity.

Finally, the elaboration of superhydrophobic photo-sensors was also reported.[455] The authors fabricated arrays epoxy photoresist square micropillars on n-doped crystalline Si substrates. Then, a poly(3-hexylthiophene-2,5-yl) layer with nano-roughness was deposited to form a p-n junction. The authors observed an increase in the superhydrophobic properties and the photosensitivity as the interpillar distance. Indeed, only the regions in between the pillars are responsible for the photoconductivity while the relation with the superhydrophobic properties follows the Cassie-Baxter equation.

3.12 Batteries

The technology of batteries has become a major field of researches in electronic devices because their capacity and shelf life are not able to follow the advances made in semiconductor technologies. A battery has to provide power when required and to endure prolonged periods of storage. For this last point, a mechanical separator is present in a normal battery to separate the electrolyte from the electrodes, increasing the necessary volume of the battery. To overcome these problems, the group of Simon proposed to use superhydrophobic nanostructured electrodes instead of the use a mechanical separator in order to miniaturize the system (Fig. 44).[456-458] Here, the system is based on the electrowetting phenomena.

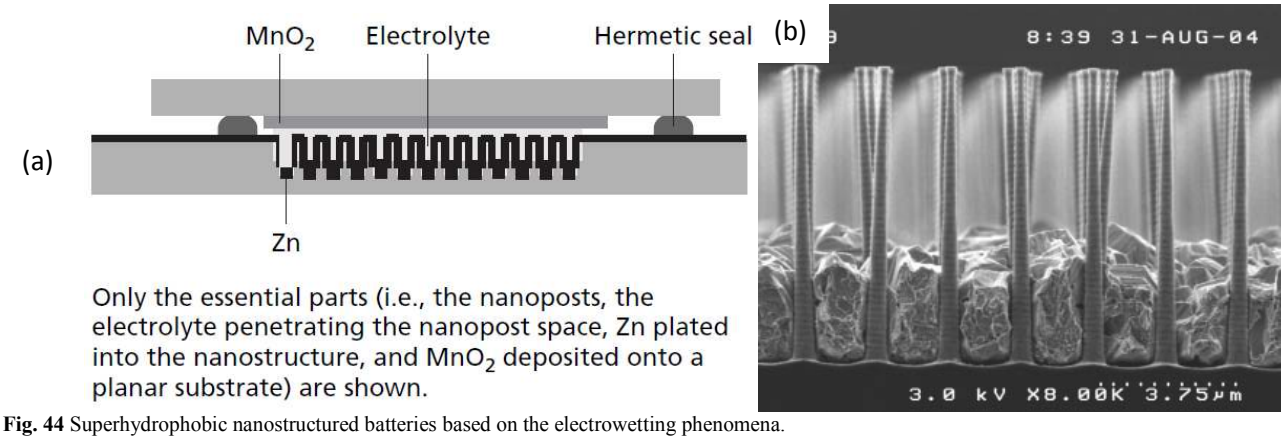

Fig. 44 Superhydrophobic nanostructured batteries based on the electrowetting phenomena. Reprinted with permission from ref. 456, copyright 2005, Wiley-VCH.

When no power is applied, the electrolyte cannot penetrate into the electrode space because of their self-cleaning properties. But, when a power is activated, that induces a Cassie-Baxter-to-Wenzel transition which highly increases the contact between the electrode and the electrolyte. Moreover, this phenomenon is extremely fast (≈ 1 ms). They also demonstrated the use of microporous honeycomb membranes disposed on the nanostructured electrodes to obtain batteries with electrically controllable permeability.[459] Indeed, the penetration of the electrolyte inside the membrane is electrically controllable.

Other research groups also showed the potential of superhydrophobic coating of batteries, fuel cells and photoelectrochemical cells.[460-462] For example, Pan et al. successfully improved the lithium storage properties of Fe_2O_3@C nanoparticles in lithium ion batteries by adding a superoleophilic and superhydrophobic polysiloxane coating.[460] Indeed, a superoleophilic and superhydrophobic can repel water while allowing the penetration of the electrolyte.

3.13 Sensors

3.13.1 Enhancing SERS effect

In the case of metal nanostructures, coherent oscillations of conduction band electrons can lead to plasmon resonance with an extremely high local electromagnetic field. This effect is called Surface-enhanced Raman scattering (SERS) and is known for metal nanoparticles in solution but also on surfaces.[463-472] This effect can be used for the detection of trace molecules. Gold nanoparticles forming Candock leaves structures were also reported in the literature through an aggregation process controlled with a polyelectrolyte film.[463] The superhydrophobic film (θ_w = 155°) also displayed excellent SERS enhancement with a factor of more than 5 compared to sputtered gold film (tests done with Rh6G). The group of Li studied the enhancing of SERS effect on superhydrophobic surfaces made of ZnO nanorods coated by Ag nanoparticles.[464] They observed a signal amplification by a 3-fold. The SERS effect of superhydrophobic surfaces obtained by assembling Ag nanocubes (size distribution: 102 ± 9 nm) using the Langmuir-Blodgett technique, coating a 25 nm Ag layer to weld the Ag nanocubes and functionalization with perfluroodecanethiol was also studied (Fig. 45).[465] The surfaces were able to detect trace molecular such as rhodamine 6G (Rh6G) down to 10^{-16} M while only 1 µL of diluted analytes were necessary. Superhydrophobic surfaces containing PS-Ag Janus particle arrays were also elaborated by site-specific electrodeposition.[466] These surfaces were able to detect highly diluted solution (femtomolar range). The group of Di Fabrizio fabricated superhydrophobic periodic array of micropillars and modified them by incorporating Ag nanoparticles on the head on the pillars.[470-472] They observed an enhancement of the SERS effect with the possibility to detect Rh6G in the fairly low atto molar range. The authors envisaged to use these surfaces to detect tumors or other important pathologies.

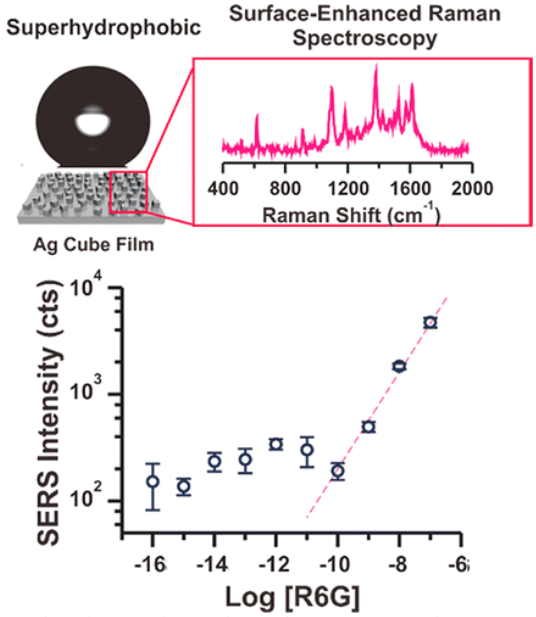

Fig. 45 Enhancing Surface-enhanced Raman scattering (SERS) using superhydrophobic Ag nanocubes. Reprinted with permission from ref. 465, copyright 2013, American Chemical Society.

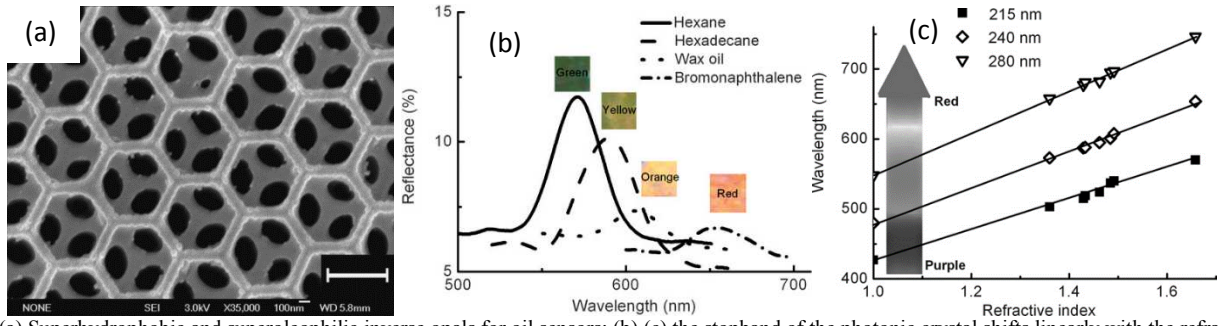

Fig. 46 (a) Superhydrophobic and superoleophilic inverse opals for oil sensors; (b) (c) the stopband of the photonic crystal shifts linearly with the refractive indices of the oils.[481]
Panel a reprinted with permission from ref. 480, copyright 2013, Wiley-VCH.

3.13.2 Classical Sensors

Following its chemical composition, a superhydrophobic material can also have interactions with various molecules in solution or gases. Here, the surface roughness can increase sensitivity of the sensors. Saito et al. used a superhydrophobic quartz crystal microbalance to detect volatile organic compounds.[473] Using nanostructured superhydrophobic by plasma-enhanced CVD of trimethylmethoxysilane, the materials could adsorb by van der Waals interactions organic compounds such as toluene and formaldehyde leading to an increase in the weight of the materials. Other research groups modified superhydrophobic materials by incorporating amine groups to interact with CO_2.[474-475] In order to detect explosives, Lei reported superhydrophobic sand by modification with PS/pyrene/tetrabutylammonium hexafluorophosphate composites.[476] The resulting materials were able to detect nitroaromatic explosive vapor such as 2,4-dinitrotoluene. One of the interests to use superhydrophobic materials was found to be to develop sensors able to detect gases or explosives dissolved in water.[477-479]

3.13.3 Sensors Based on Photonic Crystals

As described above, photonic crystals are unique materials with color or stopbands depending on structural parameters (Fig. 46).[480-482] Hence, when a product is in contact with the structure, a shift in the stopband or the color can be observed. Song et al. developed superhydrophobic and superoleophilic inverse opals for oil sensors.[480-481] They observed that, for a given pore size, the stopband of the photonic crystal shifts linearly with the refractive indices of the oils.

3.13.4 Biosensors

Many natural systems are based on complex interactions like hydrogen bonding and specific recognition. For example, protein-carbohydrate interactions concern many important biological processes such as signaling, recognition and catalysis.[483-484] Hence, the elaboration of sensors based on the sensing of carbohydrates is highly important for medical applications, diagnostic and therapeutic. The group of Sun reported the possibility to elaborate superhydrophobic surface with switchable wettability in the presence of saccharides.[485] The used copolymer contained *N*-isopropylacrylamide and a derivative containing phenylboronic acid. Its polymerization on micro and nanostructured patterned substrates led to superhydrophobic properties. Their immersion in glucose solution changed the surface wettability into superhydrophilic due to interactions between the polymer and the glucose. The same group also showed that their polymers can also interact with nucleotides such as adenosine phosphate with similar switchable wettability (Fig. 47).[486] The group of Li also reported the elaboration of superhydrophobic surfaces made of calix[4]azacrown.[487] The sensors could selectively interact with 1-butyl-3-methylimidazolium ions but only with Cl^- counterions (the tests were also realized with Br^- and PF_6^-) due to specific insertion of Cl- ions in azacrown and 1-butyl-3-methylimidazolium with the calix moiety. The interactions induced also a change in the surface hydrophobicity from superhydrophobic to superhydrophilic. Yao et al. also reported the elaboration superhydrophobic electrocatalytic sensors made of C_{60} hollow spheres by bubble-templates.[488] These sensors displayed highly sensitivity and selective detection of dopamine in the presence of ascorbic acid, and uric acid in the presence of *L*-cysteine.

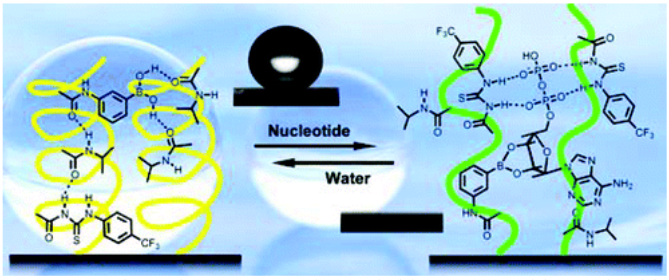

Fig. 47 Schematic representation of biosensors with nucleotide recognition and switchable superhydrophobic properties.
Reprinted with permission from ref. 486, copyright 2009, American Chemical Society.

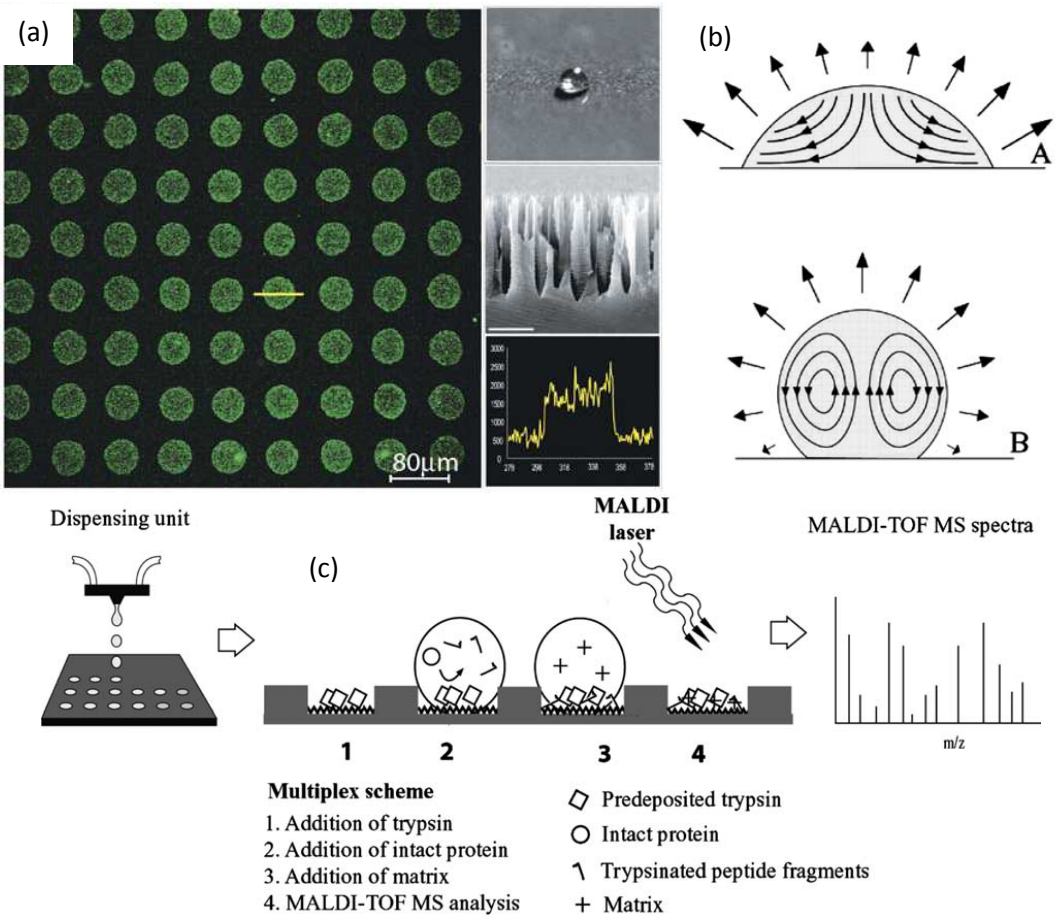

Fig. 48 Superhydrophobic surfaces to improve bioanalytical readout based on (a) porous Si and (b) evaporation of droplets containing proteins; (c) target anchor chips developed to increase the sensitivity of MALD-TOF MS.
Reprinted with permission from ref. 493, copyright 2007, Elsevier B.V.

Superhydrophobic surfaces can also find applications in immunoassays.[489-491] Shen and al. reported the advantages to use superhydrophobic polycarbonate surfaces in *Schistosoma japonicum* antibodies (SjAb) immunoassays, which consist in sensitive stripping voltammetry analysis coupled with Cu enhanced Au nanoparticles tag amplification.[490] First of all, small total volumes were required and short assay times. Moreover, the technique was quantitatively sensitive to SjAb concentrations ranging from 2 ng ml^{-1} to 15 μg mL^{-1} with a detection limit of 1.3 ng ml^{-1}.

Superhydrophobic properties can also be used to improve bioanalytical readout. For this purpose, protein microarrays are very often used.[492-494] The group of Ressine elaborated porous Si with various porosities and hydrophobicities by electrochemical etching in the presence of HF (Fig. 48a).[493-494] After ink-injection of antibodies (antirabbit IgG), the authors observed that the antibody spots are well confined to a diameter of 50 μm, allowing higher microarray density of over 15000 spots per square centimeter. The higher homogeneity of antibodies all in all the spot is due to the presence of a rotational flow during the evaporation when the surface is hydrophobic (Marangoni effect) (Fig. 48b). Such substrates were also used for MALDI-TOF MS detection. Indeed, such techniques were developed because it is not possible to obtain antibodies with no reactivity to any other proteins. Here, superhydrophobic MALDI-TOF MS target anchor chips were developed to increase the sensitivity of MALDI-TOF MS by creating hydrophilic anchor points (500 μm) by proton beam irradiation surrounded by superhydrophobic porous areas (Fig. 48c). Then, 5 μL of sample with matrix were deposited on a hydrophilic anchor point. After desorption and ionization, the authors observed an increase in detection peaks of proteins by five to sevenfold in comparison with a standard MALDI target.

The group of Alam also used the properties of superhydrophobic surfaces to concentrate ultra-diluted DNA solutions onto an electrode for non-faradaic impedance spectroscopy measurements.[495] They observed an enhancement of the detection limit by five orders of magnitude. This strategy was also used by other authors to deposit various bioactive agents or cells as well as multilayers.[496-498]

Other groups also used superhydrophobic/superhydrophilic contrast to immobilize proteins or cells in the superhydrophilic areas (Fig. 49).[499-502] Chi et al. elaborated substrates with superhydrophobic/superhydrophilic contrasts by formation of

TiO_2 nanotubes by Ti anodization and photocatalytic lithography.[499] With this method, the authors could selectively immobilize cells, proteins with reversibility, as well as various chemicals and materials such as calcium phosphate, Ag nanoparticles, drugs and biomolecules. For example, they demonstrated the SERS enhancement using Ag nanoparticles. A similar strategy was also used in the literature to immobilize and real-time monitor cells on superhydrophobic/superhydrophilic Au-TiO_2 micropatterns modified with L-cysteine and functional proteins.[500]

3.14 Drug Delivery

The elaboration of drug delivery systems is very interesting to target specifically, for example, cancerous tissues with a drug released over a period of time in a controlled manner. To obtain materials with tunable drug delivery release, electrospun poly(ε-caprolactone) fibers doped with hydrophobic poly(glycerol monostearate-*co*-ε-caprolactone) (PGC-C18) were used as superhydrophobic scaffold materials.[503-504] The authors showed that when a bioactive agent (SN-38 or CPT-11) is added in the materials, this one can be released in a controlled manner. Indeed, the displacement of the air trapped in the materials is determining in the rate of the drug delivery (Fig. 50). The hydrophobicity of the materials allows to slow down the drug release process by increasing the stability of the entrapped air layer. These materials showed efficiency against cancer cells in vitro. The same authors also showed that the air trapped can be released using high-intensity focused ultrasound.[505] Lynn et al. also reported the use of superhydrophobic polyelectrolyte multilayers, which are intrinsically hydrophilic, to promote long-term release of water-soluble agents.[506] In their system, the release rate is controlled by the slow penetration of water inside the material.

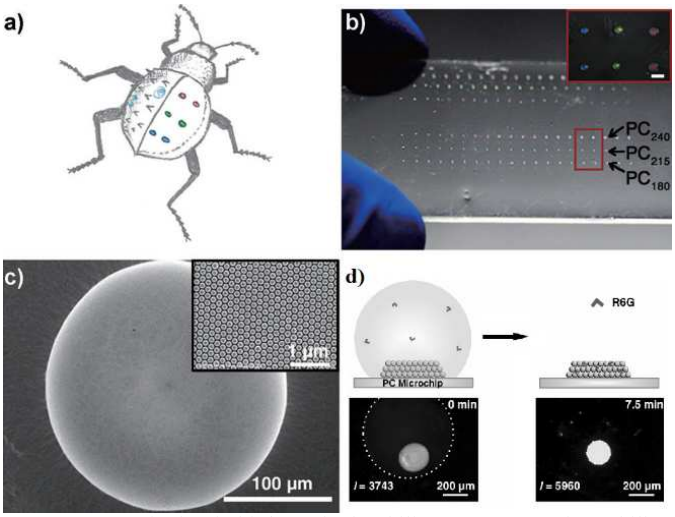

Fig. 49 Superhydrophobic/superhydrophilic contrast to immobilize proteins in the superhydrophilic areas, based on Namib desert Beetles. Reprinted with permission from ref. 502, copyright 2014, Wiley-VCH.

The drug delivery process can also be performed by encapsulation and delivery using responsive materials. Usually, drug delivery systems suffers from efficiency and poor control of the drug release. Here, superhydrophobic surfaces were used to form microgel just by deposition of droplets of the material to form spherical particles and crosslinking.[507-509] Here, pH-sensitive chitosan microgels were prepared and loaded with the antitumoral drug 5-fluorouracil (Fig. 51).[507-508] The surface was coated with pectin to prevent premature leakage of the drug and improve the controlled release. An encapsulation efficiency of 100% was obtained for microgels in the range 200-600 µm. The release rate depended on the pH. Such materials enhanced the cytotoxic effect of 5-fluorouracil and can be used to treat colon cancer. Using this strategy, temperature-sensitive microgels of dextran-methacrylated and poly(*N*-isopropylacrylamide) were also prepared and loaded with insulin and bovine serum albumin (BSA).[509] The rate of the release was depending on the bead's composition and the temperature.

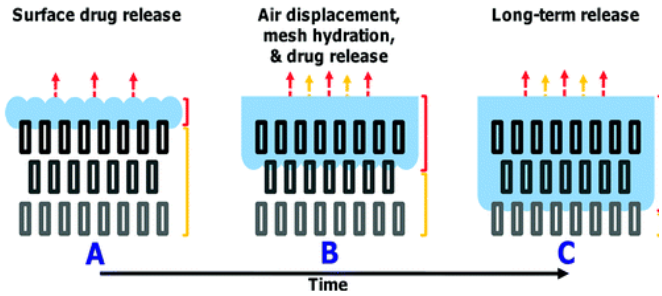

Fig. 50 Schematic representation of drug delivery systems based on the displacement of the air trapped on superhydrophobic materials. Reprinted with permission from ref. 503, copyright 2012, American Chemical Society.

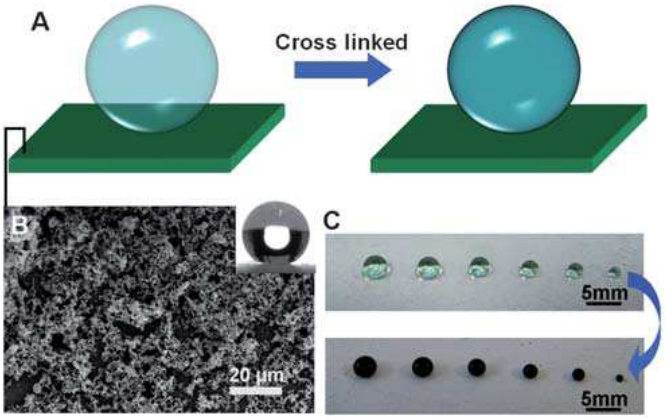

Fig. 51 Elaboration of drug delivery systems by deposition of droplets and cross-linking on superhydrophobic surfaces.[508]

3.15 Heterogeneous Catalysis

Catalysts are extremely used in chemistry to increase the rate of reactions. In the case of catalysis, the surface wettability of the supported catalysis seems to be important for their activity. As a consequence the study of superhydrophobic catalysis seems to be an interesting way. Heterogeneous catalysts can in certain conditions show higher activities than homogenous catalysts.

The group of Xiao reported this effect using superhydrophobic mesoporous polymers made of divinylbenzene and an imidazolium moiety containing trifluoromethanesulfonate counterions (Fig. 52).[510-511] They observed an increase in transesterification to form biodiesel. Similar results were also reported using superhydrophobic mesoporous polymers made of divinylbenzene and *p*-styrene sulfonic acid.[512-513] Moreover, with *p*-styrene sulfonyl chloride, they functionalized the polymer with 1,2-diphenylethylenediamine and used it for the coordination of a ruthenium catalyst ($[RuCl_2(p\text{-cymene})_2]$).[514] Due to their good wettability to ketones and their high ability to transfer product from the catalyst into water phase, these heterogeneous catalysts showed higher activities in asymmetric transfer hydrogenation of ketones than their corresponding homogeneous catalysts.

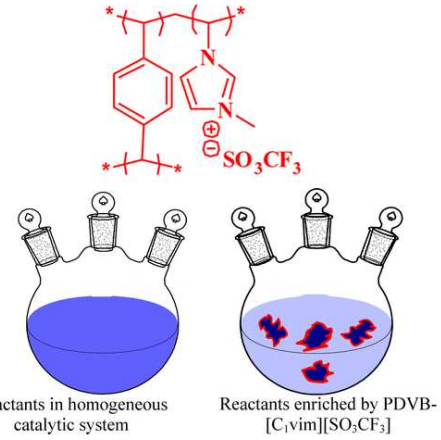

Fig. 52 Superhydrophobic mesoporous polymers made of divinylbenzene and an imidazolium moiety containing trifluoromethanesulfonate counterions, as heterogeneous catalysts for transesterification to form biodiesel.
Reprinted with permission from ref. 510, copyright 2012, American Chemical Society.

Superhydrophobic catalysts were also reported by incorporating cobalt in silica nanoparticles and their functionalization with 3,3,3-trifluoro-propyl groups.[515] Due to their higher wettability to organic molecules and their higher repellency to water (product of reaction), these catalysts showed higher catalytic activity for selective oxidation of hydrocarbons than a hydrophilic one. Gold nanoparticles were also encapsulated in silica core-shell sphere containing isobutyl groups to reach superhydrophobic with yolk-shell nanostructures after HF etching.[516] These surfaces enhanced the catalytic performance in the reduction of nitroaromatic compound. Nanostructured surfaces containing Co, Ni and CoNi allows were also studied in the literature.[517] Superhydrophobic films with various nanostructures such as nanosheets or urchin-like structures were obtained a magnetic-field-induced deposition process. The authors reported an excellent catalytic effect for the reduction of *p*-nitrophenol with sodium borohydride with a high durability of the catalysts. The group of Song also reported the catalytic effect of hybrid materials.[518] Combining calixarene with EuW_{10}, highly hydrophobic films ($\theta_w > 139°$) were obtained with a high efficiency in extractive oxidative desulfurization. Superhydrophobic organo-titanosilicate with covalently linked phenyl groups were also reported by Fan et al. They showed that promising catalytic activity in the epoxidation of olefins using H_2O_2 aqueous solutions.[519]

4. Conclusions

In this review, we gave a very recent overview of potential applications of superhydrophobic materials, which are characterized by extremely high water contact angle and various adhesion properties. Such materials have been elaborated by studying and mimicking natural surfaces. Here, we have extremely detailed each application including anti-icing, anti-corrosion and anti-bacteria coatings, microfluidic devices, textiles, oil/water separation, water desalination/purification, optical devices, sensors, batteries and catalysts. Now, we found that at least two parameters seem to be essential for many applications: the presence of air on superhydrophobic materials with self-cleaning properties (Cassie-Baxter state) and the robustness of the superhydrophobic properties (stability of the Cassie-Baxter state). This review opens new ways to researchers to envisage new strategies to industrialists to advance in the commercialization of these materials.

Notes and references

[a] *Univ. Nice Sophia Antipolis, LPMC, UMR 7336, CNRS, Parc Valrose, 06100 Nice, France*
Fax: (+33)4-92-07-61-56; Tel: (+33)4-92-07-61-59;
E-mail:Frederic.GUITTARD@unice.fr

† Footnotes should appear here. These might include comments relevant to but not central to the matter under discussion, limited experimental and spectral data, and crystallographic data.
Electronic Supplementary Information (ESI) available: [details of any supplementary information available should be included here]. See DOI: 10.1039/b000000x/

1 a) K. Koch and W. Barthlott, *Philos. Trans. R. Soc., A*, 2009, **367**, 1487; b) H. J. Ensikat, P. Ditsche-Kuru, C. Neinhuis and W. Barthlott, *Beilstein J. Nanotechnol.*, 2011, **2**, 152.
2 C. Neinhuis and W. Barthlott, *Ann. Bot.*, 1997, **79**, 667.
3 W. Barthlott and C. Neinhuis, *Planta*, 1997, **202**, 1.
4 S. Yang, J. Ju, Y. Qiu, Y. He, X. Wang, S. Dou, K. Liu and L. Jiang, *Small*, 2014, **10**, 294.
5 K. M. Wisdom, J. A. Watson, X. Qu, F. Liu, G. S. Watson and C.-H. Chen, *Proc. Natl. Acad. Sci. U. S. A.*, 2013, **110**, 7992.
6 R. Hensel, A. Finn, R. Helbig, H.-G. Braun, C. Neinhuis, W.-J. Fischer and C. Werner, *Adv. Mater.*, 2014, **26**, 2029.
7 R. Hensel, R. Helbig, S. Aland, H.-G. Braun, A. Voigt, C. Neinhuis, C. Werner, *Langmuir*, 2013, **29**, 1100.
8 R. Helbig, J. Nickerl, C. Neinhuis, C. Werner, *PLoS One*, 2011, **6**, e25105.

9 D. G. Stavenga, S. Foletti, G. Palasantzas and K. Arikawa, *Proc. R. Soc. B*, 2006, **273**, 661.
10 a) X. Gao, X. Yan, X. Yao, L. Xu, K. Zhang, J. Zhang, B. Yang and L. Jiang, *Adv. Mater.*, 2007, **19**, 2213; Z. Sun, T. Liao, K. Liu, L. Jiang, J. H. Kim and S. X. Dou, *Small*, DOI: 10.1002/smll.201400516.
11 Y. Zheng, X. Gao and L. Jiang, *Soft Matter*, 2007, **3**, 178.
12 E. Miyako, T. Sugino, T. Okazaki, A. Bianco, M. Yudasaka and S. Iijima, *ACS Nano*, 2013, **10**, 8736.
13 E. P. Ivanova, J. Hasan, H. K. Webb, V. K. Truong, G. S. Watson, J. A. Watson, V. A. Baulin, S. Pogodin, J. Y. Wang, M. J. Tobin, C. Loebbe and R. J. Crawford and, *Small*, 2012, **8**, 2489.
14 N. J. Shirtcliffe, G. McHale and M. I. Newton, *Langmuir*, 2009, **25**, 14121.
15 A. R. Parker and C. R. Lawrence, *Nature*, 2001, **414**, 33.
16 W. Barthlott, T. Schimmel, S. Wiersch, K. Koch, M. Brede, M. Barczewski, S. Walheim, A. Weis, A. Kaltenmaier, A. Leder and H. F. Bohn, *Adv. Mater.*, 2010, **22**, 2325.
17 G. S. Watson, B. W. Cribb and J. A. Watson, *Acta Biomater.*, 2010, **6**, 4060.
18 D. L. Hu, B. Chan and J. W. M. Bush, *Nature*, 2003, **423**, 663.
19 D. Y. Lee, D. H. Lee, S. G. Lee, K. Cho, *Soft Matter*, 2012, **8**, 4905.
20 R. N. Wenzel, *Ind. Eng. Chem.*, 1936, **28**, 988.
21 a) A. B. D. Cassie, S. Baxter, *Trans. Faraday Soc.*, 1944, **40**, 546; b) S. Baxter, A. B. D. Cassie, *J. Text. Inst.*, *Trans.* 1945, **36**, T67.
22 A. Marmur, *Langmuir*, 2008, **24**, 7573.
23 A. Marmur, *Soft Matter*, 2013, **9**, 7900.
24 T. Darmanin, E. Taffin de Givenchy, S. Amigoni and F. Guittard, *Adv. Mater.*, 2013, **25**, 1378.
25 T. Darmanin and F. Guittard, *Prog. Polym. Sci.*, 2014, **39**, 656.
26 E. Celia, T. Darmanin, E. Taffin de Givenchy, S. Amigoni and F. Guittard, *J. Colloid Interface Sci.*, 2013, **402**, 1.
27 M. Wolfs, T. Darmanin and F. Guittard, *Polym. Rev.*, 2013, **53**, 460.
28 A. Marmur, *Contact Angle, Wettability Adhes.* 2009, **6**, 3.
29 T. Young, *Philos. Trans. R. Soc. London* 1805, **95**, 65.
30 Y.-L. Zhang, H. Xia, E. Kim and H.-B Sun, *Soft Matter*, 2012, **8**, 11217.
31 X. Zhang, F. Shi, J. Niu, Y. Jiang and Z. Wang, *J. Mater. Chem.*, 2008, **18**, 621.
32 L. Cao, H.-H. Hu and D. Gao, *Langmuir*, 2007, **23**, 4310.
33 a) E. Bormashenko, *Philos. Trans. R. Soc., A*, 2010, **365**, 4695; b) E. Bormashenko, T. Stein, G. Whyman, Y. Bormashenko and R. Pogreb, *Langmuir*, 2006, **22**, 9982.
34 J.-L. Liu, X.-Q. Feng, G. Wang and S.-W. Yu, *J. Phys.: Condens. Matter* 2007, **19**, 356002/1.
35 F. J. Wang, S. Lei, J. F. Ou, M. S. Xue and W. Li, *Appl. Surf. Sci.*, 2013, **276**, 397.
36 K. Koch, B. Bhushan and W. Barthlott, *Soft Matter*, 2008, **4**, 1943-1963.
37 H. Bellanger, T. Darmanin, E. Taffin de Givenchy and F. Guittard, *Chem. Rev.*, 2014, **114**, 2694
38 R. Rakitov and S. N. Gorb, *Proc. R. Soc. B*, 2013, **280**, 20122391.
39 a) J. Bico, U. Thiele and D. Quere, *Colloids Surf., A* 2002, **206**, 41; b) K. Kurogi, H. Yan and K. Tsujii, *Colloids Surf., A* 2008, **317**, 592.
40 a) R. M. Fillion, A. R. Riahi and A. Edrisy, *Renewable Sustainable Energy Rev.*, 2014, **32**, 797; b) Y. Yingdi, L. Nengzhen, X. Xiangao, X. Yiming, Z. Qinghua and Z. Xiaoli, *Prog. Chem.*, 2014, **26**, 214.
41 a) P. Tourkine, M. Le Merrer and D. Quéré, *Langmuir*, 2009, **25**, 7214; b) M. He, J. Wang, H. Li, X. Jin, J. Wang, B. Liu and Y. Song, *Soft Matter*, 2010, **6**, 2396.
42 M. He, J. Wang, H. Lia and Y. Song, *Soft Matter*, 2011, **7**, 3993.
43 A. Alizadeh, M. Yamada, R. Li, W. Shang, S. Otta, S. Zhong, L. Ge, A. Dhinojwala, K. R. Conway, V. Bahadur, A. J. Vinciquerra, B. Stephens and M. L. Blohm, *Langmuir*, 2012, **28**, 3180.
44 L. Boinovich, A. M. Emelyanenko, V. V. Korolev and A. S. Pashinin, *Langmuir*, 2014, **30**, 1659.
45 S. Jung, M. Dorrestijn, D. Raps, A. Das, C. M. Megaridis and D Poulikakos, *Langmuir*, 2011, **27**, 3059.
46 S. A. Kulinich and M. Farzaneh, *Appl. Surf. Sci.*, 2009, **255**, 8153.
47 L. Cao, A. K. Jones, V. K. Sikka, J. Wu and D. Gao, *Langmuir*, 2009, **25**, 12444.
48 A. J. Meuler, J. D. Smith, K. K. Varanasi, J. M. Mabry, G. H. McKinley and R. E. Cohen, *ACS Appl. Mater. Interfaces*, 2010, **2**, 3100.
49 A. J. Meuler, G. H. McKinley and R. E. Cohen, *ACS Nano*, 2010, **4**, 7048.
50 S. A. Kulinich and M. Farzaneh, *Langmuir*, 2009, **25**, 8854.
51 M. A. Sarshar, C. Swarctz, S. Hunter, J. Simpson and C.-H. Choi, *Colloid Polym. Sci.*, 2013, **291**, 427.
52 J. B. Boreyko, B. R. Srijanto, T. D. Nguyen, C. Vega, M. Fuentes-Cabrera and C. P. Collier, *Langmuir*, 2013, **29**, 9516.
53 L. Mishchenko, B. Hatton, V. Bahadur, J. A. Taylor, T. Krupenkin and J. Aizenberg, *ACS Nano*, 2010, **4**, 7699.
54 a) S. A. Kulinich, S. Farhadi, K. Nose and X. W. Du, *Langmuir*, 2011, **27**, 25; b) L. B. Boinovich, A. M. Emelyanenko, V. K. Ivanov and A. S. Pashinin, *ACS Appl. Mater. Interfaces*, 2013, **5**, 2549; c) S. A. Kulinich and M. Farzaneh, *Cold Reg. Sci. Technol.*, 2011, **65**, 60; d) S. Farhadi, M. Farzaneh, S. A. Kulinich, *Appl. Surf. Sci.*, 2011, **257**, 6264.
55 J. Chen, J. Liu, M. He, K. Li, D. Cui, Q. Zhang, X. Zeng, Y. Zhang, J. Wang and Y. Song, *Appl. Phys. Lett.*, 2012, **101**, 111603/1.
56 K. K. Varanasi, T. Deng, J. D. Smith, M. Hsu and N. Bhate, *Appl. Phys. Lett.*, 2010, **97**, 234102/1.
57 M. Nosonovsky and V. Hejazi, *ACS Nano*, 2012, **6**, 8488.
58 V. Hejazi, K. Sobolev and M. Nosonovsky, *Sci. Rep.*, 2013, **3**, 2194.
59 a) T. Jing, Y. Kim, S. Lee, D. Kim, J. Kim and W. Hwang, *Appl. Surf. Sci.*, 2013, **276**, 37; b) L. Wang, M. Wen, M. Zhang, L. Jiang and Y. Zheng, *J. Mater. Chem. A*, 2014, **2**, 3312.
60 V. Bahadur, L. Mishchenko, B. Hatton, J. A. Taylor, J. Aizenberg and T. Krupenkin, *Langmuir*, 2011, **27**, 14143.
61 M. Ruan, W. Li, B. Wang, B. Deng, F. Ma and Z. Yu, *Langmuir*, 2013, **29**, 8482.
62 M. Song, Y. Liu, S. Cui, L. Liu and M. Yang, *Appl. Surf. Sci.*, 2013, **283**, 19.
63 Y. Wang, J. Xue, Q. Wang, Q. Chen and J. Ding, *ACS Appl. Mater. Interfaces*, 2013, **5**, 3370.
64 L. Huang, Z. Liu, Y. Liu and Y. Gou, *Int. J. Therm. Sci.*, 2011, **50**, 432.
65 X. Li, B. Yang, Y. Zhang, G. Gu, M. Li and L. Mao, *J. Sol-Gel Sci. Technol.*, 2014, **69**, 441.

66 H. Wang, L. Tang, X. Wu, W. Dai and Y. Qiu, *Appl. Surf. Sci.*, 2007, **253**, 8818.
67 a) P. Kim, T.-S. Wong, J. Alvarenga, M. J. Kreder, W. E. Adorno-Martinez and J. Aizenberg, *ACS Nano*, 2012, **6**, 6569; b) H. A. Stone, *ACS Nano*, 2012, **6**, 6536.
68 L. Ejenstam, L. Ovaskainen, I. Rodriguez-Meizoso, L. Wagberg, J. Pan, A. Swerin and P. M. Claesson, *J. Colloid Interface Sci.*, 2013, **412**, 56.
69 D. Yu and J. Tian, *J. Colloid Interface Sci.*, 2014, **445**, 75.
70 J. Ou, W. Hu, M. Xue, F. Wang and W. Li, *ACS Appl. Mater. Interfaces*, 2013, **5**, 3101.
71 J. Ou, M. Liu, W. Li, F. Wang, M. Xue and C. Li, *ACS Appl. Mater. Interfaces*, 2012, **258**, 4724.
72 T. Ishizaki and M. Sakamoto, *Langmuir*, 2011, **27**, 2375.
73 H. Liu, S. Szunerits, W. Xu and R. Boukherroub, *ACS Appl. Mater. Interfaces*, 2009, **1**, 1150.
74 L. Feng, Y. Che, Y. Liu, X. Qiang, Y. Wang, *Appl. Surf. Sci.*, 2013, **283**, 367.
75 F. Zhang, S. Chen, L. Dong, Y. Lei, T. Liu and Y. Yin, *Appl. Surf. Sci.*, 2011, **257**, 2587.
76 T. He, Y. Wang, Y. Zhang, Q. Iv, T. Xu and T. Liu, *Corros. Sci.*, 2009, **51**, 1757.
77 P. Wang, R. Qiu, D. Zhang, Z. Lin and B. Hou, *Electrochim. Acta*, 2010, **56**, 517.
78 P. Wang, D. Zhang, R. Qiu, and J. Wu, *Corros. Sci.*, 2014, **83**, 317.
79 P. Wang, D. Zhang and R. Qiu, *Corros. Sci.*, 2012, **54**, 77.
80 P. Wang, D. Zhang, R. Qiu and B. Hou, *Corros. Sci.*, 2011, **53**, 2080.
81 Y. Fan, Z. Chen, J. Liang, Y. Wang and H. Chen, *Surf. Coat. Technol.*, 2014, **244**, 1.
82 a) L. Zhao, Q. Liu, R. Gao, J. Wang, W. Yang and L. Liu, *Corros. Sci.*, 2014, **80**, 177; b) T. Ning, W. Xu and S. Lu, *Appl. Surf. Sci.*, 2011, **258**, 1359.
83 Y. Liu, X. Yin, J. Zhang, S. Yu, Z. Han and L. Ren, *Electrochem. Acta*, 2014, **125**, 395.
84 A. V. Rao, S. S. Latthe, S. A. Mahadik, C. Kappenstein, *Appl. Surf. Sci.*, 2011, **257**, 5772.
85 Y. Fan, C. Li, Z. Chen and H. Chen, *Appl. Surf. Sci.*, 2012, **258**, 6531.
86 N. Valipour Motlagh, F. Ch. Birjandi, J. Sargolzaei and N. Shahtahmassebi, *Appl. Surf. Sci.*, 2013, **283**, 636.
87 Y. Hu, S. Huang, S. Liu and W. Pan, *Appl. Surf. Sci.*, 2012, **258**, 7460.
88 T. T. Isimjan, T. Wang and S. Rohani, *Chem. Eng. J.*, 2012, **210**, 182.
89 R. Gao, Q. Liu, J. Wang, X. Zhang, W. Yang, J. Liu and L. Liu, *Chem. Eng. J.*, 2014, **241**, 352.
90 L. Liu, F. Xu, Z. Yu and P. Dong, *Appl. Surf. Sci.*, 2012, **258**, 8928.
91 T. Ishizaki, J. Hieda, N. Saito, N Saito and O. Takai, *Electrochim. Acta*, 2010, **55**, 7094.
92 B. Grignard, A. Vaillant, J. de Coninck, M. Piens, A. M. Jonas, C. Detrembleur and C. Jerome, *Langmuir*, 2011, **27**, 335.
93 S. Yuan, S. O. Pehkonen, B. Liang, Y. P. Ting, K. G. Neoh and E. T. Kang, *Corros. Sci.*, 2011, **53**, 2738.
94 C.-J. Weng, C.-H. Chang, C.-W. Peng, S.-W. Chen, J.-M. Yeh, C.-L. Hsu and Y. Wei, *Chem. Mater.*, 2011, **23**, 2075.
95 C.-W. Peng, K.-C. Chang, C.-J. Weng, M.-C. Lai, C.-H. Hsu, S.-C. Hsu, Y.-Y. Hsu, W.-I. Hung, Y. Wei and J.-M. Yeh, *Electrochim. Acta*, 2013, **95**, 192; b) K.-C. Chang, H.-I. Lu, C.-W. Peng, M.-C. Lai, S.-C. Hsu, M.-H. Hsu, Y.-K. Tsai, C.-H. Chang, W.-I. Hung, Y. Wei and J.-M. Yeh, *ACS Appl. Mater. Interfaces*, 2013, **5**, 1460.
96 D. Zhu, X. Lu and Q. Lu, Langmuir, 2014, 30, 4671.
97 C.-W. Peng, K.-C. Chang, C.-J. Weng, M.-C. Lai, C.-H. Hsu, S.-C. Hsu, S.-Y. Li, Y. Wei and J.-M. Yeh, *Polym. Chem.*, 2013, **4**, 926.
98 A. C. C. de Leon, R. B. Pernites and R. C. Advincula, *ACS Appl. Mater. Interfaces*, 2012, **4**, 3169–3176.
99 Q. F. Xu and J. N. Wang, *New J. Chem.*, 2009, **33**, 734.
100 C.-J. Weng, C.-H. Chang, I.-L. Lin, J.-M. Yeh, Y. Wei, C.-L. Hsu and P. H. Chen, *Surf. Coat. Technol.*, 2012, **207**, 42.
101 X. H. Xu, Z. Z. Zhang, F. Guo, J. Yang, X. T. Zhu, *Appl. Surf. Sci.*, 2011, **257**, 7054.
102 J. Hasan, H. K. Webb, V. K. Truong, S. Pogodin, V. A. Baulin, G. S. Watson, J. A. Watson, R. J. Crawford and E. P. Ivanova, *Appl. Microbiol. Biotechnol.*, 2013, **97**, 9257.
103 B. Yin, T. Liu and Y. Yin, *Langmuir*, 2012, **28**, 17019.
104 T. Liu, B. Yin, T. He, N. Guo, L. Dong and Y. Yin, *ACS Appl. Mater. Interfaces*, 2012, **4**, 4683.
105 L. Shen, B. Wang, J. Wang, J. Fu, C. Picart and J. Ji, *ACS Appl. Mater. Interfaces*, 2012, **4**, 4476.
106 H. Yang, W. You, Q. Shen, X. Wang, J. Sheng, D. Cheng, X. Cao and C. Wu, *RSC Adv.*, 2014, **4**, 2793.
107 J.-S. Chung, B. G. Kim, S. Shim, S.-E. Kim, E.-H. Sohn, J. Yoon and J.-C. Lee, *J. Colloid Interface Sci.*, 2012, **366**, 64.
108 K. Yamauchi, Y. Yao, T. Ochiai, M. Sakai, Y. Kubota and G. Yamauchi, *J. Nanotechnol.*, 2011, **2011**, 380979/1.
109 Y. Yao, K. Yamauchi, G. Yamauchi, T. Ochiai, T. Murakami and Y. Kubota, *J. Biomater. Nanobiotechnol.*, 2012, **3**, 421.
110 M. S. Khalil-Abad and M. E. Yazdanshenas, *J. Colloid Interface Sci.*, 2010, **351**, 293.
111 C.-H. Xue, J. Chen, W. Yin, S.-T. Jia and J.-Z. Ma, *Appl. Surf. Sci.*, 2012, **258**, 2468.
112 I. S. Bayer, D. Fragouli, A. Attanasio, B. Sorce, G. Bertoni, R. Brescia, R. Di Corato, T. Pellegrino, M. Kalyva, S. Sabella, P. P. Pompa, R. Cingolani and A. Athanassiou, *ACS Appl. Mater. Interfaces*, 2011, **3**, 4024.
113 B. Simoncic, B. Tomsic, L. Cerne, B. Orel, I. Jerman, J. Kovac, M. Zerjav and A. Simoncic, *J. Sol-Gel Sci. Technol.*, 2012, **61**, 340.
114 A. Berendjchi, R. Khajavi and M. E. Yazdanshenas, *Nanoscale Res. Lett.*, 2011, **6**, 594.
115 B. Simoncic, B. Tomsic, L. Cerne, B. Orel, I. Jerman, J. Kovac, M. Zerjav and A. Simoncic, *J. Sol-Gel Sci. Technol.*, 2012, **61**, 340.
116 T. Sun, H. Tan, D. Han, Q. Fu and L. Jiang, *Small*, 2005, **1**, 959.
117 J. Zhao, L. Song J. Yin and W. Ming, *Chem. Commun.*, 2013, **49**, 9191.
118 J. Ballester-Beltrán, P. Rico, D. Moratal, W. Song, J. F. Mano and M. Salmerón-Sánchez, *Soft Matter*, 2011, **7**, 10803.
119 T. Ishizaki, N. Saito and O. Takai, *Langmuir*, 2010, **26**, 8147.
120 T.-J. Ko, E. Kim, S. Nagashima, K. H. Oh, K.-R. Lee, S. Kim and M.-W. Moon, *Soft Matter*, 2013, **9**, 8705.
121 E. S. Leibner, N. Barnthip, W. Chen, C. R. Baumrucker, J. V. Badding, M. Pishko and E. A. Vogler, *Acta Biomater.*, 2009, **5**, 1389.
122 Q. Huang, L. Lin, Y. Yang, R. Hu, E. A. Vogler and C. Lin, *Biomaterials*, 2012, **33**, 8213.

123 J. Li, Q. Han, Y. Zhang, W. Zhang, M. Dong, F. Besenbacher, R. Yang and C. Wang, *ACS Appl. Mater. Interfaces*, 2013, **5**, 9816.
124 J.-Y. Shiu and P. Chen, *Adv. Funct. Mater.*, 2007, **17**, 2680.
125 R. B. Pernites, C. M. Santos, M. Maldonado, R. R. Ponnapati, D. F. Rodrigues and R. C. Advincula, *Chem. Mater.*, 2012, **24**, 870.
126 S. H. Yoon, N. Rungraeng, W. Song and S. Jun, *J. Food Eng.*, 2014, **131**, 135.
127 C. Hu, S. Liu, B. Li, H. Yang, C. Fan and W. Cui, *Adv. Healthcare Mater.*, 2013, **2**, 1314.
128 X. Zhang, L. Wang and E. Levaenen, *RSC Adv.*, 2013, **3**, 12003.
129 N. J. Shirtcliffe, G. McHale and M. I. Newton, *PLoS One*, 2012, **7**, e36983.
130 C. Jin, Y. Jiang, T. Niu and J. Huang, *J. Mater. Chem.*, 2012, **22**, 12562.
131 C. P. Stallard, K. A. McDonell, O. D. Onayemi, J. P. O'Gara and D. P. Dowling, *Biointerphases*, 2012, **7**, 31.
132 B. J. Privett, J. Youn, S. A. Hong, J. Lee, J. Han, J. H. Shin and M. H. Schoenfisch, *Langmuir*, 2011, **27**, 9597.
133 C. R. Crick, S. Ismail, Jonathan Pratten and I. P. Parkin, *Thin Solid Films*, 2011, **519**, 3722.
134 L. R. Freschauf, J. McLane, H. Sharma and M. Khine, *PLoS One*, 2012, **7**, e40987.
135 E. Fadeeva, V. K. Truong, M. Stiesch, B. N. Chichkov, R. J. Crawford, J. Wang and E. P. Ivanova, *Langmuir*, 2011, **27**, 3012.
136 J. Ma, Y. Sun, K. Gleichauf, J. Lou and Q. Lin, *Langmuir*, 2011, **27**, 10035.
137 F. Poncin-Epaillard, J. M. Herry, P. Marmey, G. Legeay, D. Debarnot and M. N. Bellon-Fontaine, *Mater. Sci. Eng. C*, 2013, **33**, 1152.
138 J. Tarrade, T. Darmanin, E. Taffin de Givenchy, F. Guittard, D. Debarnot and F. Poncin-Epaillard, *Appl. Surf. Sci.*, 2014, **292**, 782.
139 A. Rawal, *Langmuir*, 2012, **28**, 3285.
140 G. Whyman and E. Bormashenko, *Langmuir*, 2011, **27**, 8171.
141 E. Bormashenko, *Colloids Surf., A*, 2008, **324**, 47.
142 Y. Yoo, J. B. You, W. Choi and S. G. Im, *Polym. Chem.*, 2013, **4**, 1664.
143 a) H. Zhou, H. Wang, H. Niu, A. Gestos, X. Wang and T. Lin, *Adv. Mater.*, 2012, **24**, 2409; b) H. Zou, S. Lin, Y. Tu, G. Liu, J. Hu, F. Li, L. Miao, G. Zhang, H. Luo, F. Liu, C. Hou and M. Hu, *J. Mater. Chem. A*, 2013, **1**, 11246.
144 a) Y. Zhao, Z. Xu, X. Wang and T. Lin, *Langmuir*, 2012, **28**, 6328; b) B. Deng, R. Cai, Y. Yu, H. Jiang, C. Wang, J. Li, L. Li, Ming Yu, J. Li, L. Xie, Q. Huang and C. Fan, *Adv. Mater.*, 2010, **22**, 5473.
145 a) J. Zhang, B. Li, L. Wu and A. Wang, *Chem. Commun.*, 2013, **49**, 11509; c) L. Wu, J. Zhang, B. Li and A. Wang, *J. Mater. Chem. B*, 2013, **1**, 4756; b) H. Zhou, H. Wang, H. Niu, A. Gestos and T. Lin, *Adv. Funct. Mater.*, 2013, **23**, 1664.
146 a) T. Darmanin and F. Guittard, *J. Am. Chem. Soc.*, 2009, **131**, 7928; b) T. Darmanin, and F. Guittard, *Macromol. Chem. Phys.*, 2013, **214**, 2036.
147 a) J. Tarrade, T. Darmanin, E. Taffin de Givenchy and F. Guittard, *RSC Adv.*, 2013, **3**, 10848; b) H. Bellanger, T. Darmanin, E. Taffin de Givenchy and F. Guittard, *Colloids Surf., A*, 2013, **433**, 47.
148 a) H. Bellanger, T. Darmanin, E. Taffin de Givenchy and F. Guittard, *RSC Adv.*, 2013, **3**, 5556; b) H. Bellanger, T. Darmanin, E. Taffin de Givenchy and F. Guittard, *J. Mater. Chem. A*, 2013, **1**, 2896.
149 a) P. Conte, T. Darmanin and F., *React. Funct. Polym.*, 2014, **74**, 46; b) H. Bellanger, T. Darmanin and F. Guittard, *Langmuir*, 2012, **28**, 186.
150 W. Choi, A. Tuteja, S. Chhatre, J. M. Mabry, R. E. Cohen and G. H. McKinley, *Adv. Mater.*, 2009, **21**, 2190.
151 H. Wang, Y. Xue, J. Ding, L. Feng, X. Wang and T. Lin, *Angew. Chem., Int. Ed.*, 2011, **50**, 11433.
152 B. Leng, Z. Shao, G. de With and W. Ming, *Langmuir*, 2009, **25**, 2456.
153 G. R. J. Artus, J. Zimmermann, F. A. Reifler, S. A. Brewer and S. Seeger, *Appl. Surf. Sci.*, 2012, **258**, 3835.
154 C. Shillingford, N. MacCallum, T.-S. Wong, P. Kim and J. Aizenberg, *Nanotechnoogy*, 2014, **25**, 014019/1.
155 X. Zhou, Z. Zhang, X. Xu, X. Men and X. Zhu, *Appl. Surf. Sci.*, 2013, **276**, 571.
156 C. Pereira, C. Alves, A. Monteiro, C. Magén, A. M. Pereira, A. Ibarra, M. R. Ibarra, P. B. Tavares, J. P. Araújo, G. Blanco, J. M. Pintado , A. P. Carvalho, J. Pires, M. F. R. Pereira and C. Freire, *ACS Appl. Mater. Interfaces*, 2011, **3**, 2289.
157 D. D. Lovingood, W. B. Salter, K. R. Griffith, K. M. Simpson, J. D. Hearn and J. R. Owens, *Langmuir*, 2013, **29**, 15043.
158 L. Wang, X. Zhang, B. Li, P. Sun, J. Yang, H. Xu and Y. Liu, *ACS Appl. Mater. Interfaces*, 2011, **3**, 1277.
159 L. Wang, X. Zhang, B. Li, P. Sun, J. Yang, H. Xu and Y. Liu, *ACS Appl. Mater. Interfaces*, 2011, **3**, 1277.
160 W. Duan, A. Xie, Y. Shen, X. Wang, F. Wang, Y. Zhang and J. Li, *Ind. Eng. Chem. Res.*, 2011, **50**, 4441.
161 Y. Zhao, Z. Xu, X. Wang and T. Lin, *Appl. Surf. Sci.*, 2013, **286**, 364.
162 A. L. Mohamed, M. A. El-Sheikh and A. I. Waly, *Carbohydr. Polym.*, 2014, **102**, 727.
163 M. Zhang and C. Wang, *Carbohydr. Polym.*, 2013, **96**, 396.
164 D. Tian, X. Zhang, X. Wang, J. Zhai and L. Jiang, *Phys. Chem. Chem. Phys.*, 2011, **13**, 14606.
165 Z. X. Jiang, L. Geng and Y. D. Huang, *J. Phys. Chem. C*, 2010, **14**, 9370.
166 C. Wang, T. Yao, J. Wu, C. Ma, Z. Fan, Z. Wang, Y. Cheng, Q. Lin and B. Yang, *ACS Appl. Mater. Interfaces*, 2009, **1**, 2613.
167 Q. Pan, M. Wang and H. Wang, *Appl. Surf. Sci.*, 2008, **254**, 6002.
168 D.-D. La, T. A. Nguyen, S. Lee, J. W. Kim and Y. S. Kim, *Appl. Surf. Sci.*, 2011, **257**, 5705.
169 Z. Cheng, M. Du, K. Fu, N. Zhang and K. Sun, *ACS Appl. Mater. Interfaces*, 2012, **4**, 5826.
170 F. Wang, S. Lei, M. Xue, J. Ou and W. Li, *Langmuir*, 2014, **30**, 1281.
171 B. Wang and Z. Guo, *Appl. Phys. Lett.*, 2013, **103**, 063704/1.
172 H. Li, Y. Li and Q. Liu, *Nanoscale Res. Lett.*, 2013, **8**, 183.
173 D. Tian, X. Zhang, J. Zhai and L. Jiang, *Langmuir*, 2011, **27**, 4265.
174 D. Tian, Z. Guo, Y. Wang, W. Li, X. Zhang, J. Zhai and L. Jiang, *Adv. Funct. Mater.*, 2014, **24**, 536.
175 H. Li, M. Zheng, S. Liu, L. Ma, C. Zhu and Z. Xiong, *Surf. Coat. Technol.*, 2013, **224**, 88.
176 C.-F. Wang, F.-S. Tzeng, H.-G. Chen and C.-J. Chang, *Langmuir*, 2012, **28**, 10015.
177 J. Wu, J. Chen, K. Qasim, J. Xia, W. Lei, B.-p. Wang, *J. Chem. Technol. Biotehnol.*, 2012, **87**, 427.
178 H. Li, M. Zheng, L. Ma, C. Zhu and S. Lu, *Mater. Res. Bull.*, 2013, **48**, 25.

179 C. Gao, Z. Sun, K. Li, Y. Chen, Y. Cao, S. Zhang and L. Feng, *Energy Environ. Sci.*, 2013, **6**, 1147.
180 H. Yang, X. Zhang, Z.-Q. Cai, P. Pi, D. Zheng, X. Wen, J. Cheng and Z.-r. Yang, *Surf. Coat. Technol.*, 2011, **205**, 5387.
181 H. Yang, P. Pi, Z.-Q. Cai, X. Wen, X. Wang, J. Cheng and Z.-r. Yang, *Appl. Surf. Sci.*, 2010, **256**, 4095.
182 C. Lee and S. Baik, *Carbon*, 2010, **48**, 2192.
183 C. H. Lee, N. Johnson, J. Drelich and Y. K. Yap, *Carbon*, 2011, **49**, 669.
184 Y. Yang, H. Li, S. Cheng, G. Zou, C. Wang and Q. Lin, *Chem. Commun.*, 2014, **50**, 2900.
185 C. R. Crick, J. A. Gibbins and I. P. Parkin, *J. Mater. Chem. A*, 2013, **1**, 5943.
186 M. W. Lee, S. An, S. S. Latthe, C. Lee, S. Hong and S. S. Yoon, *ACS Appl. Mater. Interfaces*, 2013, **5**, 10597.
187 T. An, S. J. Cho, W. Choi, J. H. Kim, S. T. Lim and G. Lim, *Soft Matter*, 2011, **7**, 9867.
188 B. Wang, J. Li, G. Wang, W. Liang, Y. Zhang, L. Shi, Z. Guo and W. Liu, *ACS Appl. Mater. Interfaces*, 2013, **5**, 1827.
189 F. Liu, M. Ma, D. Zang, Z. Gao and C. Wang, *Carbohydr. Polym.*, 2014, **103**, 480.
190 X. Zhang, T. Geng, Y. Guo, Z. Zhang and P. Zhang, *Chem. Eng. J.*, 2013, **231**, 414.
191 Z.-Y. Deng, W. Wang, L.-H. Mao, C.-F. Wang and S. Chen, *J. Mater. Chem. A*, 2014, **2**, 4178.
192 M. Zhang, C. Wang, S. Wang and J. Li, *Carbohydr. Polym.*, 2013, **97**, 59.
193 C.-H. Xue, P.-T. Ji, P. Zhang, Y.-R. Li and S.-T. Jia, *Appl. Surf. Sci.*, 2013, **284**, 464.
194 F. Zhao, L. Liu, F. Ma and L. Liu, *RSC Adv.*, 2014, **4**, 7132.
195 N. Chen and Q. Pan, *ACS Nano*, 2013, **7**, 6875.
196 W. Zhang, Z. Shi, F. Zhang, X. Liu, J. Jin and L. Jiang, *Adv. Mater.*, 2013, **25**, 2071.
197 M. Huang, Y. Si, X. Tang, Z. Zhu, B. Ding, L. Liu, G. Zheng, W. Luo and J. Yu, *J. Mater. Chem. A*, 2013, **1**, 14071.
198 X. Tang, Y. Si, J. Ge, B. Ding, L. Liu, G. Zheng, W. Luo and J. Yu, *Nanoscale*, 2013, **5**, 11657.
199 S. U. Patel and G. G. Chase, *Sep. Purif. Technol.*, 2014, **126**, 62.
200 W. Lei, D. Portehault, D. Liu, S. Qin and Y. Chen, *Nat. Commun.*, 2013, **4**, 1777.
201 J. Wang, Y. Zheng and A. Wang, *Chem. Eng. J.*, 2012, **213**, 1.
202 B. Wang, R. Karthikeyan, X.-Y. Lu, J. Xuan and M. K. H. Leung, *Ind. Eng. Chem. Res.*, 2013, **52**, 18251.
203 Z.-Y. Wu, C. Li, H.-W. Liang, Y.-N. Zhang, X. Wang, J.-F. Chen and S.-H. Yu, *Sci. Rep.*, 2014, **4**, 4079.
204 H. Hu, Z. Zhao, Y. Gogotsi and J. Qiu, *Environ. Sci. Technol. Lett.*, 2014, **1**, 214.
205 Q. Zhu, Y. Chu, Z. Wang, N. Chen, L. Lin, F. Liu and Q. Pan, *J. Mater. Chem. A*, 2013, **1**, 5386.
206 H. Sun, A. Li, Z. Zhu, W. Liang, X. Zhao, P. La and W. Deng, *ChemSusChem*, 2013, **6**, 1057.
207 M. Guix, J. Orozco, M. Garcia, W. Gao, S. Sattayasamitsathit, A. Merkoci, A. Escarpa and J. Wang, *ACS Nano*, 2012, **6**, 4445.
208 A. Li, H.-X. Sun, D.-Z. Tan, W.-J. Fan, S.-H. Wen, X.-J. Qing, G.-X. Li, S.-Y. Li and W.-Q. Deng, *Energy Environ. Sci.*, 2011, **4**, 2062.
209 X. Chen, Y. Wu, B. Su, J. Wang, Y. Song and L. Jiang, *Adv. Mater.*, 2012, **24**, 5884.
210 C. Ruan, K. Ai, X. Li and L. Lu, *Angew. Chem., Int. Ed.*, 2014, XX.
211 a) M. Liu, S. Wang, Z. Wei, Y. Song and L. Jiang, *Adv. Mater.*, 2009, **21**, 665; b) X. Liu, J. Zhou, Z. Xue, J. Gao, J. Meng, S. Wang and L. Jiang, *Adv. Mater.*, 2012, **24**, 3401.
212 a) Z. Cheng, H. Lai, Y. Du, K. Fu, R. Hou, C. Li, N. Zhang and K. Sun, *ACS Appl. Mater. Interfaces*, 2014, **6**, 636; b) B. Wang and Z. Guo, *Chem. Commun.*, 2013, **49**, 9416.
213 D. Tian, X. Zhang, Y. Tian, Y. Wu, X. Wang, J. Zhai and L. Jiang, *J. Mater. Chem.*, 2012, **22**, 19652.
214 Q. Wen, J. Di, L. Jiang, J. Yu and R. Xu, *Chem. Sci.*, 2013, **4**, 591.
215 J. Zeng and Z. Guo, *Colloids Surf., A*, 2014, **444**, 283.
216 W. Zhang, Y. Zhu, X. Liu, D. Wang, J. Li, L. Jiang and J. Jin, *Angew. Chem., Int. Ed.*, 2014, **53**, 856.
217 Z. Xue, S. Wang, L. Lin, L. Chen, M. Liu, L. Feng and L. Jiang, *Adv. Mater.*, 2011, **23**, 4270.
218 B. Jing, H. Wang, K.-Y. Lin, P. J. McGinn, C. Na and Y. Zhu, *Polymer*, 2013, **54**, 5771.
219 Q. Zhu and Q. Pan, *ACS Nano*, 2014, **8**, 1402.
220 W. Ma, H. Xu and A. Takahara, *Adv. Mater. Interfaces*, 2014, XXX.
221 Y. Cao, N. Liu, C. Fu, K. Li, L. Tao, L. Feng and Y. Wei, *ACS Appl. Mater. Interfaces*, 2014, **6**, 2026.
222 L. Zhang, Z. Zhang and P. Wang, *NPG Asia Mater.*, 2012, **44**, e8.
223 T. Darmanin, J. Tarrade, E. Celia and F. Guittard, *J. Phys. Chem. C*, 2014, **118**, 2052.
224 T. Darmanin, J. Tarrade, E. Celia, H. Bellanger and F. Guittard, *ChemPlusChem*, 2014, **79**, 382.
225 T. Darmanin and F. Guittard, *Soft Matter*, 2013, **9**, 5982.
226 A. K. Kota, Y. Li, J. M. Mabry and A. Tuteja, *Adv. Mater.*, 2012, **24**, 5838.
227 S. Pan, A. K. Kota, J. M. Mabry and A. Tuteja, *J. Am. Chem. Soc.*, 2013, **135**, 578.
228 T. Darmanin and F. Guittard, *J. Colloid Interface Sci.*, 2013, **408**, 101.
229 S. Taleb, T. Darmanin and F. Guittard, *ACS Appl. Mater. Interfaces*, submitted.
230 J. A. Howarter and J. P. Youngblood, *Adv. Mater.*, 2007, **19**, 3838.
231 J. A. Howarter and J. P. Youngblood, *Macromol. Rapid Commun.*, 2008, **29**, 455.
232 J. Yang, Z. Zhang, X. Xu, X. Zhu, X. Men and X. Zhou, *J. Mater. Chem.*, 2012, **22**, 2834.
233 Z. Ma, Y. Hong, L. Ma and M. Su, *Langmuir*, 2009, **25**, 5446.
234 J. Ge, Y. Si, F. Fu, J. Wang, J. Yang, L. Cui, B. Ding, J. Yu and G. Sun, *RSC Adv.*, 2013, **3**, 2248.
235 J. Yang, A. Raza, Y. Si, L. Cui, J. Ge, B. Ding and J. Yu, *Nanoscale*, 2014, **4**, 7549.
236 S. J. Cho, H. Nam, H. Ryu and G. Lim, *Adv. Funct. Mater.*, 2013, **23**, 5577.
237 X. Li, C. Wang, Y. Yang, X. Wang, M. Zhu and B. S. Hsiao, *ACS Appl. Mater. Interfaces*, 2014, **6**, 2423.
238 D. Yoon, C. Lee, J. Yun, W. Jeon, B. J. Cha and S. Baik, *ACS Nano*, 2012, **6**, 5980.
239 B. Zhang, L. Liu, S. Xie, F. Shen, H. Yan, H. Wu, Y. Wan, M. Yu, H. Ma, L. Li and J. Li, *RSC Adv.*, 214, 4, 16561.
240 Y. Liao, R. Wang and A. G. Fane, *J. Membr. Sci.*, 2013, **440**, 77.

241 C. Yang, X.-M. Lia, J. Gilron, D.-f. Kong, Y. Yin, Y. Oren, C. Linder and T. He, *J. Membr. Sci.*, 2014, **456**, 155.
242 J. Zhang, Z. Song, B. Li, Q. Wang, S. Wang, *Desalination*, 2013, **324**, 1.
243 A. Razmjou, E. Arifin, G. Dong, J. Mansouri and V. Chen, *J. Membr. Sci.*, 2012, **415**–**416**, 850.
244 S. Meng, J. Mansouri, Y. Ye and V. Chen, *J. Membr. Sci.*, 2014, **450**, 48.
245 B. Zhang, L. Liu, S. Xie, F. Shen, H. Yan, H. Wu, Y. Wan, M. Yu, H. Ma, L. Li and J. Li, *RSC Adv.*, 2014, 4, 16561.
246 S. S. Madaeni, S. Zinadini and V. Vatanpour, *Sep. Purif. Technol.*, 2013, **111**, 98.
248 J. Liu, J. Jin, Y. Li, H.-W. Huang, C. Wang, M. Wu, L.-H. Chen and B.-L. Su, *J. Mater. Chem. A*, 2014, **2**, 5051.
249 H. Cao, Y. Xiao, Y. Lu, J. Yin, B. Li, S. Wu and X. Wu, *Nano Res.*, 2010, **3**, 863.
250 H. Cao, H. Zheng, K. Liu and R. Fu, *Cryst. Growth Des.*, 2010, 10, 597.
251 M. Macias-Montero, A. Borras, Z. Saghi, P. Romero-Gomez, J. R. Sanchez-Valencia, J. C. Gonzalez, A. Barranco, P. Midgley, J. Cotrino and A. R. Gonzalez-Elipe, *J. Mater. Chem.*, 2012, **22**, 1341.
252 C. R. Crick, J. C. Bear, A. Kafizas and I. P. Parkin, *Adv. Mater.*, 2012, **24**, 3505.
253 T. Kamegawa, Y. Shimizu and H. Yamashita, *Adv. Mater.*, 2012, **24**, 3697.
254 X. Wang, Y. Shen, A. Xie, L. Qiu, S. Li and Y. Wang, *J. Mater. Chem.*, 2011, **21**, 9641.
255 G. D. Bixler and B. Bhushan, *Nanoscale*, 2014, **6**, 76.
256 G. D. Bixler and B. Bhushan, *Nanoscale*, 2013, **5**, 7685.
257 B. Bhushan, *Beilstein J. Nanotechnol.*, 2011, **2**, 66.
258 O. I. Vinogradova and A. L. Dubov, *Mendeleev Commun.*, 2012, **22**, 229.
259 G. McHale, M. R. Flynn and M. I. Newton, *Soft Matter*, 2011, **7**, 10100.
260 B. Su, M. Li and Q. Lu, *Langmuir*, 2010, **26**, 6048.
261 C. Lee and C.-J. Kim, *Phys. Rev. Lett.*, 2011, **106**, 014502/1.
262 Y. Zhou, M. Li, B. Su and Q. Lu, *J. Mater. Chem.*, 2009, **19**, 3301.
263 G. McHale, M. I. Newton and N. J. Shirtcliffe, *Soft Matter*, 2010, **6**, 714.
264 O. I. Vinogradova, N. F. Bunkin, N. V. Churaev, O. A. Kiseleva, A. V. Lobeyev and B. W. Ninham, *J. Colloid Interface Sci.*, 1995, **173**, 443.
265 C. Cottin-Bizonne, J.-L. Barrat, L. Bocquet and E. Charlaix, *Nat. Mater.*, 2003, **2**, 237.
266 A. V. Belyaev and O. I. Vinogradova, *Soft Matter*, 2010, **6**, 4563.
267 R. J. Daniello, N. E. Waterhouse and J. P. Rothstein, *Phys. Fluids*, 2009, **21**, 085103/1.
268 M. B. Martell, J. B. Perot and J. P. Rothstein, *J. Fluid Mech.*, 2009, **620**, 31.
269 B. R. Elbing, E. S. Winkel, K. A. Lay, S. L. Ceccio, D. R. Dowling and M. Perlin, *J. Fluid Mech.*, 2008, **612**, 201.
270 J. Ou and J. P. Rothstein, *Phys. Fluids*, 2005, **17**, 103606/1.
271 Y. Wu, Y. Xue, X. Pei, M. Cai, H. Duan, W. T. S. Huck, F. Zhou and Q. Xue, *J. Phys. Chem. C*, 2014, **218**, 2564.
272 M. Wilson, *Phys. Today*, 2009, **62**, 16.
273 J. Zhou, A. V. Belyaev, F. Schmid and O. I. Vinogradova, *J. Chem. Phys.*, 2012, **136**, 194706/1.
274 A. V. Belyaev and O. I. Vinogradova, *Phys. Rev. Lett.*, 2011, **107**, 098301/1.
275 T. V. Nizkaya, E. S. Asmolov and O. I. Vinogradova, *Soft Matter*, 2013, **9**, 11671.
276 Y. P. Cheng C. J. Teo and B. C. Khoo, *Phys. Fluids*, 2009, **21**, 122004/1.
277 M. A. Samaha, H. V. Tafreshi and M. Gal-el-Hak, *Phys. Fluids*, 2011, **23**, 012001/1.
278 S. Lyu, D. C. Nguyen, D. Kim, W. Hwang and B. Yoon, *Appl. Surf. Sci.*, 2013, **286**, 206.
279 Z. Ming, L. Jian, W. Chunxia, Z. Xiaokang and C. Lan, *Soft Matter*, 2011, **7**, 4391.
280 Y. C. Jung and B. Bhushan, *ACS Nano*, 2009, **3**, 4155.
281 N. Vourdas, A. Tserepi, A. G. Boudouvic and E. Gogolides, *Microelectron. Eng.*, 2008, **85**, 1124.
282 F. Mumm, A. T. J. van Helvoort and P. Sikorski, *ACS Nano*, 2009, **3**, 2647.
283 J. A. Schatz, J. V. Vykoukal and P. R. C. Gascoyne, *Lab Chip*, 2004, **4**, 11.
284 J. Zhou, S. Yang, X. Y. Zeng, J. H. Wu, G. P. Chen and Y. P. Huang, *J. Adhes. Sci. Technol.*, 2012, **26**, 2087.
285 Y. Zhao and S. K. Cho, *Lab Chip*, 2006, **6**, 137.
286 S. Xing, R. S. Harake and T. Pan, *Lab Chip*, 2011, **11**, 3642.
287 G. Londe, A. Chunder, A. Wesser, L. Zhai and H. J. Cho, *Sens. Actuators, B*, 2008, **132**, 431.
288 M. C. Draper, C. R. Crick, V. Orlickaite, V. A. Turek, I. P. Parkin and J. B. Edel, *Anal. Chem.*, 2013, **85**, 5405.
289 L. Hong and T. Pan, *Microfluid. Nanofluid.*, 2011, **10**, 991.
290 X.-D. Zhao, H.-M. Fan, J. Luo, J. Ding, X.-Y. Liu, B.-S. Zou and Y.-P. Feng, *Adv. Funct. Mater.*, 2011, **21**, 184.
291 G. R. Willmott, C. Neto and S. C. Hency, *Faraday Discuss.*, 2010, **146**, 233.
292 Y.-H. Chang, Y.-T. Huang, M. K. Lo, C.-F. Lin, C.-M. Chen and S.-P. Feng, *J. Mater. Chem. A*, 2014, **2**, 1985.
293 F. Lapierre, M. Jonsson-Niedziolka, Y. Coffinier, R. Boukherroub and V. Thomy, *Microfluid. Nanofluid.*, 2013, **15**, 327.
294 T. N. Krupenkin, J. A. Taylor, T. M. Schneider and S. Yang, *Langmuir*, 2004, **20**, 3824.
295 M. Barberoglou, V. Zorba, A. Pagozidis, C. Fotakis and E. Stratakis, *Langmuir*, 2010, **26**, 13007.
296 J. L. Campbell, M. Breedon, K. Latham and K. Kalantar-zadeh, *Langmuir*, 2008, **24**, 5091.
297 Z. Han, B. Tay, C. Tan, M. Shakerzadeh and K. Ostrikov, *ACS Nano*, 2009, **3**, 3031.
298 E. Bormashenko, R. Pogreb, T. Stein, G. Whyman and M. Hakham-Itzhaq, *Appl. Phys. Lett.*, 2009, **95**, 264102/1.
299 N. Kumari, S. V. Garimella, *Langmuir*, 2011, **27**, 10342.
300 A. Torkkeli, J. Saarilahti, A. Haara, H. Harla, T. Soukka and P. Tolonen, *Proc. IEEE MEMS 2001*, 2001, 475.
301 A. Accardo, F. Mecarini, M. Leoncini, F. Brandi, E. Di Cola, M. Burghammer, C. Riekel and E. Di Fabrizio, *Lab Chip*, 2013, **13**, 332.
302 N. Verplanck, E. Galopin, J.-C. Camart, V. Thomy, Y. Coffinier and R. Boukherroub, *Nano Lett.*, 2007, **7**, 813.

303 F. Lapierre, V. Thomy, Y. Coffinier, R. Blossey and R. Boukherroub, *Langmuir*, 2009, **25**, 6551.
304 N. Verplanck, Y. Coffinier, V. Thomy, and R. Boukherroub, *Nanoscale Res. Lett.*, 2007, **2**, 577.
305 P. Brunet, F. Lapierre, Y. Coffinier, V. Thomy, and R. Boukherroub, *Langmuir*, 2008, **24**, 11203.
306 F. Lapierre, Y. Coffinier, V. Thomy, and R. Boukherroub, *Langmuir*, 2013, **29**, 13346.
307 S. J. Lee, S. Lee and K. H. Kang, *Appl. Phys. Lett.*, 2012, **100**, 081604/1.
308 W. Y. L. Ling, A. Neild and T. W. Ng, *Langmuir*, 2012, **28**, 17656.
309 M. S. Dhindsa, N. R. Smith, J. Heikenfeld, P. D. Rack, J. D. Fowlkes, M. J. Doktycz, A. V. Melechko and M. L. Simpson, *Langmuir*, 2006, **22**, 9030.
310 A. Egatz-Gomez, J. Schneider, P. Aella, D. Yang, P. Dominguez-Garcia, S. Lindsay, S. T. Picraux, M. A. Rubio, S. Melle, M. Marquez and A. A. Garcia, *Appl. Surf. Sci.*, 2007, **254**, 330.
311 R. Prakash, D. P. Papageorgiou, A. G. Papathanasiou and K. V. I. S. Kaler, *Sens. Actuators, B*, 2013, **182**, 351.
312 N F. Mumm, A. T. J. van Helvoort and P. Sikorski, *ACS Nano*, 2009, **3**, 2647.
313 Y. Koc, A. J. de Mello, G. McHale, M. I. Newton, P. Roach and N. J. Shirtcliffe, *Lab Chip*, 2008, **8**, 582.
314 S. M. Oliveira, W. Song, N. M. Alves and J. F. Mano, *Soft Matter*, 2011, **7**, 8932.
315 C. Lu, Y. Xie, Y. Yang, M. M.-C. Cheng, C.-G. Koh, Y. Bai and L. J. Lee, *Anal. Chem.*, 2007, **79**, 994.
316 S. L. S. Freire and B. Tanner, *Langmuir*, 2013, **29**, 9024.
317 K. Tsougeni, P. S. Petrou, D. P. Papageorgiou, S. E. Kakabakos, A. Tserepi and E. Gogolides, *Sens. Actuators, B*, 2012, **161**, 216.
318 a) M. Cao, J. Ju, K. Li, S. Dou, K. Liu and Lei Jiang, *Adv. Funct. Mater.,* DOI: 10.1002/adfm.201303661; b) X. Heng, M. Xiang, Z. Lu and C. Luo, *ACS Appl. Mater. Interfaces*, DOI: 10.1021/am4053267; c) J. Ju, H. Bai, Y. Zheng, T. Zhao, R. Fang and L. Jiang, *Nat. Commun.*, 2012, **3**, 1247.
319 A. Roth-Nebelsick, M. Ebner, T. Miranda, V. Gottschalk, D. Voigt, S. Gorb, T. Stegmaier, J. Sarsour, M. Linke and W. Konrad, *J. R. Soc. Interface*, 2012, **9**, 1965.
320 a) H. G. Andrews, E. A. Eccles, W. C. E. Schofield and J. P. S. Badyal, *Langmuir*, 2011, **27**, 3798; b) Y. Zheng, H. Bai, Z. Huang, X. Tian, F.-Q. Nie, Y. Zhao, J. Zhai and L. Jiang, *Nature*, 2010, **463**, 640.
321 L. Zhai, M. C. Berg, F. C. Cebeci, Y. Kim, J. M. Milwid, M. F. Rubner and R. E. Cohen, *Nano Lett.*, 2006, **6**, 1213.
322 a) K. Tsougeni, D. Papageorgiou, A. Tserepi and E. Gogolides, *Lab Chip*, 2010, **10**, 462–469; b) F. Lapierre, G. Piret, H. Drobecq, O. Melnyk, Y. Coffinier, V. Thomy and R. Boukherroub, *Lab Chip*, 2011, **11**, 1620.
323 a) M. P. Sousa and J. F. Mano, *ACS Appl. Mater. Interfaces*, 2013, **5**, 3731; b) M. P. Sousa and J. F. Mano, *Cellulose*, 2013, **20**, 2185.
324 a) M. Elsharkawy, T. M. Schutzius and C. M. Megaridis, *Lab Chip*, 2014, **14**, 1168; b) S. Xing, J. Jiang and T. Pan, *Lab Chip*, 2013, **13**, 1937.
325 J. Zhao, X. Zhang, N. Chen and Q. Pan, *ACS Appl. Mater. Interfaces*, 2012, **4**, 3706.
326 X. Zhang, J. Zhao, Q. Zhu, N. Chen, M. Zhang and Q. Pan, *ACS Appl. Mater. Interfaces*, 2011, **3**, 2630.
327 Q. Pan and M. Wang, *ACS Appl. Mater. Interfaces*, 2009, **1**, 420.
328 H. Jin, M. Kettunen, A. Laiho, H. Pynnoenen, J. Paltakari, A. Marmur, O. Ikkala and R. H. A. Ras, *Langmuir*, 2011, **27**, 1930.
329 M. Xiao, X Guo, M. Cheng, G. Ju, Y. Zhang and F. Shi, *Small*, 2014, **10**, 859.
330 M. Xiao, M. Cheng, Y. Zhang and F. Shi, *Small*, 2013, **9**, 2509.
331 D. Tian, Y. Song and L. Jiang, *Chem. Soc. Rev.*, 2013, **44**, 5184.
332 K. Nakata, S. Nishimoto, A. Kubo, D. Tryk, T. Ochiai, T. Murakami and A Fujishima, *Chem. Asian J.*, 2009, **4**, 984.
333 S. Nishimoto, A. Kubo, K. Nohara, X. Zhang, N. Taneichi, T. Okui, Z. Liu, K. Nakata, H. Sakai, T. Murakami, M. Abe, T. Komine and A Fujishima, *Appl. Surf. Sci.*, 2009, **255**, 6221.
334 H. Zhao and K.-L. Law, *ACS Appl. Mater. Interfaces*, 2012, **4**, 4288.
335 H. Zhao, K.-L. Law and V. Sambhy, *Langmuir*, 2011, **27**, 5927.
336 H. Zhao and K.-L. Law, *Langmuir*, 2012, **28**, 11812.
337 Y. Rahmawan, L. Xu and S. Yang, *J. Mater. Chem. A*, 2013, **1**, 2955
338 J. Bravo, L. Zhai, Z. Wu, R. E. Cohen and M. F. Rubner, *Langmuir*, 2007, **23**, 7293.
339 X. Zhu, Z. Zhang, G. Ren, X. Men, B. Ge and X. Zhou, *J. Colloid Interface Sci.*, 2014, **421**, 141.
340 Y.-L. Zhang, J.-N. Wang, Y. He, Y. He, B.-B. Xu, S. Wei and F.-S. Xiao, *Langmuir*, 2011, **27**, 12585.
341 P. Vukusic and J. R. Sambles, *Nature*, 2003, **424**, 852.
342 S.-y. Takemura, D. G. Stavenga and K. Arikawa, *J. Exp. Biol.*, 2007, **210**, 3075.
343 A. R. Parker, Z. Hegedus and R. A. Watts, *Proc. R. Soc. Lond. B*, 1998, **265**, 811.
344 a) P. Qu, F. Chen, H. Liu, Q. Yang, J. Lu, J. Si, Y. Wang and X. Hou, *Opt. Express*, 2012, **20**, 5775; b) J. Huang, X. Wang and Z. L. Wang, *Nanotechnology*, 2008, **19**, 025602/1.
345 W.-L. Min, B. Jiang and P. Jiang, *Adv. Mater.*, 2008, **20**, 3914.
346 Y. Li, J. Zhang, S. Zhu, H. Dong, F. Jia, Z. Wang, Y. Tang, L. Zhang, S. Zhang and B. Yang, *Langmuir*, 2010, **26**, 9842.
347 B. Kiraly, S. Yang and T. J. Huang, *Nanotechnology*, 2013, **24**, 245704/1.
348 M. Cao, X. Song, J. Zhai, J. Wang and Y. Wang, *J. Phys. Chem. B*, 2006, **110**, 15858.
349 N. Nishikawa, S. Sakiyama, S. Yamazoe, Y. Kojima, E.-i. Nishihara, T. Tsujioka, H. Mayama, S. Yokojima, S. Nakamura and K. Uchida, *Langmuir*, 2013, **29**, 8164.
350 C.-H. Liu, P.-L. Niu and C.-K. Sung, *J. Phys. D: Appl. Phys.*, 2014, **47**, 015401/1.
351 X. Gao, *Encyclopedia of Nanotechnology*, 2012, p. 117.
352 K. Rykaczewski, *Langmuir*, 2012, **28**, 7720.
353 K. Rykaczewski, W. A. Osborn, J. Chinn, M. L. Walker, J. H. J. Scott, W. Jones, C. Hao, S. Yao and Z. Wang, *Soft Matter*, 2012, **8**, 8786.
354 R. D. Narhe and D. A. Beysens, *Europhys. Lett.*, 2006, **75**, 98.
355 C.-H. Chen, Q. Cai, C. Tsai, C.-L. Chen, G. Xiong, Y. Yu, and Z. Ren, *Appl. Phys. Lett.*, 2007, **90**, 173108/1.
356 K.-C. Park, H. J. Choi, C.-H. Chang, R. E. Cohen, G. H. McKinley and G. Barbastathis, *ACS Nano*, 2012, **6**, 3789.
357 S. Manakasettarn, T.-H. Hsu, G. Myhre, S. Pau, J. A. Taylor and T. Krupenkin, *Opt. Mater. Express*, 2012, **2**, 214.

358 Y. Lai, Y. Tang, J. Gong, D. Gong, L. Chi, C. Lin and Z. Chen, *J. Mater. Chem.*, 2012, **22**, 7420.
359 N. L. Tarwal, A. V. Rajgure, A. I. Inamdar, R. S. Devan, I. Y. Kim, S. S. Suryavanshi, Y. R. Ma, J. H. Kim and P. S. Patil, *Sens. Actuators, A*, 2013, **199**, 67.
360 T. J. Athauda, P. Hari and R. R. Ozer, *ACS Appl. Mater. Interfaces*, 2013, **5**, 6237.
361 S. He, M. Zheng, L. Yao, X. Yuan, M. Li, L. Ma and W. Shen, *Appl. Surf. Sci.*, 2010, **256**, 2557.
362 X. B. Ji, W. C. Lu and H. P. Ma, *Cryst. Res. Technol.*, 2012, **47**, 1121.
363 M. G. Gong, Y. Z. Long, X. L. Xu. H. D. Zhang and B. Sun, in *Nanowires: Recent Advances*, ed. X. Peng, InTech, 2012, ch. 5, p.77.
364 Z. Guo, X. Chen, J. Li, J.-H. Liu and X.-J. Huang, *Langmuir*, 2011, **27**, 6193.
365 W. Jia, B. Jia, X. Wu and F. Qu, *CrystEngComm*, 2012, **14**, 7759.
366 S. Schicho, A. Jaouad, C. Sellmer, D. Morris, V. Aimez and R. Ares, *Mater. Lett.*, 2013, **94**, 86.
367 P. Shen, N. Uesawa, S. Inasawa, Y. Yamaguchi, *Langmuir*, 2010, **26**, 13522.
368 A. Pakdel, Y. Bando, D. Shtansky and D. Goldberg, *Surf. Innovations*, 2013, **1**, 32.
369 H. Cao, Y. Xiao and R. Liang, *CrystEngComm*, 2011, **13**, 5688.
370 Y. Xiao, H. Cao, K. Liu, S. Zhang and V. Chernow, *Nanotechnology*, 2010, **21**, 145601/1.
371 Y. W. Hu, H. R. He and Y. M. Ma, *Adv. Mater. Res.*, 2011, **412**, 163.
372 R. Su, H. Liu, T. Kong, Q. Song, N. Li, G. Jin and G. Cheng, *Langmuir*, 2011, **27**, 13220.
373 Z. Shen, C. Hou, S. Liu and Z. Guan, *J. Appl. Polym. Sci.*, 2014, **131**, 40400.
374 B. N. Sahoo and B. Kandasubramanian, *RSC Adv.*, 2014, **4**, 11331.
375 X. Fan, X. Li, D. Tian, J. Zhai and L. Jiang, *J. Colloid Interface Sci.*, 2012, **366**, 1.
376 Q. Zhang, J. Yang, C.-F. Wang, Q.-L. Chen and S. Chen, *Colloid Polym. Sci.*, 2013, **291**, 717.
377 L. Zhu, S. Yang, J. Yang, C.-F. Wang, L. Chen and S. Chen, *Mater. Lett.*, 2013, **99**, 54.
378 Y. Zhang, Q. Zhang, C.-F. Wang and S. Chen, *Ind. Eng. Chem. Res.*, 2013, **52**, 11590.
379 L. Hou, C. Wang, L. Chen and S. Chen, *J. Mater. Chem.*, 2010, **20**, 3863.
400 M. Yoon, Y. Kim and J. Cho, *ACS Nano*, 2011, **5**, 5417.
401 Q. Wang, W. Hou and Y. Zhang, *Appl. Surf. Sci.*, 2009, **256**, 664.
402 H. Matsukizono and R.-H. Jin, *Langmuir*, 2011, **27**, 6338.
403 O. Sato, S. Kubo and Z.-Z. Gu, *Acc. Chem. Res.*, 2009, **42**, 1.
404 J. Wang, Y. Zhang, S. Wang, Y. Song and L. Jiang, *Acc. Chem. Res.*, 2011, **44**, 405.
405 C. W. Mason, *J. Phys. Chem.*, 1926, **30**, 383.
406 M. Srinivasarao, *Chem. Rev.*, 1999, **99**, 1935.
407 J. Yong, Q. Yang, F. Chen, D. Zhang, G. Du, H. Bian, J. Si and X. Hou, *RSC Adv.*, 2014, **4**, 8138.
408 P. P. Goodwyn, Y. Maezono, N. Hosoda and K. Fujisaki, *Naturwissenschaften*, 2009, **96**, 781.
409 H. Kasukawa, N. Oshima and R. Fujii, *Zool. Sci.*, 1987, **4**, 243.
410 J. N. Lythgoe and J. Shand, *J. Physiol.*, 1982, **325**, 23.
411 L. M. Maethger, M. F. Land, U. E. Siebeck and N. J. Marshall, *J. Exp. Biol.*, 2003, **206**, 3607.
412 A. R. Tao, D. G. DeMartini, M. Izumi, A. M. Sweeney, A. L. Holt, D. E. Morse, *Biomaterials*, 2010, **31**, 793.
413 V. Welch, J. P. Vigneron, V. Lousse and A. Parker, *Phys. Rev. E*, 2006, **73**, 041916/1.
414 A. R. Parker, V. L. Welch, D. Driver, N. Martini, *Nature*, 2003, **426**, 786.
415 M. Rassart, P. Simonis, A. Bay, O. Deparis and J. P. Vigneron, *Phys. Rev. E*, 2009, **80**, 031910/1.
416 J. P. Vigneron, J. M. Pasteels, D. M. Windsor, Z. Vértesy, M. Rassart, T. Seldrum, J. Dumont, O. Deparis, V. Lousse, L. P. Biró, D. Ertz and V. Welch, *Phys. Rev. E*, 2007, **76**, 031907/1.
417 P. Vukusic, J. R. Sambles, C. R. Lawrence and R. J. Wootton, *Nature*, 2001, **410**, 36.
418 P. Vukusic, J. R. Sambles and C. R. Lawrence, *Nature*, 2000, **404**, 457.
419 J.-Y. Shiu, C.-W. Kuo, P. Chen and C.-Y. Mou, *Chem. Mater.*, 2004, **16**, 561.
420 G. Zhang, D. Wang, Z.-Z. Gu and H. Moehwald, *Langmuir*, 2005, **16**, 9143.
421 J. Zhang, L. Xue and Y. Han, *Langmuir*, 2005, **21**, 5.
422 J. T. Han, X. Xu and K. Cho, *Langmuir*, 2005, **21**, 6662.
423 S. Zhang, X.-W. Zhao, H. Xu, R. Zhu, Z.-Z. Gu, *J. Colloid Interface Sci.*, 2007, **316**, 168.
424 Y. Xia, B. Gates, Y. Yin and Y. Lu, *Adv. Mater.*, 2000, **12**, 693.
425 Hiroshi Fudouzi, *Sci. Technol. Adv. Mater.*, 2011, **12**, 064704/1.
426 H. Cong, B. Yu, S. Wang, L. Qi, J. Wang and Y. Ma, *Opt. Express*, 2013, **21**, 17831.
427 J.-N. Wang, R.-Q. Shao, Y.-L. Zhang, L. Guo, H.-B. Jiang, D.-X. Lu and H.-B. Sun, *Chem. Asian J.*, 2012, **7**, 301.
428 H. Ge, Y. Song, L. Jiang and D. Zhu, *Thin Solid Films*, 2006, **515**, 1539.
429 S.-i. Shinohara, T. Seki, T. Sakai, R. Yoshida and Y. Takeoka, *Angew. Chem., Int. Ed.*, 2008, **47**, 9039.
430 E. Tian, J. Wang, Y. Zheng, Y. Song, L. Song and D. Zhu, *J. Mater. Chem.*, 2008, **18**, 1116.
431 A. M. Brozell, M. A. Muha, A. Abed-Amoli, D. Bricarello and A. N. Parikh, *Nano Lett.*., 2007, **7**, 3822.
432 E. Tian, Y. Ma, L. Cui, J. Wang, Y. Song, L. Song and D. Zhu, *Macromol. Rapid Commun.*, 2009, **30**, 1719.
433 J. Wang, Y. Men, H. Ge, Z. Sun, Y. Zheng, Y. Song and D. Zhu, *Macromol. Chem. Phys.*, 2006, **207**, 596.
434 L. Cui, Y. Zhang, J. Wang, Y. Ren, Y. Song and L. Jiang, *Macromol. Rapid Commun.*, 2009, **30**, 598.
435 L. Cui, Y. Li, J. Wang, E. Tian, X. Zhang, Y. Zhang, Y. Song and L. Jiang, *J. Mater. Chem.*, 2009, **19**, 5499.
436 Y. Huang, J. Zhou, B. Su, L. Shi, J. Wang, S. Chen, L. Wang, J. Zi, Y. Song and L. Jiang, *J. Am. Chem. Soc.*, 2012, **134**, 17053.
437 J. Wang, Y. Wen, X. Feng, Y. Song and L. Jiang, *Macromol. Rapid Commun.*, 2006, **27**, 188.
438 Z.-Z. Gu, H. Uetsuka, K. Takahashi, R. Nakajima, H. Onishi, A. Fujishima and O. Sato, *Angew. Chem. Int. Ed.*, 2003, **42**, 894.
439 Z.-Z. Gu, A. Fujishima and O. Sato, *Angew. Chem. Int. Ed.*, 2002, **114**, 2171.

440 X. Chen, L. Wang, Y. Wen, Y. Zhang, J. Wang, Y. Song, L. Jiang and D. Zhu, *J. Mater.Chem.*, 2008, **18**, 2262.
441 J. Zhou, H. Li, L. Ye, J. Liu, J. Wang, T. Zhao, L. Jiang and Y. Song, *J. Phys. Chem. C*, 2010, **114**, 22303.
442 L. Xu, J. Wang, Y. Song and L. Jiang, *Chem. Mater.*, 2008, **20**, 3554.
443 J. Lie, G. Liang, X. Zhu and S. Yang, *Adv. Funct. Mater.*, 2012, **22**, 2980.
444 D. Wu, Q.-D. Chen, H. Xia, J. Jiao, B.-B. Xu, X.-F. Lin, Y. Xu and H.-B. Sun, *Soft Matter*, 2010, **6**, 263.
445 Y. Liu, A. Das, S. Xu, Z. Lin, C. Xu, Z. L. Wang, A. Rohatgi and C. P. Wong, *Adv. Energy Mater.*, 2012, **2**, 47.
446 Y. Gao, I. Gereige, A. El Labban, D. Cha, T. T. Isimjan and P. M. Beaujuge, *ACS Appl. Mater. Interfaces*, 2014, **6**, 2219.
447 R. Asmatulu, M. Ceylan and N. Nuraje, *Langmuir*, 2011, **27**, 504.
448 H. C. Barshilia, S. John and V. Mahajan, *Sol. Energy Mater. Sol. Cells*, 2012, **107**, 219.
449 Y.-B. Park, H. Im, M. Im and Y.-K. Choi, *J. Mater. Chem.*, 2011, **21**, 633.
450 J.-H. Kong, T.-H. Kim, J. H. Kim, J.-K. Park, D.-W. Lee, S.-H. Kim and J.-M. Kim, *Nanoscale*, 2014, **6**, 1453.
451 S.-H. Lee, K.-S. Han, J.-H. Shin, S.-Y. Hwang and H. Lee, *Prog. Photovoltaics*, 2013, **21**, 1056.
452 S. Y. Heo, J. K. Koh, G. Kang, S. H. Ahn, W. S. Chi, K. Kim and J. H. Kim, *Adv. Energy Mater.*, 2014, 4, 1300632/1.
453 J. Zhu, C.-M. Hsu, Z. Yu, S. Fan and Y. Cui, *Nano Lett.*, 2010, **10**, 1979.
454 N. T. Panagiotopoulos, E. K. Diamanti, L. E. Koutsokeras, M. Baikousi, E. Kordatos, T. E. Matikas, D. Gournis and P. Patsalas, *ACS Nano*, 2012, **6**, 10475.
455 A. Milionis, R. Giannuzzi, I. S. Bayer, E. L. Papadopoulou, R. Ruffilli, M. Manca and A. Athanassiou, *ACS Appl. Mater. Interfaces*, 2013, **5**, 7139.
456 V. A. Lifton, S. Simon and R. E. Frahm, *Bell Lab. Tech. J.*, 2005, **10**, 81.
457 V. A. Lifton and S. Simon, *NSTI Nanotech 2005, NSTI Nanotechnology Conference and Trade Show*, Anaheim, CA, United States, 2005, **2**, 726.
458 V. Lifton and S. Simon, *Proc. Power Sources Conf.*, 2006, **42nd**, 123.
459 V. A. Lifton, J. A. Taylor, B. Vyas, P. Kolodner, R. Cirelli, N. Basavanhally, A. Papazian, R. Frahm, S. Simon and T. Krupenkin, *Appl. Phys. Lett.*, 2008, **93**, 043112/1.
460 Q. Zhu, N. Chen, F. Tao and Q. Pan, *J. Mater. Chem.*, 2012, **22**, 15894.
461 W. Li, X. Wang, Z. Chen, M. Waje and Y. Yan, *Langmuir*, 2005, **21**, 9386.
462 S. C. Tan, F. Yan, L. I. Crouch, J. Robertson, M. R. Jones and M. E. Welland, *Adv. Funct. Mater.*, 2013, **23**, 5556.
463 W.-K. Wang, M.-L. Zheng, W.-Q. Chen, F. Jin, Y.-Y. Cao, Z.-S. Zhao and X.-M. Duan, *Langmuir*, 2011, **27**, 3249.
464 F. Xu, Y. Zhang, Y. Sun, Y. Shi, Z. Wen and Z. Li, *J. Phys. Chem. C*, 2011, **115**, 9977.
465 H. K. Lee, Y. H. Lee, Q. Zhang, I. Y. Phang, J. M. R. Tan, Y. Cui and X. Y. Ling, *ACS Appl. Mater. Interfaces*, 2013, **5**, 11409.
466 S. Yang, P. J. Hricko, P.-H. Huang, S. Li, Y. Zhao, Y. Xie, F. Guo, L. Wang and T. J. Huang, *J. Mater. Chem. C*, 2014, **2**, 542.
467 Y. Hu, S. Liu, S. Huang and W. Pan, *Thin Solid Films*, 2010, **519**, 1314.
468 Q.-X. Zhang, Y.-X. Chen, Z. Guo, H.-L. Liu, D.-P. Wang and X.-J. Huang, *ACS Appl. Mater. Interfaces*, 2013, **5**, 10633.
469 B.-B. Xu, Y.-L. Zhang, W.-Y. Zhang, X.-Q. Liu, J.-N. Wang, X.-L. Zhang, D.-D. Zhang, H.-B. Jiang, R. Zhang and H.-B. Sun, *Adv. Opt. Mater.*, 2013, **1**, 56.
470 F. Gentile, M. L. Coluccio, N. Coppede, F. Mecarini, G. Das, C. Liberale, L. Tirinato, M. Leoncini, G. Perozziello, P. Candeloro, F. De Angelis and E. Di Fabrizio, *ACS Appl. Mater. Interfaces*, 2012, **4**, 3213.
471 F. Gentile, M. L. Coluccio, A. Accardo, G. Marinaro, E. Rondanina, S. Santoriello, S. Marras, G. Das, L. Tirinato, G. Perozziello, F. De Angelis, C. Dorigoni, P. Candeloro, and E. Di Fabrizio, *Microelectron. Eng.*, 2012, **97**, 349.
472 F. Gentile, G. Das, M. L. Coluccio, F. Mecarini, A. Accardo, L. Tirinato, R. Tallerico, G. Cojoc, C. Liberale, P. Candeloro, P. Decuzzi, F. De Angelis and E. Di Fabrizio, *Microelectron. Eng.* 2010, **87**, 798.
473 N. Andreeva, T. Ishizaki, P. Baroch and N. Saito, *Sens. Actuators, B* 2012, **164**, 15.
474 Y. Lv, X. Yu, J. Jia, S.-T. Tu, J. Yan and E. Dahlquist, *Appl. Energy* 2012, **90**, 167.
475 R. Begag, H. Krutka, W. Dong, D. Mihalcik, W. Rhine, G. Gould, J. Baldic and P. Nahass, *Greenhouse Gas Sci. Technol.* 2013, **3**, 30.
476 X. Sun, Y. Liu, S. Mopidevi, Y. Meng, F. Huang, J. Parisi, M.-P. Nieh, C. Cornelius, S. L. Suib and Y. Lei, *Sens. Actuators, B* 2014, **195**, 52.
477 D. J. Cho, S. E. Kim, E. Seo, M. C. Lee, J. M. Lee and J. S. Ko, *Sens. Actuators, B* 2013, **188**, 347.
478 K. Malzahn, J. R. Windmiller, G. Valdes-Ramirez, M. J. Schoening and J. Wang, *Analyst* 2011, **136**, 2912.
479 Y. Zhao, M. Qin, A. Wang and D. Kim, *Adv. Mater.* 2013, **25**, 4561.
480 H. Li, J. Wang, L. Yang and Y. Song, *Adv. Funct. Mater.*, 2008, **18**, 3258.
481 H. Li, L. Chang, J. Wang, L. Yang and Y. Song, *J. Mater. Chem.*, 2008, **18**, 5098.
482 F. Song, H. Su, J. Han, D. Zhang and Z. Chen, *Nanotechnology*, 2009, **20**, 495502/1.
483 S. J. Williams and G. J. Davie, *Trends Biotechnol.*, 2001, **19**, 356.
484 T. D. James, K. R. A. S. Sandanayake and S. Shinkai, *Angew. Chem., Int. Ed.*, 1996, **35**, 1910.
485 G. Qing, X. Wang, L. Jiang, H. Fuchs and T. Sun, *Soft Matter*, 2009, **5**, 2759.
486 G. Qing, X. Wang, H. Fuchs and T. Sun, *J. Am. Chem. Soc.*, 2009, **131**, 8370.
487 N. Feng, H. Zhao, J. Zhan, D. Tian and H. Li, *Org. Lett.*, 2012, **14**, 1958.
488 L. Wei, Y. Lei, H. Fu and J. Yao, *ACS Appl. Mater. Interfaces*, 2012, **4**, 1594.
489 H. He, Y. Yuan, W. Wang, N.-R. Chiou, A. J. Epstein and L. J. Lee, *Biomicrofluidics*, 2009, **3**, 022401/1.
490 J. Nie, Y. Zhang, H. Wang, S. Wang and G. Shen, *Biosens. Bioelectron.*, 2012, **33**, 23.
491 Y. Zhang, H. Wang, J. Li, J. Nie, Y. Zhang, G. Shen and R. Yu, *Biosens. Bioelectron.*, 2011, **26**, 3272.

492 A. I. Neto, C. A. Custodio, W. Song and J. F. Mano, *Soft Matter*, 2011, **7**, 4147.
493 A. Ressine, G. Marko-Varga and T. Laurell, *Biotechnol. Ann. Rev.*, 2007, **13**, 149.
494 A. Ressine, D. Finnskog, G. Marko-Varga and T. Laurell, *Nanobiotechnology*, 2008, **4**, 18.
495 A. Ebrahimi, P. Dak, E. Salm, S. Dash, S. V. Garimella, R. Bashir and M. A. Alam, *Lab Chip*, 2013, **13**, 4248.
496 A. C. Lima, C. A. Custodio, C. Alvarez-Lorenzo and J. F. Mano, *Small*, 2013, **9**, 2487.
497 A. Accardo, L. Tirinato, D. Altamura, T. Sibillano, C. Giannini, C. Riekel and E. Di Fabrizio, *Nanoscale*, 2013, **5**, 2295.
498 A. Accardo, F. Gentile, F. Mecarini, F. De Angelis, M. Burghammer, E. Di Fabrizio and C. Riekel, *Langmuir* 2010, **26**, 15057.
499 Y. Lai, L. Lin, F. Pan, J. Huang, R. Song, Y. Huang, C. Lin, H. Fuchs and L. Chi, *Small* 2013, **9**, 2945.
500 X. Li, Y. Liu, A. Zhu, Y. Luo, Z. Deng and Y. Tian, *Anal. Chem.* 2010, **82**, 6512.
501 F. Gentile, M. L. Coluccio, E. Rondanina, S. Santoriello, D. Di Mascolo, A. Accardo, M. Francardi, F. De Angelis, P. Candeloro and E. Di Fabrizio, *Microelectron. Eng.* 2013, **111**, 272.
502 J. Hou, H. Zhang, Q. Yang, M. Li, Y. Song and L. Jiang, *Angew. Chem., Int. Ed.*, 2014, DOI: 10.1002/anie.201400686.
503 S. T. Yohe, Y. L. Colson and M. W. Grinstaff, *J. Am. Chem. Soc.*, 2012, **134**, 2016.
504 S. T. Yohe, V. L. M. Herrera, Y. L. Colson and M. W. Grinstaff, *J. Control. Release*, 2012, **162**, 92.
505 S. T. Yohe, J. A. Kopechek, T. M. Porter, Y. L. Colson and M. W. Grinstaff, *Adv. Healthcare Mater.*, 2013, **2**, 1204.
506 U. Manna, M. J. Kratochvil and D. M. Lynn, *Adv. Mater.*, 2013, **25**, 6405.
507 A. M. Puga, A. C. Lima, J. F. Mano, A. Concheiro and C. Alvarez-Lorenzo, *Carbohydr. Polym.*, 2013, **98**, 331.
508 W. Song, A. C. Lima, J. F. Mano, *Chem. Commun.*, 2010, **6**, 5868.
509 A. C. Lima, W. Song, B. Blanco-Fernandez, C. Alvarez-Lorenzo and J. F. Mano, *Pharm. Res.*, 2011, **28**, 1294.
510 F. Liu, L. Wang, Q. Sun, L. Zhu, X. Meng and F.-S. Xiao, *J. Am. Chem. Soc.*, 2012, **134**, 16948.
511 F. Liu, W. Li, Q. Sun, L. Zhu, X. Meng, Y.-H. Guo and F.-S. Xiao, *ChemSusChem*, 2011, **4**, 1059.
512 I. Noshadi, R. K. Kumar, B. Kanjilal, R. Parnas, H. Liu, J. Li and F. Liu, *Catal. Lett.*, 2013, **143**, 792.
513 P. Xia, F. Liu, C. Wang, S. Zuo and C. Qi, *Catal. Commun.*, 2012, **26**, 140.
514 Q. Sun, Y. Jin, L. Zhu, L. Wang, X. Meng and F.-S. Xiao, *Nano Today*, 2013, **8**, 342.
515 C. Chen, J. Xu, Q. Zhang, Y. Ma, L. Zhou and M. Wang, *Chem. Commun.*, 2011, **47**, 1336.
516 S. Shi, M. Wang, C. Chen, J. Gao, H. Ma, J. Ma and J. Xu, *Chem. Commun.*, 2013, **49**, 9591.
517 H. Li, J. Liao, Y. Du, T. You, W. Liao and L. Wen, *Chem. Commun.*, 2013, **49**, 1768.
518 X.-M. Zhou, W. Chen and Y.-F. Song, *Eur. J. Inorg. Chem.*, 2014, **2014**, 812.
519 H. Zhou, L. Xiao, X. Liu, S. Li, H. Kobayashi, X. Zheng and J. Fan, *Chem. Commun.*, 2012, **48**, 6954.

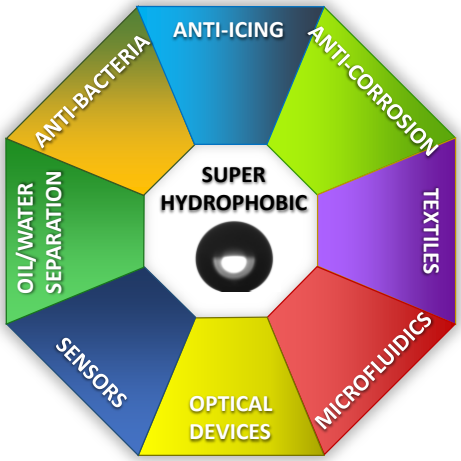

This review highlights the recent advances made in the potential applications of superhydrophobic materials.